SUMMARY REPORT

THE SRICOS–EFA METHOD

BRIAUD J.-L., CHEN H.-C., CHANG K.-A., OH S.J., CHEN S., WANG J., LI Y., KWAK K., NARTJAHO P., GUDARALLI R., WEI W., PERGU S., CAO Y.W., TING F.

TEXAS A&M UNIVERSITY

JANUARY 2011

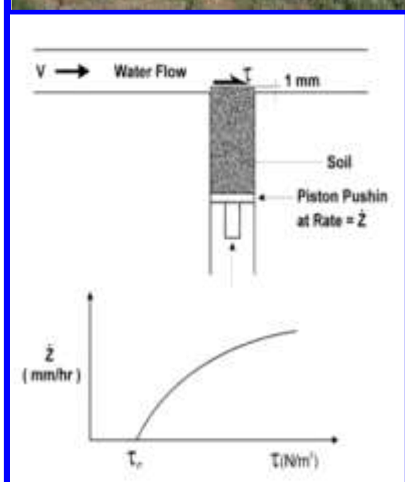

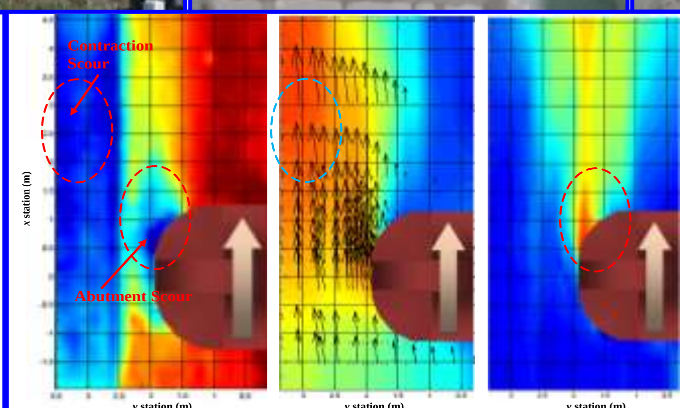

(a) Scour pattern after 320 hours

(b) Initial time averaged velocity

(c) Initial turbulence intensity

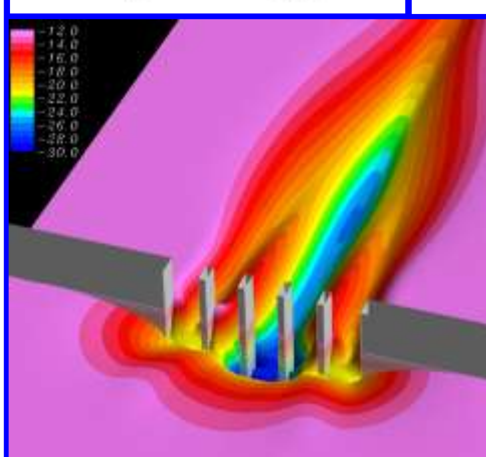

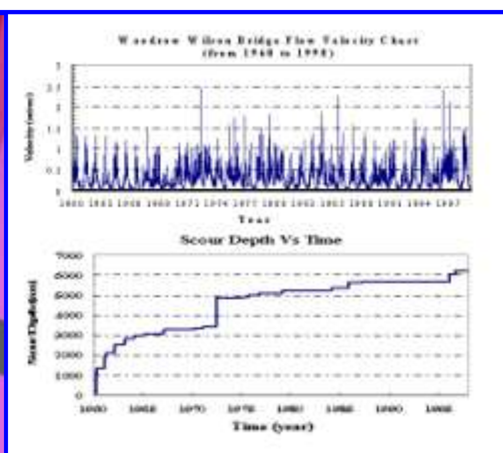

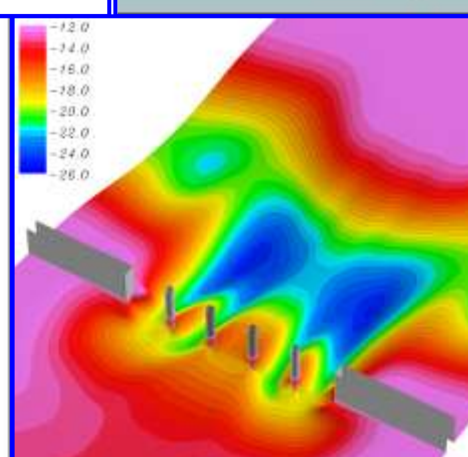

TABLE OF CONTENTS

Page

LIST OF FIGURES

Page

LIST OF TABLES

INTRODUCTION

Most prediction equations to estimate bridge scour depths have been developed on the basis of laboratory flume test results using coarse grained soil. Unfortunately these same equations are also used for fine grained soil which have much lower erosion rate than coarse grained soil. It usually takes less than a day for coarse grained soil to reach the maximum scour depth around a bridge support under a constant flow rate but for a fine grained soil the scour depth developed in a day maybe a small percent of the maximum scour depth because of the slower erosion rate. Studies of bridge scour depths in fine grained soils with consideration of soil erodibility and time dependence have been performed at Texas A&M University since 1990.

The SRICOS-EFA (Scour Rate In COhesive Soil – Erosion Function Apparatus) method has been developed starting in early 1990s by Briaud and his coworkers for fine grained soils. This method allows the user to predict the scour depth as a function of time; it is based on two main parameters, the maximum scour depth and the maximum shear stress before scour begins. The equation to calculate the maximum scour depth was developed on the basis of flume test results and dimensional analysis, while the maximum shear stress was developed on the basis of three-dimensional (3D) numerical computation results.

The SRICOS-EFA program allows users to perform the complex pier scour, contraction scour and abutment scour alone, also it can handle the combined scour of the pier, contraction and abutment scour (integrated SRICOS-EFA method). It automates the calculations of all the parameters such as maximum initial shear stress, initial scour rate, maximum scour depth, and transformation of the discharge into velocity. It also automates the computations to handle multi-flood hydrograph and multi-layer soil systems.

BASIC CONCEPT OF SRICOS

The scour phenomenon in fine grained soils is much slower and more dependent on soil properties than that in coarse grained soils. Applying the equations developed to predict depth of scour in coarse grained soils to fine grained soils without the consideration of time yields overly conservative scour depths. Therefore, a scour analysis method for fine grained materials needs to consider the effect of time and soil properties as well as hydraulic parameters. Once the SRICOS (Scour Rate In COhesive Soils) method was developed to predict the scour depth versus time around a cylindrical bridge pier founded in fine grained soils, it has been expanded to contraction scour and abutment scour.

The SRICOS method is highly dependent on the maximum scour depth and the shear stress between the flow and soil interface. The procedure of SRICOS method is consisted with following steps.

1. Obtain standard 76.2 mm diameter Shelby tube samples as close to the pier as possible.
2. Test the sample in the EFA to get the erodibility curve ($\dot{z}$ vs. τ).
3. Determine the maximum shear stress τ_{max}.
4. Obtain the initial scour rate $(\dot{z}_i)$ corresponding to τ_{max}.
5. Develop the complete scour depth y_s vs. t curve.
6. Predict the depth of scour by reading the y_s vs. t at the time corresponding to the duration of the flood using

$$y_s(t) = \frac{t}{\frac{1}{\dot{z}_i} + \frac{t}{y_s}} \tag{1}$$

where t is time (hour), y_s is the maximum pier scour depth (mm), τ_{max} is the maximum shear stress on the channel bed

EFA TEST

An apparatus measuring the erosion function was developed in the early 1990s, called the EFA (Erosion Function Apparatus), and it is shown in Figure 1(Briaud *et al.*, 2001; Briaud *et al.*, 1999). The principle is to go to the site where erosion is being investigated, collect samples within the depth of concern, bring them back to the laboratory, and test them in the EFA. The 75 mm outside diameter sampling tube is placed through the bottom of the conduit where water flows at a constant velocity. The soil or rock is pushed out of the sampling tube only as fast as it is eroded by the water flowing over it.

For fine grained and coarse grained soils, ASTM standard thin wall steel tube samples are favored. If such samples cannot be obtained (e.g.: coarse grained soils), Split Spoon SPT samples are obtained and the coarse grained soil is reconstituted in the thin wall steel tube. Fortunately in the case of erosion of coarse grained soils, soil disturbance does not affect the results significantly. If it is representative of the rock erosion process to test a 75 mm diameter rock sample, the rock core is placed in the thin wall steel tube and tested in the EFA. The rate of erosion can be very different for different soils.

The test result consists of the erosion rate $\dot{z}$ versus shear stress τ curve (Figure 1). For each flow velocity V, the erosion rate $\dot{z}$ (mm/hr) is simply obtained by dividing the length of sample eroded by the time required to do so.

$$\dot{z} = \frac{h}{t} \tag{2}$$

where h is the length of soil sample eroded in a time t. The length h is 1 mm and the time t is the time required for the sample to be eroded flush with the bottom of the pipe (visual inspection through a Plexiglas window).

After several attempts at measuring the shear stress τ in the apparatus it was found that the best way to obtain τ was by using the Moody Chart (Moody, 1944) for pipe flows.

$$\tau = \frac{1}{8} f \rho V^2 \tag{3}$$

where τ is the shear stress on the wall of the pipe; *f* is the friction factor obtained from the Moody Chart (Figure 2); ρ is the mass density of water (1,000 kg/m^3); and V is the mean flow velocity in the pipe. The friction factor *f* is a function of the pipe Reynolds Number Re and the pipe roughness ε / D. The Reynolds Number is ν / VD where *D* is the pipe diameter and ν is the kinematic viscosity of water ($10^{-6}\, m^2/s$ at $20°\mathrm{C}$). Since the pipe in the EFA has a rectangular cross section, *D* is taken as the hydraulic diameter $D = 4A/P$ where *A* is the cross-sectional flow area, *P* is the wetted perimeter, and the factor 4 is used to ensure that the hydraulic diameter is equal to the diameter for a circular pipe. For a rectangular cross-section pipe:

$$D = 2ab/(a+b) \tag{4}$$

where *a* and *b* are the dimensions of the sides of the rectangle. The relative roughness ε / D is the ratio of the average height of the roughness elements on the pipe surface over the pipe diameter *D*. The average height of the roughness elements ε is taken equal to $0.5D_{50}$ where D_{50} is the mean grain size for the soil. The factor 0.5 is used because it is assumed that the top half of the particle protrudes into the flow while the bottom half is buried in the soil mass.

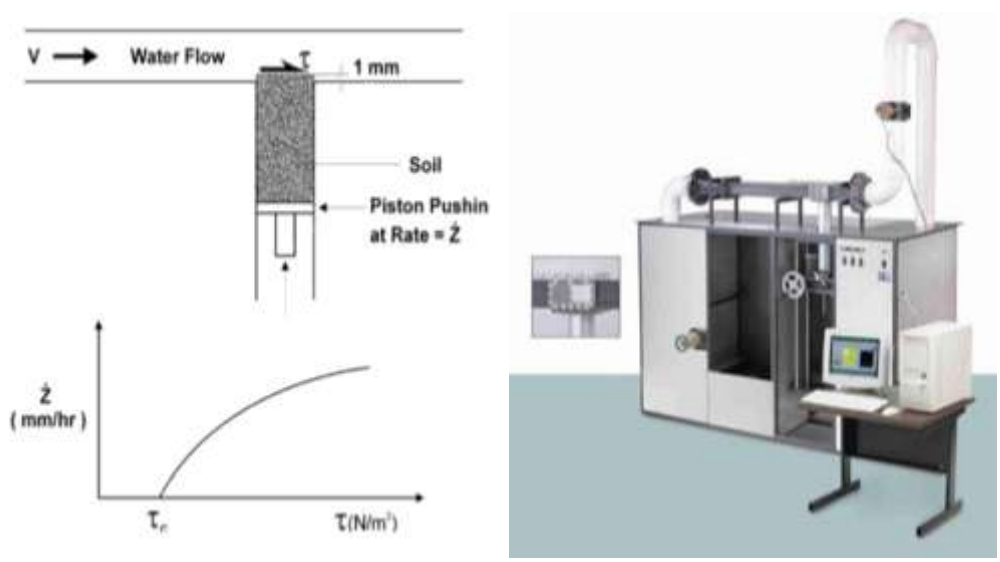

Figure 1 – EFA (Erosion Function Apparatus) to measure erodibility (Briaud *et al.*, 1999).

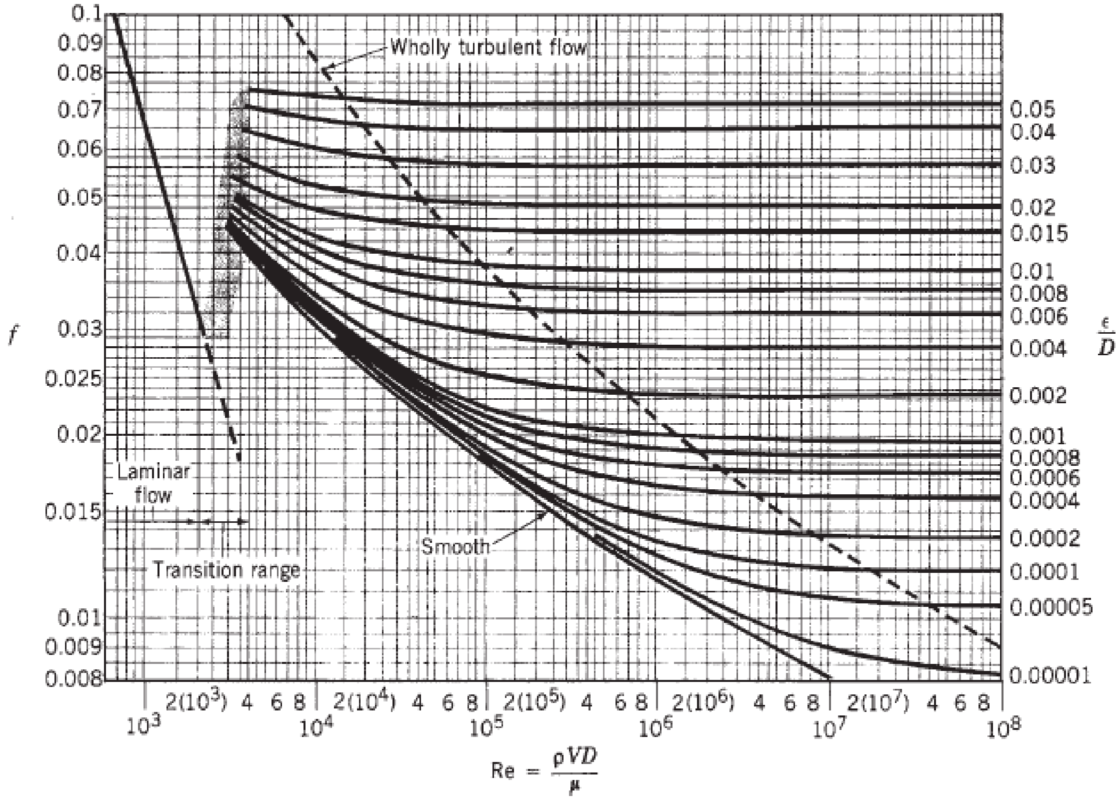

Figure 2 – Moody Chart (reprinted with permission from (Munson *et al.*, 1990)

The categories of erosion rate for different soils are proposed on the basis of 15 years of erosion testing experience using EFA (Erosion Function Apparatus). In order to classify a soil or rock, the erosion function is plotted on the category chart and the erodibility category number for the material tested is the number for the zone in which the erosion function fits. Note that using the water velocity is less representative and leads to more uncertainties than using the shear stress; indeed the velocity and the shear stress are not linked by a constant. Nevertheless the velocity chart is presented because it is easier to gage a problem in terms of velocity.

Categories are used in many fields of engineering: soil classification categories, hurricane strength categories, earthquake magnitude categories. Such categories have the advantage of quoting one number to represent a more complex condition. Briaud (Briaud, 2008) proposed Erosion categories in order to bring erodibility down in complexity from an erosion rate vs shear stress function to a category number. Such a classification system can be presented in terms of velocity (Figure 3) or shear stress (Figure 4).

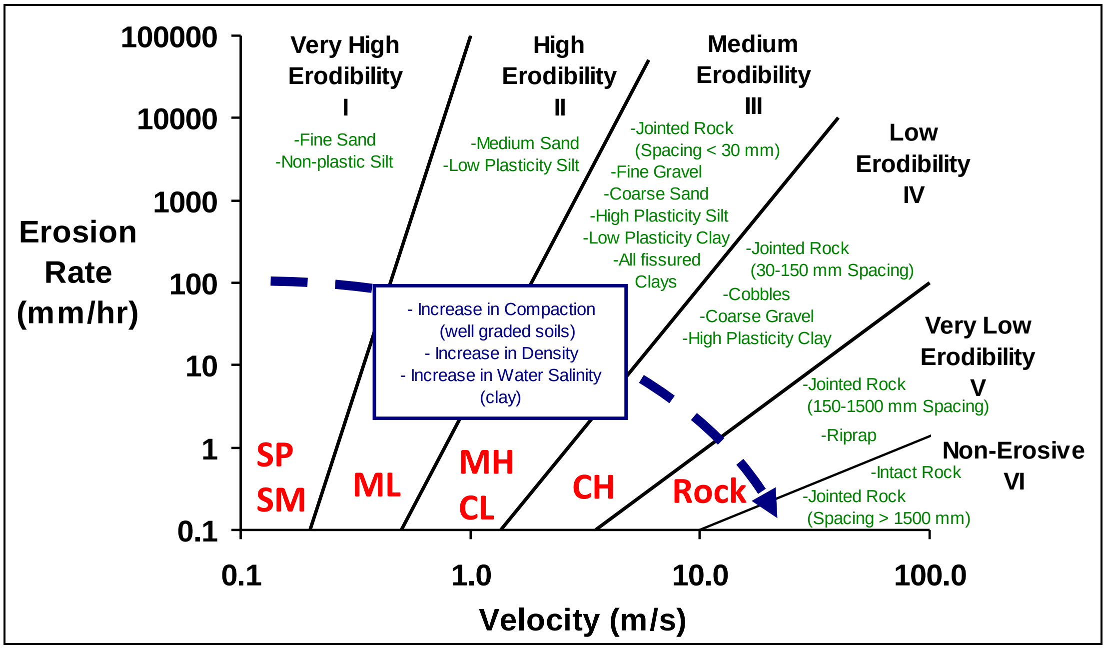

Figure 3 – Proposed erosion categories for soils and rocks based on velocity (Briaud, 2008).

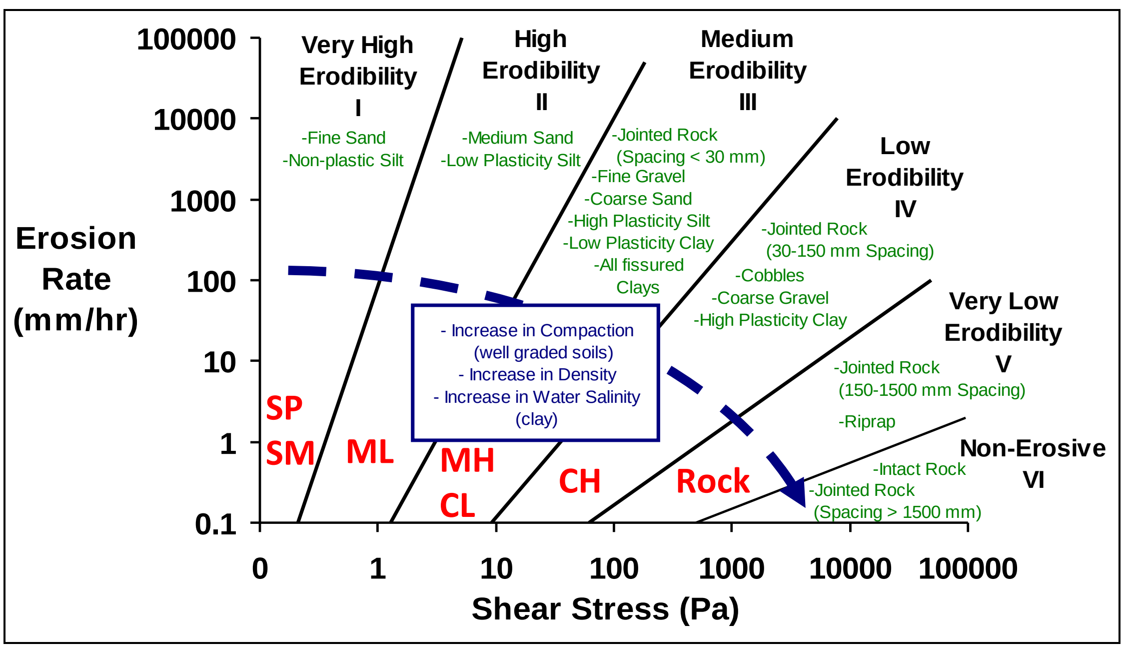

Figure 4 – Proposed erosion categories for soils and rocks based on shear stress (Briaud, 2008).

PET (POCKET ERODOMETER TEST)

Over the last 20 years, several tools have been developed in an effort to quantify the erodibility of a soil; however, they all require a significant amount of time for set up and sample preparation. The Pocket Erodometer Test (PET) is a simple test which can be performed in a few seconds with an inexpensive, compact, and very light instrument. The Pocket Erodometer is a regulated mini jet impulse generating device. The jet is aimed horizontally at the vertical face of the sample. The depth of the hole in the surface of the sample created by 20 impulses of water is recorded. The hole depth is compared to an erosion chart to determine the erodibility category of the soil. This erosion category allows the engineer to make preliminary decisions in erosion related work.

Many different options were considered during the development of the Pocket Erodometer including the most appropriate device, velocity range, direction of application, distance from the face of the sample, and repeatability from one person to another. The actual device chosen for the Pocket Erodometer measures 105 mm by 77 mm by 18 mm, has a nozzle velocity of approximately 8 m/s, and a nozzle hole diameter of approximately 0.5 mm. This velocity was selected because it showed measureable and varied erosion depths for a number of different soil samples, while keeping most of the sample intact for further testing.

It was important to obtain the nozzle exit velocity of each device tested during the development of the Pocket Erodometer. Figure 5 shows the calibration set up. The Pocket Erodometer is placed at a chosen height (around 1 m), aimed horizontally, and a water impulse is imparted. The particle motion equations are used:

$$x = v_{0x} t \tag{5}$$

$$H = \frac{1}{2} g t^2 \tag{6}$$

where x and H are defined on Figure 4, v_{0x} is the horizontal nozzle velocity, t is the time and g is the gravity acceleration. Eliminating t between Eq. (5) and (6) gives:

$$v_{0x} = \frac{x}{\sqrt{\frac{2H}{g}}} \tag{7}$$

This procedure gives a reproducible determination of the nozzle velocity. The calibration can be run inside or outside, but variables such as wind which are neglected in the equations can affect the results. A table or other stable object can be used as a base for the Pocket Erodometer so that *H* is well known and constant throughout the calibration process. The Pocket Erodometer should be placed on the table and pointed in such a way that the water jet initially travels horizontally. The operator should squeeze the trigger 20 times at a rate of 1 squeeze per second. Because the water stream is not a single particle there will be some scatter in how far the water travels horizontally before hitting the ground (Figure 4). A mark should be made at the two ends of the majority of the water on the floor surface. The extreme outliers should be ignored. These end values of *x* should be averaged and used in Eq. (7).

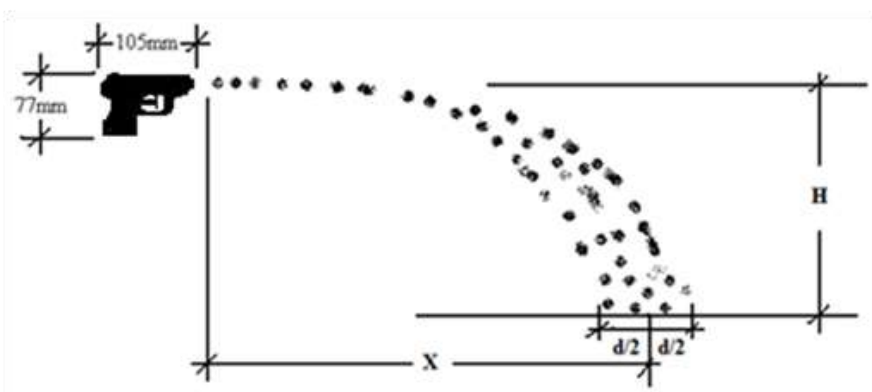

Figure 5 – Schematic of calibration dimensions.

To avoid having to plot the results from the PET in terms of erosion rate on the EFA erodibility chart while in the field, categories were developed based on the erosion depths for each PET. Figure 6 shows the PET depth ranges overlaid on the EFA erosion category chart. Each PET range corresponds to the category in which the EFA erosion function would lie.

The recommendations in Figure 6 are based on a limited number of PETs and should be used with caution until further tests are performed to corroborate these early results. It should be noted that, unlike the EFA erosion chart shown in Figure 5, the PET erosion chart (Figure 6) only contains five categories. The PET is not suitable for rock erosion testing. Soils exhibiting no noticeable erosion using the Pocket Erodometer should be further distinguished by testing them in the EFA or other appropriate erosion device.

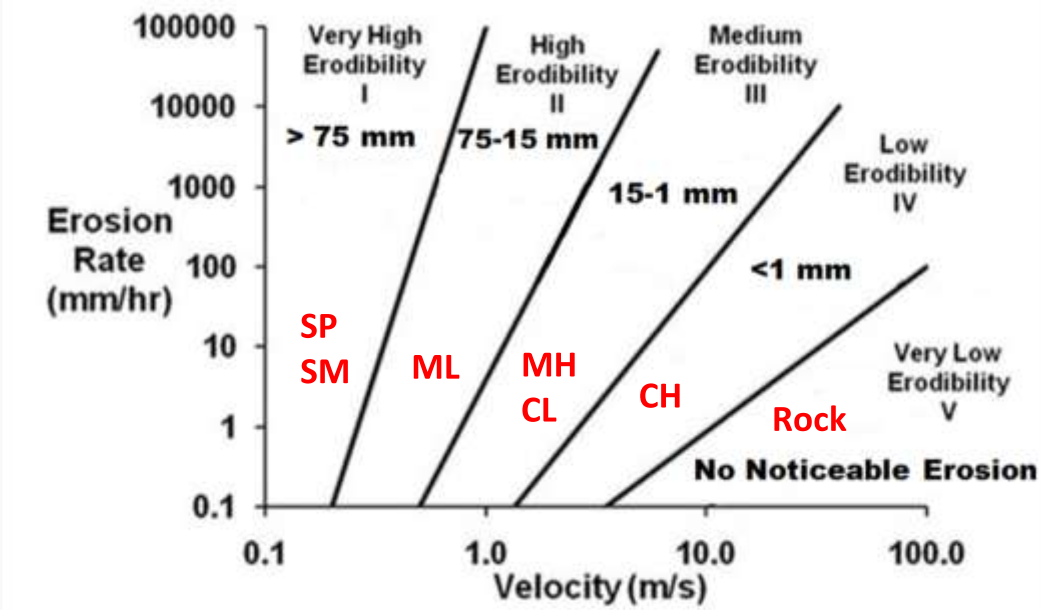

Figure 6 – PET erosion depth ranges shown on EFA categories.

It is recommended that the calibration steps be taken before beginning each testing session to ensure a nozzle velocity of $8m/s \pm 0.5m/s$ for each test. The device should have a nozzle aperture of approximately 0.5 mm and an impulse duration of 0.1s for each squeeze. If using a continuous device with the specified nozzle aperture and velocity, it should be run for 2 s for each PET. The procedure of standard Pocket Erodometer (PE) is:

1. Place the sample horizontally either on a flat surface or by holding it in your hand. Note: The test cannot be run with the jet pointed vertically.
2. Smooth the surface to remove any uneven soil. You want to begin with a smooth and vertical surface, so that it is easy to measure the erosion depth.
3. Hold the Pocket Erodometer (PE) pointed at the smooth end of the sample, 50 mm away from the face.
4. Keeping the jet of water from the PE aimed horizontally at a constant location, squeeze the trigger 20 times at a rate of 1 squeeze per second, forming an indentation in the

surface of the sample. Each squeeze should fully compress the trigger and then the trigger should be fully released before it is re-compressed.

5. Using the end of a digital caliper or an appropriate measuring tool, measure the depth of the hole created.

6. The test should be repeated at least 3 times in different locations across the face of the sample and an average should be used to ensure a good estimate.

7. Determine the erosion category using Figure 6.

MULTI-FLOOD AND MULTI-LAYER ANALYSIS

The SRICOS method was developed with consideration of multi-flood and multi-layer system to apply it to actual cases of scour. The multi-flood system and multi-layer system were studied by Kwak (Kwak, 2000), and they are summarized as:

Multi-flood analysis

The hydrograph of a river indicates how the velocity varies with time. The fundamental basis of the accumulation algorithms is that the velocity histogram is a step function with a constant velocity value for each time step. For example, a flood followed by bigger flood in a uniform soil is assumed (Figure 7). The flood 1 lasting a time t_1, with a velocity V_1, and a flood 2 lasting time t_2 with a velocity V_2 are assumed. A scour depth $y_{s1}(t)$ is reached at time t_1 (Point A on Figure 7 (b)) after the flood 1, and then a scour depth $y_{s2}(t)$ is reached at time t_1 (Point B on Figure 7 (c)). These scour depths $y_{s1}(t)$ and $y_{s2}(t)$ can be calculated by equation (8) and (9).

$$y_{s1}(t) = \frac{t_1}{\frac{1}{\dot{z}_{i1}} + \frac{t_1}{y_{s1}}} \tag{8}$$

$$y_{s2}(t) = \frac{t_2}{\frac{1}{\dot{z}_{i2}} + \frac{t_2}{y_{s2}}} \tag{9}$$

The scour depth $y_{s1}(t)$ also could have been created by flood 2 in a time t_e The time t_e is called the equivalent time, and equation (10) can be obtained by using equations (8) and (9) with assumption of $y_{s1}(t) = y_{s2}(t)$.

$$t_e = \frac{t_1}{\frac{\dot{z}_{i2}}{\dot{z}_{i1}} + t_1 \dot{z}_{i2} \left(\frac{1}{y_{s1}} - \frac{1}{y_{s2}} \right)} \tag{10}$$

When flood 2 starts, even though $y_{s1}(t)$ was occurred by flood 1 during t_1, $y_{s1}(t)$ is equivalent to $y_{s2}(t)$ by flood 2 during the equivalent time t_e. Therefore, y_s vs. t curve proceeds from point B on Figure 7 (c) to point C after t_1. The y_s vs. t curve for the sequent flood 1 and 2 follows the path OA on the curve during flood 1, and then switches to BC on the curve during flood 2. This is shown as the curve OAC on Figure 7 (d).

In opposite case in which a flood is followed by a smaller flood, if $y_{s1}(t)$ is bigger than y_{s2}, a smaller flood cannot develop any additional scour.

In the general case, the complete velocity hydrograph is divided into a series of partial flood events lasting Δt. The scour depth due to sequent floods in the hydrograph will be handled by following the procedure in Figure 7 (d).

Multi-layer analysis

In the multi-flood analysis, the soil is assumed to be uniform. Whereas, in reality, the soil involves different layers and the layer characteristics can vary significantly with depth. Therefore, it is required to have an accumulation process which can handle the case of multi-layer. The SRICOS method handles this problem by assuming that a flow with constant velocity of V develops scour on the channel bottom consisted with the first layer with a thickness of Δy_1 and a second layer with a thickness of Δy_2 (Figure 8 (a)). The y_s vs. t curves for layer 1 and layer 2 are given by equations (8) and (9) (Figure 8 (b), Figure 8 (c)). If y_{s1} exceeds the thicknessΔy_1, then layer 2 will also be involved in the scour process. In this case, the scour depth Δy_1 (point A on Figure 8 (b)) in layer 1 is reached after a time t_1, and it is equivalent to scour depth on layer 2 during equivalent time t_e (point B on Figure 8 (c)). Therefore, when layer 2 starts to be eroded, the y_s vs. t curve proceeds from point B to point C on Figure 8 (c). The combined scour process for the two-layer system corresponds to the path OAC on Figure 8 (d).

In reality, there may be a series of soil layers with different erosion functions. The computations proceed by stepping forward in time. The time steps are Δt long, the velocity is the one for the corresponding flood event, and the erosion function ($\dot{z}$ vs τ) is the one for the soil layer corresponding to the current scour depth (bottom of the scour hole). When Δt is such that the scour depth enters a new soil layer, the computations follow the process described in Figure 8 (d).

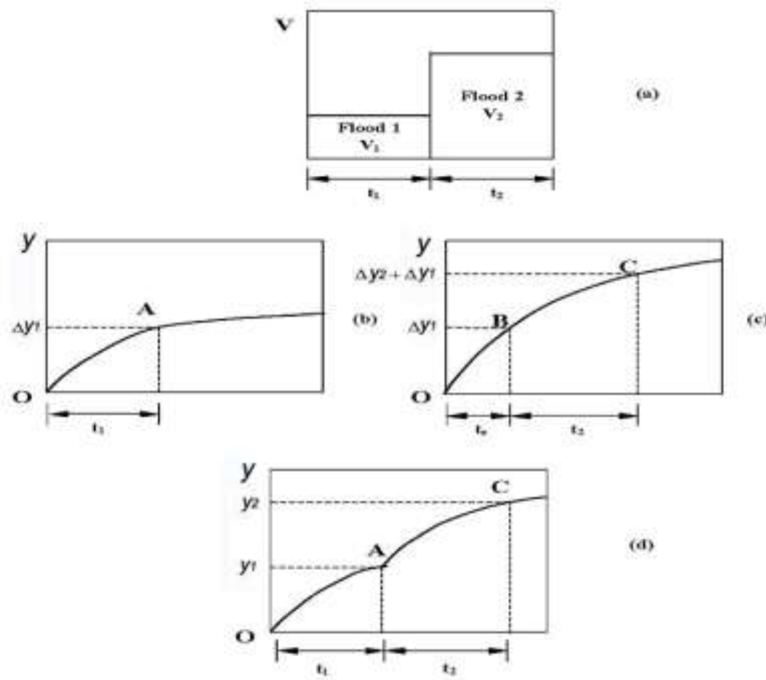

Figure 7 – Scour due to a sequence of two flood events.

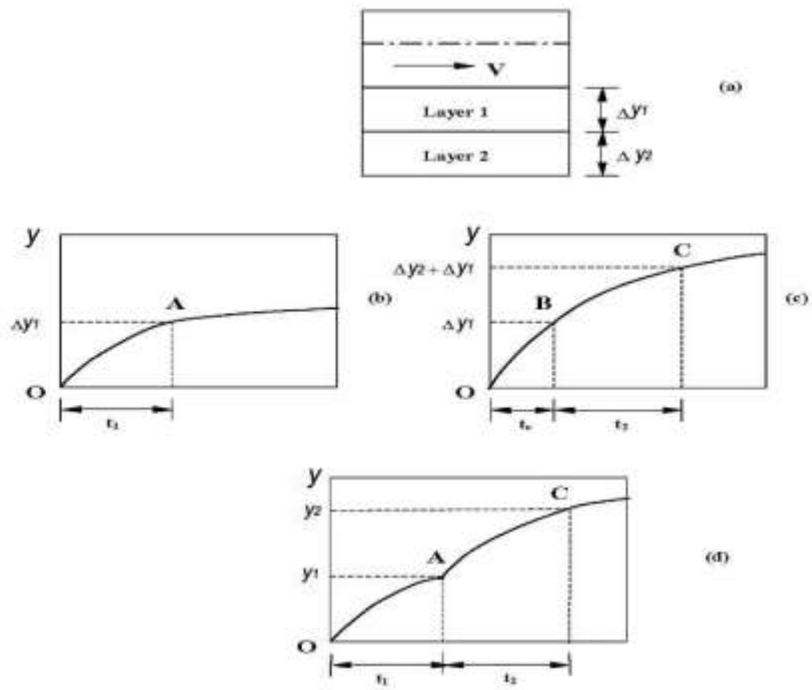

Figure 8 – Scour on multi-layers.

PIER SCOUR

Maximum scour depth

Gudavalli (Gudavalli, 1997) conducted 43 flume tests with 2 types of sand (D_{50} = 0.6 mm, 0.14 mm) and 3 types of clay (Porcelain, Armstone and Bentonite clay) in a deep water condition ($y_1 / a \geq 1.43$ where y_1 is the approach water depth and a is the pier diameter). A variable slope flume with a width of 0.45 m was used for experiments with 25 mm and 75 mm diameter piers, and a concrete flume with a width of 1.5 m was used for experiments with 25 mm, 75 mm, 150 mm and 210 mm diameter piers. Based on these flume tests, Gudavalli proposed the following equation.

$$y_{s(Pier)}(mm) = 0.18\left(\frac{aV_1}{\nu}\right)^{0.635} \tag{11}$$

where $y_{s(Pier)}$ is the maximum pier scour depth, a is the width of the pier, V_1 is the mean velocity at the location of the pier if the pier was not there, and ν is the kinematic viscosity of water (10^{-6}

m^2/s at 20 ℃)

Briaud and his coworkers (Briaud *et al.*, 2004) conducted a series of flume tests for complex pier scour with a Porcelain clay as channel bed material. Complex pier refers to the fact that the condition for the pier is more complex than a cylindrical pier in deep water. The complexity is brought about by shallow water, rectangular piers, attack angle, and other factors. The 1.5 m wide, 30.5 m long and 3.5 m deep concrete flume was used to conduct the complex pier scour tests. Correction factors for equation (11) were proposed as follows.

$$y_{s(Pier)}(mm) = 0.18 \cdot K_w \cdot K_{sp} \cdot \left(\frac{a'V}{v}\right)^{0.635} \qquad (12)$$

where a' is the projected pier width perpendicular to the flow for a rectangular pier, K_w is the correction factor for water depth effect, and K_{sp} is the correction factor for pier spacing.

The left term in equation (11) and (12) has the dimension of length, but the right term is dimensionless. In addition, these equations do not include the erosion resistance of the soil, and lead to the odd conclusions that for given geometric and flow conditions all soils scour to the same depth. One would expect that highly erosion resistant soils would lead to much smaller maximum scour depths than soils with low erosion resistance.

Oh (Oh, 2009; Oh *et al.*, 2011) re-analyzed databases obtained from of flume test results had been conducted at Texas A&M University (Briaud *et al.*, 2004; Gudavalli, 1997), and proposed equation (13) for the maximum complex pier scour depth after data analysis.

$$\frac{y_{s(Pier)}}{a'} = 2.2 \cdot K_w \cdot K_1 \cdot K_L \cdot K_{sp} \cdot \left(2.6 \cdot Fr_{(pier)} - Fr_{c(pier)}\right)^{0.7} \qquad (13)$$

where $Fr_{(pier)}$ is Froude number based on approach velocity and *a'*, $Fr_{c(pier)}$ is Froude number based on critical velocity, $y_{s(pier)}$ is the maximum complex pier scour depth and *a'* is the projected pier width. All correction factors for complex pier are following, and parameters are schematized in Figure 9

$$K_w = \begin{cases} 0.89\left(\dfrac{y_1}{a'}\right)^{0.33} & , \text{for } \dfrac{y_1}{a'} < 1.43 \\ 1.0 & , \text{else} \end{cases} \qquad K_{sp} = \begin{cases} 2.9\left(\dfrac{S}{a'}\right)^{-0.91} & , \text{for } \dfrac{S}{a'} < 3.42 \\ 1.0 & , \text{else} \end{cases}$$

$$K_L = 1.0, \quad \text{for whole range of } L/a \qquad K_1 = \text{value in Table 1}$$

$$Fr_{(pier)}\left(= \frac{V_1}{\sqrt{g \cdot a'}} \right), \quad Fr_{c(pier)} = \frac{V_c}{\sqrt{g \cdot a'}}, \quad a' = a\left(\cos\theta + \frac{L}{a} \cdot \sin\theta \right)$$

Table 1 - Correction factor for pier nose shape (K_1) (Richardson *et al.*, 2001)

Shape of pier nose	K_1	Shape of pier nose	K_1
Square nose	1.1	Circular cylinder	1.0
Round nose	1.0	Sharp nose	0.9

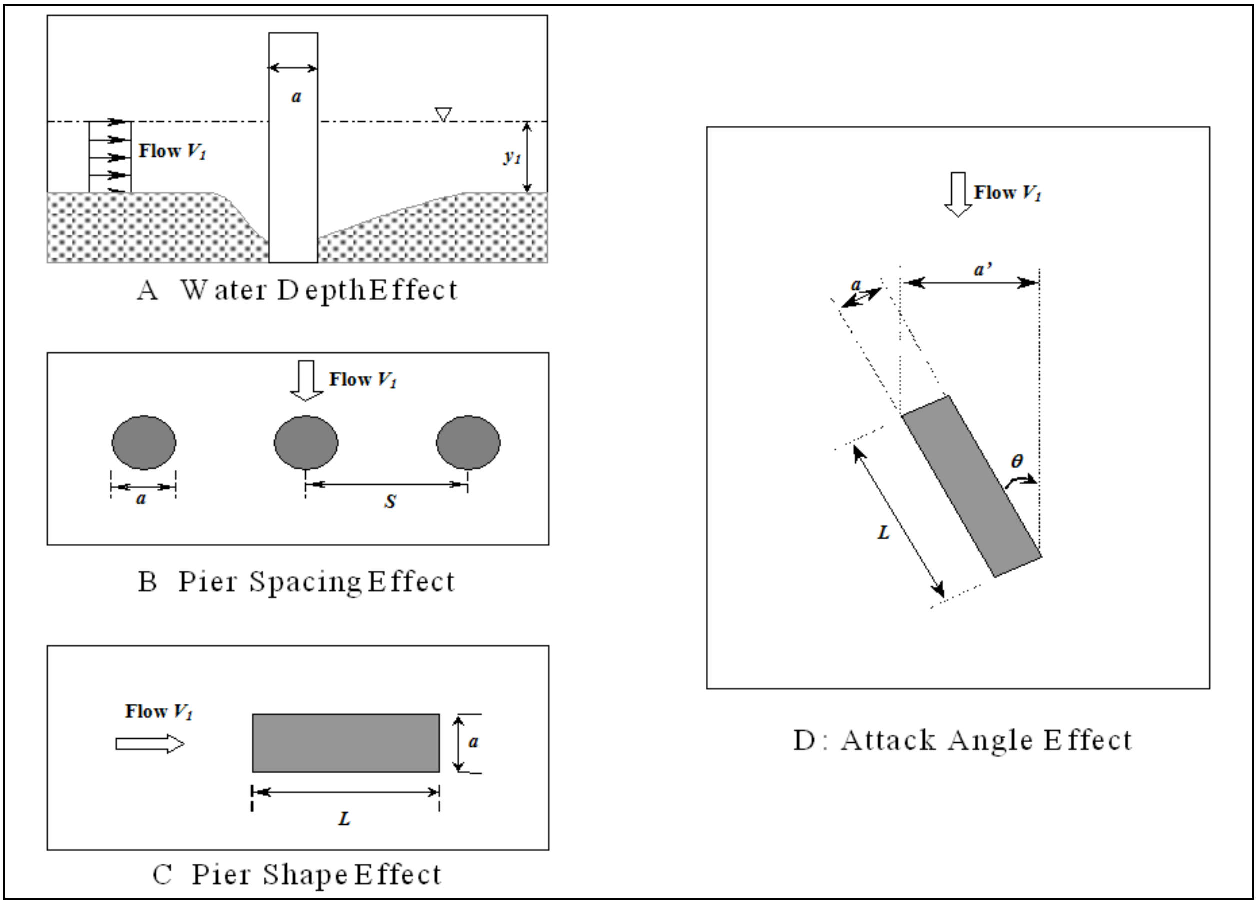

Figure 9 – Schematic definition of pier parameters.

Maximum shear stress around pier

Nurtjahyo (Nurtjahyo, 2003) conducted a series of 3D numerical simulation by varying water depth, pier spacing, pier shape, and attack angle, and found several correction factors applicable to the maximum shear stress equation for single circular pier in deepwater condition (Wei *et al.*, 1997), for shallow water depth effect, pier spacing effect, pier shape effect and attack angle effect. Then equation (14) for the maximum shear stress occurring around pier in complex condition was developed.

$$\tau_{\max(pier)} = k_w k_{sh} k_{sp} k_\theta \cdot 0.094 \rho V_1^2 \left[\frac{1}{\log \mathrm{Re}} - \frac{1}{10} \right] \tag{14}$$

$$k_w = 1 + 16 \exp\left(-4y/a\right) \qquad k_{sh} = 1.15 + 7\exp\left(-4L/a\right)$$

$$k_\theta = 1 + 1.5\left(\theta/90\right)^{0.57} \qquad k_{sp} = 1 + 5\exp\left(-1.1S/a\right)$$

where k_w, is the correction factor for water depth, k_{sp}, is the correction factor for pier spacing, k_{sh}, is the correction factor for pier shape, k_θ. is the correction factor for attack angle. All parameters are schematized in Figure 9

CONTRACTION SCOUR

Maximum and uniform contraction scour depth

Li (Li, 2002) and Oh (Oh, 2009) found that the normalized contraction scour depth by the water depth was linearly dependent on the difference of Froude number, and was irrelevant to the contraction length and shape after data regression. The prediction equation of the maximum contraction scour depth and the uniform contraction scour depth for both rectangular channel and compound channel can be expressed as equation (15) and (16), respectively.

$$\frac{y_{s(Cont)}}{y_{m1}} = 1.27\left(1.83 Fr_{m2} - Fr_{mc}\right) \tag{15}$$

$$\frac{y_{s(uni\_Cont)}}{y_{m1}} = 0.94\left(1.83 Fr_{m2} - Fr_{mc}\right) \tag{16}$$

where $y_{s(Cont)}$ is the maximum contraction scour depth, $y_{s(uni\_Cont)}$ is the uniform contraction scour depth, y_{m1} is the main channel depth at the approach section, $Fr_{m2}\left(=\dfrac{V_1/C_R}{\sqrt{gy_{m1}}}\right)$ is Froude number of the main channel at bridge section, $C_R\left(=\left(Q-Q_{block}\right)/Q\right)$ is contraction ratio, $Fr_{mc}\left(=\dfrac{V_{mc}}{\sqrt{gy_{m1}}}=\dfrac{\sqrt{\tau_c/\rho}}{gny_{m1}^{1/3}}\right)$ is the critical Froude number on the main channel at bridge section, Q is the total discharge, Q_{block} is the discharge blocked by approach embankment

Note that equation (15) and (16) do not include correction factor for the contraction transition angle because the transition angle cannot change the uniform flow velocity although it can affect the local velocity pattern around the end of abutment or contraction inlet. However, the transition angle impacts on the location of the maximum contraction scour: the smoother transition move the location to the farther downstream.

Maximum shear stress of contraction

Nurtjahyo (Nurtjahyo, 2003) studied the maximum shear stress of contraction by conducting another series of 3D numerical simulation, and proposed equation (17). Equation (17) was developed by correcting the maximum shear stress equation at the bottom of an open channel without contraction (Munson *et al.*, 1990).

$$\tau_{\max(Cont)}=k_R k_{Wa} k_\theta k_w \rho g n^2 V_1^2 R_h^{-\frac{1}{3}} \tag{17}$$

$$k_R=0.62+0.38\left(A_1/A_2\right)^{1.75} \qquad k_\theta=1.0+0.9\left(\theta/90\right)^{1.5}$$

$$k_{Wa}=\begin{cases}0.77+1.36\left(\dfrac{W_a}{L_1-L_2}\right)-1.98\left(\dfrac{W_a}{L_1-L_2}\right)^2, & \text{for } \dfrac{W_a}{L_1-L_2}\le 0.35\\ 1.0, & \text{otherwise}\end{cases}$$

where R_h is the hydraulic radius, θ is the transition angle (in degree), W_a is the top width of the abutment, A_1 is the channel area at approach section, A_2 is the channel area at bridge section, k_R is the correction factor for the contraction ratio, k_θ is the correction factor for the transition angle,

k_{Wa} is the correction factor for the contraction length, and k_w is the correction factor for the water depth and it is 1.0 for all conditions. The schematic definition for the calculation of both maximum scour depth and shear stress of contraction scour is shown in Figure 10.

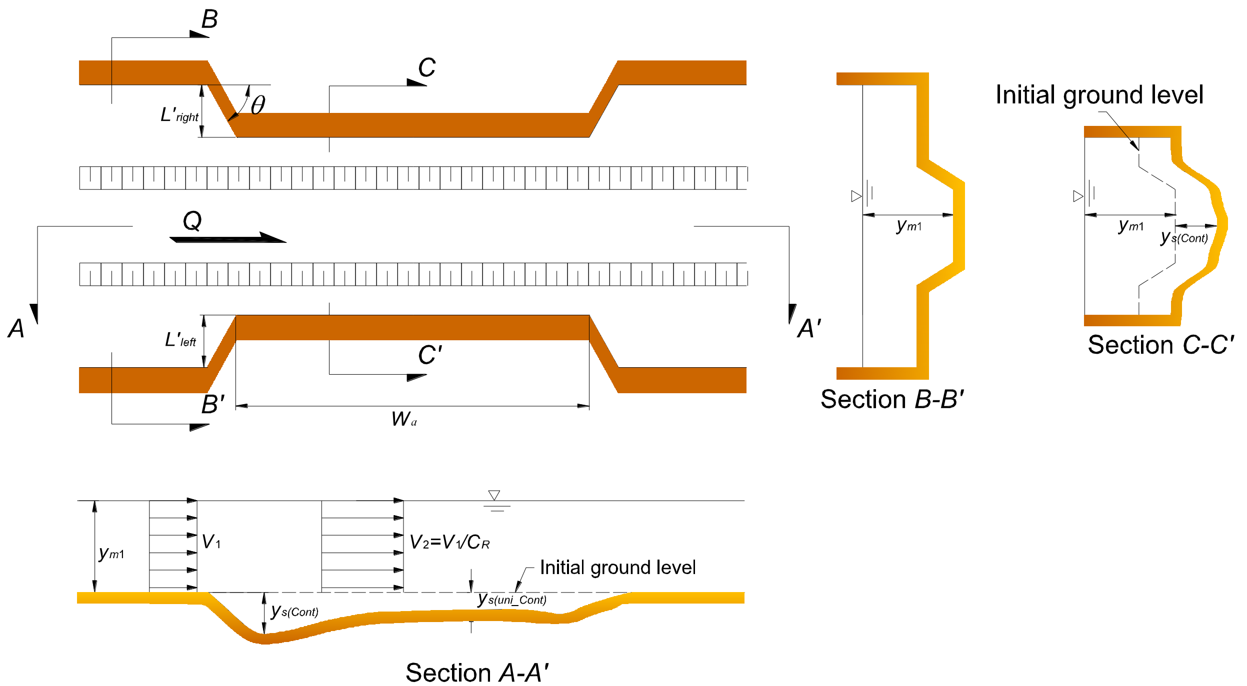

Figure 10 - Schematic definition of contraction scour parameters.

ABUTMENT SCOUR

Briaud and his coworkers conducted another research for abutment scour in fine grained soil. The equation to predict the maximum abutment scour depth was proposed after a series of flume tests, and the equation to predict the maximum shear stress around the toe of abutment was obtained after a series of 3 D numerical analyses.

Maximum abutment scour depth

The equation to predict the maximum abutment scour depth was proposed after data analysis obtained from flume results (Briaud *et al.*, 2009; Briaud and Oh, 2010). In their research, the hydraulic condition, the channel geometry, the shape of abutment, the length of abutment and the abutment alignment were varied to simulate possible conditions which should be considered for bridge design. Although a large size flume was used for lab tests, it was impossible to simulate long setback condition - short abutment on very wide floodplain. In order to consider all possible field conditions, the approach used in Maryland SHA Bridge Scour Program (ABSCOUR, 2007) was adopted to calculate the local velocity around the abutment. The method for converting the hydraulic data to the local velocity is detailed in equation (18). The definition of degree of setback is illustrated in Figure 11. The equation (19) to predict the maximum abutment scour depth was proposed using the flume test results and local velocity obtained from equation (18).

$$V_{f2} = \begin{cases} \dfrac{0.5 \cdot Q}{A_2}, \text{ for short setback } \left((L_f - L') \le 5 y_{m1} \right) \\ \dfrac{Q_{fp1}}{A_{f2}}, \text{ for long setback } \left(L' \le 0.25 L_f \right) \\ \text{otherwise use a linearly interpolated velocity between} \\ \dfrac{0.5 \cdot Q}{A_2} \text{ for } (L_f - L') = 5 y_{m1} \text{ and } \dfrac{Q_{fp1}}{A_{f2}} \text{ for } L' = 0.25 L_f \end{cases} \tag{18}$$

where $0.5 \cdot Q$ is the total discharge of half channel $\left(0.5 \cdot Q_{m1} + Q_{fp1}\right)$, Q_{fp1} is the discharge on the floodplain at the approach section immediately upstream of the abutment, Q_{m1} is the discharge in the main channel at the same line with Q_{fp1}, A_2 is total flow area at the contracted section, A_{f2} is the flow area on the floodplain at the contracted section, L_f is the width of floodplain, L' is the length of abutment

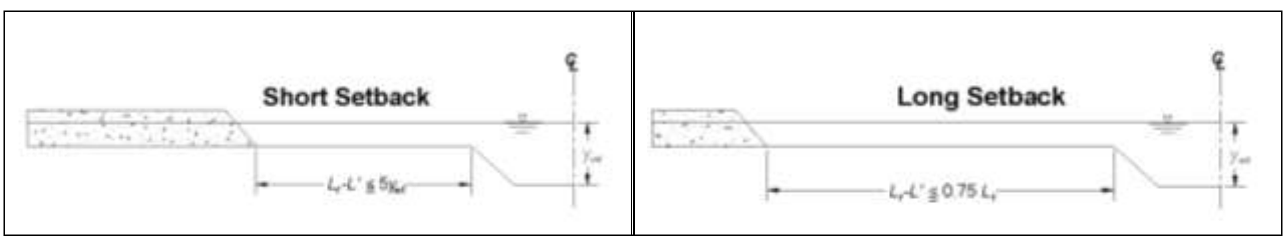

Figure 11 – Definition of degree of setback.

$$\begin{aligned} \frac{y_{s(Abut)}}{y_{f1}} &= K_1 \cdot K_2 \cdot K_L \cdot K_G \cdot K_p \cdot K_{\mathrm{Re}} \cdot 7.94 \cdot \left(1.65 \cdot Fr_{f2} - Fr_{fc}\right) \\ &= K_1 \cdot K_2 \cdot K_L \cdot K_G \cdot K_p \cdot 243 \cdot \mathrm{Re}_{f2}^{-0.28} \cdot \left(1.65 \cdot Fr_{f2} - Fr_{fc}\right) \end{aligned} \tag{19}$$

$$K_1 = \begin{cases} 1.22 & \text{for vertical-wall abutment} \\ 1.0 & \text{for wing-wall abutment} \\ 0.73 & \text{for spill-through abutment with 2:1 Slope} \\ 0.59 & \text{for spill-through abutment with 3:1 Slope} \end{cases}$$

$$K_2 = \begin{cases} 1.0 - 0.005\left|\theta - 90°\right| & \text{for } 60° \le \theta \le 120° \\ 0.85 & \text{otherwise} \end{cases}$$

$$K_G = \begin{cases} 1.0 & \text{for compound channel} \\ 0.42 & \text{for rectangular channel} \end{cases}$$

$$K_L = \begin{cases} -0.23\dfrac{L_f - L'}{y_{f1}} + 1.35 & \text{for } \dfrac{L_f - L'}{y_{f1}} < 1.5 \\ 1.0 & \text{otherwise} \end{cases}$$

$$K_p = \begin{cases} 0.92 \cdot \left(d_1 / d_{deck}\right) + 1.0 & \text{for } d_1 / d_{deck} < 1.0 \\ 0.21\left(d_1 / d_{deck}\right)^2 - 1.27\left(d_1 / d_{deck}\right) + 2.97 & \text{for } 1.0 \le d_1 / d_{deck} \le 3.0 \\ 1.0 & \text{for } 3.0 < d_1 / d_{deck} \end{cases}$$

where K_1 is the correction factor for the abutment shape, K_2 is the correction factor for the abutment skew, K_G is the correction factor for the channel geometry, K_L is the correction factor for the abutment location, K_p is the correction factor for pressure flow, d_1 is the distance from water surface to the low chord of the bridge at upstream face of the bridge, h is the distance from the low chord of the bridge to the river bottom before scour starts, $Fr_{2(Abut)}\left(= \dfrac{V_{f2}}{\sqrt{g \cdot y_{f1}}}\right)$ is Froude number around the toe of abutment, $Fr_{fc}\left(= \dfrac{V_c}{\sqrt{g \cdot y_{f1}}}\right)$ is critical Froude number around the toe of abutment, ν is the kinematic viscosity of water ($10^{-6} m^2 / s$ at $20°C$), $\mathrm{Re}_{f2} = \left(\dfrac{V_{f2} \cdot y_{f1}}{\nu}\right)$ is Reynolds number around the toe of abutment.

Maximum shear stress around the toe of abutment

A series of 3 D numerical simulation for the study of the maximum shear stress around the toe of abutment was conducted, and equation (20) was proposed after data regression using simulation results (Briaud *et al.*, 2009; Chen, 2008).

$$\tau_{\max(Abut)} = 12.45 k_{Cr} k_{sh} k_{Fr} k_s k_{sk} k_L k_o \rho V_1^2 \,\mathrm{Re}^{-0.45} \tag{20}$$

$$k_{Cr} = 3.65\frac{q_2}{q_1} - 2.91 \qquad k_{sh} = 0.85 \times \left(\frac{L'}{W_a}\right)^{-0.24}$$

$$k_{Fr} = \begin{cases} 2.07Fr + 0.8 & \text{for } Fr > 0.1 \\ 1.0 & \text{for } Fr \leq 0.1 \end{cases} \qquad k_s = \begin{cases} 1.0 & \text{vertical-wall abutment} \\ 0.65 & \text{wing-wall abutment} \\ 0.58 & \text{spill-through abutment} \end{cases}$$

$$k_L = \begin{cases} 1.0 & \text{for } \left(L_f - L'\right)/y_f \leq -2 \\ 0.6(L_f - L')/y_f + 1.2 & \text{for } -2 < (L_f - L')/y_f \leq 0 \\ -1.2(L_f - L')/y_f + 1.2 & \text{for } 0 < (L_f - L')/y_f \leq 1 \\ 1.0 & \text{for } 1 \leq (L_f - L')/y_f \end{cases}$$

$$k_o = \begin{cases} 0.92 \cdot \left(d_1/d_{deck}\right) + 1.0 & \text{for } d_1/d_{deck} < 1.0 \\ 0.21\left(d_1/d_{deck}\right)^2 - 1.27\left(d_1/d_{deck}\right) + 2.97 & \text{for } 1.0 \leq d_1/d_{deck} \leq 3.0 \\ 1.0 & \text{for } 3.0 < d_1/d_{deck} \end{cases}$$

where $\mathrm{Re}\left(= V_1 W_a / \nu\right)$ is the Reynolds number defined with top width of the abutment, q_1 is the unit discharge at approach section, q_2 is the unit discharge at bridge section, d_1 is the distance from the water surface to the low chord of the bridge at upstream face of the bridge, d_{deck} is the thickness of the bridge deck, k_{sh} is the correction factor for the aspect ratio of the approach embankment, k_{Fr} is the correction factor for Froude number, k_s is the correction factor for abutment shape, $k_{sk}\left(=1.0\right)$ is the correction factor for abutment alignment, k_o is the correction factor for overtopping

Definitions for pressure flow in equation (19) and (20) are shown in Figure 13.

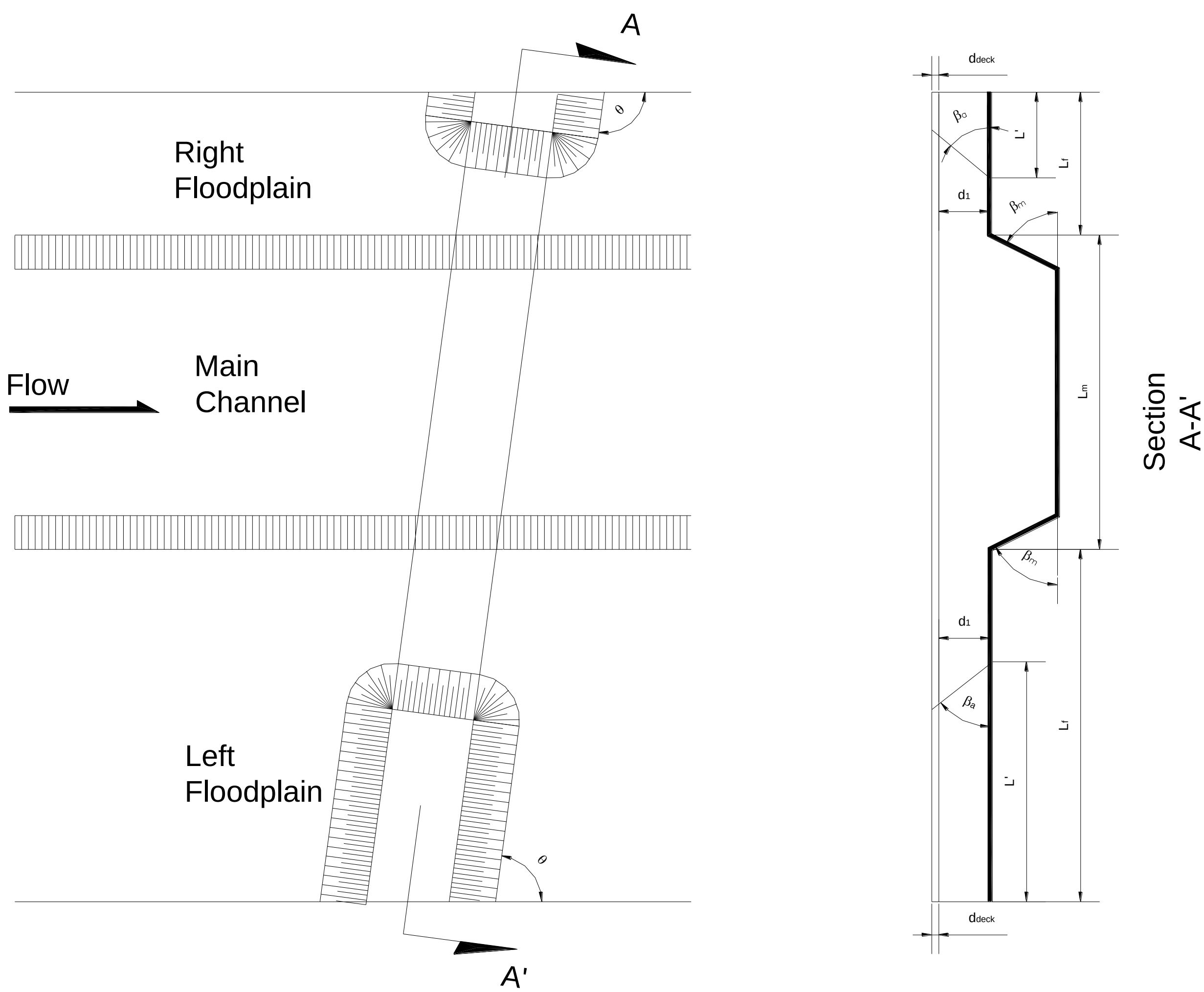

Figure 12 – Schematic definition of abutment scour parameters.

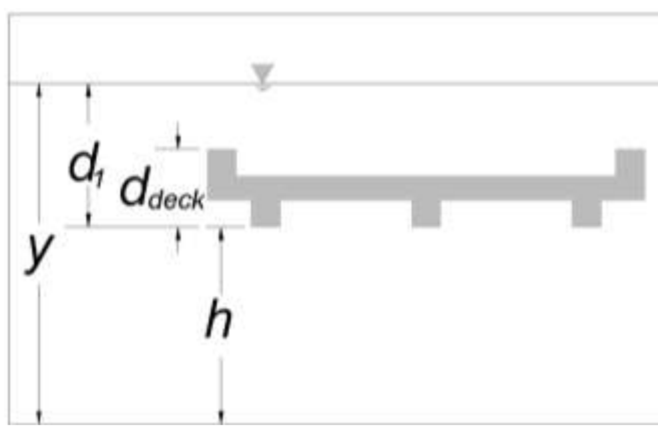

Figure 13 – Definitions for pressure flow near a bridge abutment.

EQUIVALENT TIME

The SRICOS-EFA computer program is required to predict the scour depth versus time curve as explained in the preceding section. An attempt was made to simplify the method to the point where only hand calculations would be needed. This requires the consideration of an equivalent uniform soil and an equivalent time for a constant velocity history. Studies to find the equivalent time were conducted by Kwak (Kwak, 2000) for pier scour and Wang (Wang, 2004) for contraction scour.

The equivalent uniform soil is characterized by an average $\dot{z}$ versus τ curve over the anticipated scour depth. The equivalent time t_{equiv} is the time required for the maximum velocity in the hydrograph to create the same scour depth as the one created by the complete hydrograph. The equivalent time t_{equiv} for pier scour was obtained for 55 cases generated from eight bridge sites, and for contraction scour was obtained for 28 cases generated from six bridge sites. For each bridge site, soil samples were collected in Shelby tubes and tested in the EFA to obtain the erosion function $\dot{z}$ versus τ curve, then the hydrograph was collected from the nearest gauge station and the SRICOS-EFA program was used to calculate the scour depth. The equivalent time equation for pier scour (Eq.(21)) and contraction scour (Eq.(22)) was obtained by multi-regression technique. The equivalent time for abutment scour will be prepared soon.

Pier scour

$$t_{equiv}\left(\text{hrs}\right) = 73\left(t_{hydro}\left(\text{years}\right)\right)^{0.126}\left(V_{\max}\left(\text{m/s}\right)\right)^{1.706}\left(\dot{z}_i\left(\text{mm/hr}\right)\right)^{-0.20} \qquad (21)$$

Contraction scour

$$t_{equiv}\left(\text{hrs}\right) = 644.32\cdot\left(t_{hydr}\left(\text{yrs}\right)\right)^{0.4242}\cdot\left(V_{\max}\left(\text{m}/\text{s}\right)\right)^{1.648}\cdot\left(\dot{z}_{i,mean}\left(\text{mm}/\text{hr}\right)\right)^{-0.605} \qquad (22)$$

where $t_{equiv}\left(\text{hrs}\right)$ = equivalent time necessary for the highest velocity in the hydrograph to create the same scour depth as the entire hydrograph, $t_{hydro}\left(\text{years}\right)$ = the duration of the hydrograph, $V_{\max}\left(\text{m/s}\right)$ = maximum velocity in the hydrograph, $\dot{z}_i\left(\text{mm/hr}\right)$ = initial rate of scour corresponding to the maximum velocity, $\dot{z}_{i,mean}\left(\text{mm/hr}\right)$ = mean initial rate of scour corresponding to the maximum velocity

FUTURE HYDROGRAPHS AND SCOUR RISK ANALYSIS

All methods mentioned above determines the scour depth by a given sequential daily discharge values. A methodology to prepare daily discharge was suggested based on the recorded previous hydrograph or Q_{100} and Q_{500} for the predictions of possible scour depth in future (Briaud *et al.*, 2007; Briaud *et al.*, 2003; Wang, 2004). A Monte Carlo procedure assuming that the hydrograph is modeled as a stochastic process is used in the methodology, and the methodology is consisted of followings.

Existing hydrograph method

The daily discharge, Q, is considered as a random, uncorrelated variable. A suitable distribution is fitted to the data and the hydrographs are then generated as series of values sampled from such a distribution. The theoretical distribution used to model daily discharge observations needs to be defined only for positive values of Q, to have a positive skewness, and to be able to provide an accurate representation of the extreme values (i.e. good fit at the upper tail of the distribution). The mean and standard deviation can be expressed as:

$$\mu_y = \frac{1}{2}\ln\left[\frac{{\mu_Q}^2}{1+\left(\frac{\sigma_Q}{\mu_Q}\right)^2}\right] \tag{23}$$

$$\sigma_y = \sqrt{\ln\left[1+\left(\frac{\sigma_Q}{\mu_Q}\right)^2\right]} \tag{24}$$

where μ_Q and σ_Q are the mean and the standard deviation of daily discharge, respectively.

The basic procedures of existing hydrograph approach are:

1. Calculate the mean μ_Q and standard deviation σ_Q of the daily stream flow values in existing hydrograph.

2. Calculate the log-normal mean μ_y and standard deviation σ_y of the daily stream flow values by using Eq. (23) and (24).

3. Q_f (future daily stream flow) is expressed as the exponential of a normally distributed random variable.

$$Q_f = \exp\left(\mu_y + \text{random} \times \sigma_y\right) \tag{25}$$

where random is random value from a normal distribution with μ =0 and σ =1

Q_{100} and Q_{500} method

If the Q_{100} and Q_{500} are known values, the parameters of the Lognormal Distribution (mean value and standard deviation) can be calculated using the conditions:

$$\text{P}\left[Q > Q_{100}\right] = 0.01\left(\text{per year}\right) = 1/36500 \ \left(\text{per day}\right) \tag{26}$$

$$\text{P}\left[Q > Q_{500}\right] = 0.002\left(\text{per year}\right) = 1/182500 \ \left(\text{per day}\right) \tag{27}$$

where $\text{P}\left[Q > Q_{100}\right]$ and $\text{P}\left[Q > Q_{500}\right]$ are the probabilities that the daily flow will be larger than Q_{100} and Q_{500} respectively.

The values of $\text{P}\left[Q > Q_{100}\right]$ and $\text{P}\left[Q > Q_{500}\right]$ are given by the cumulative density function (CDF) of the lognormal distribution of Q evaluated at Q_{100} and Q_{500}.

$$\text{P}(Q > Q_{100}) = 1 - \frac{1}{\sigma\sqrt{2\pi}} \int_0^{Q_{100}} \frac{1}{Q} e^{\frac{-(\ln Q - \mu_y)^2}{2\sigma_y^{\,2}}} dQ = \frac{1}{2} - \frac{1}{2} erf\left(\frac{\ln Q_{100} - \mu_y}{\sqrt{2}\sigma_y}\right) \tag{28}$$

$$\text{P}(Q > Q_{500}) = 1 - \frac{1}{\sigma\sqrt{2\pi}} \int_0^{Q_{500}} \frac{1}{Q} e^{\frac{-(\ln Q - \mu_y)^2}{2\sigma_y^{\,2}}} dQ = \frac{1}{2} - \frac{1}{2} erf\left(\frac{\ln Q_{500} - \mu_y}{\sqrt{2}\sigma_y}\right) \tag{29}$$

where *erf*(*z*) is the error function (WolframMathworld, 2007). The only unknowns in Equations

(28) and (29) are μ_y and σ_y. Therefore, Q_f (future daily discharge) is expressed as Eq. (25): the exponential of a normally distributed random variable.

The Q_{100} or Q_{500} can be obtained by using the hydrograph, and Briaud (Briaud, 2008) suggested to use one simple graphical method (e.g., (Chow *et al.*, 1988)). The procedure of this method is:

1. Obtain the yearly maximum flows from the hydrograph.
2. Rank them in descending order of intensity.
3. Calculate for each flow the probability of exceedance as the rank divided by the total number of observations + 1.
4. Plot the flow versus the probability of exceedance on a semi-log paper such as the one of Figure 14.

Once the data is plotted, a linear regression is performed over 30 years of data and extrapolated to the 0.01 probability of exceedance for the 100 year flood and to the 0.002 probability of exceedance for the 500 year flood. Indeed the return period is the inverse of the probability of exceedance. There are other and more refined ways of obtaining these design floods but this simple graphical method helps understand the process and the meaning of the 100 year flood: a flood which has a 1% chance of being exceeded in any one year.

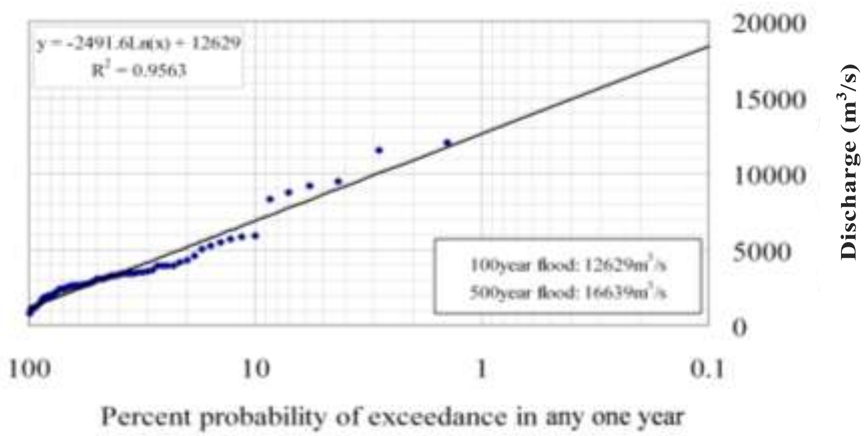

Figure 14 – Flood frequency curve obtained from measured discharge hydrograph. (Briaud *et al.*, 2003)

The probability of exceedance, R, of the design flood with a given return period T_r depends on the design life L_t of a structure.

$$R = 1 - \left(1 - 1/T_r\right)^{L_t} \tag{30}$$

If the design life of the bridge is 75 years, the probability that the flood with a return period of 100 year will be exceeded during the 75 year design life is 53% according to equation (30) and that probability is 14% for the 500 year flood. Only when one gets to the 10,000 year flood does the probability get to be lower than 1% (0.75%). Therefore looking at those numbers alone, it seems desirable to use the 10,000 year flood for design purposes. This flood is used in design in the Netherlands for regions of the country deemed critical. The USA uses the 100 and 500 year flood for design purposes in hydraulic engineering; this leads to probabilities of exceedance which are in the tens of percent. By comparison, the structural engineers use a probability of exceedance of about 0.1% for the design of bridge beams (LRFD target), and judging from measured vs. predicted pile capacity data bases (Briaud, Tucker, 1988) the geotechnical engineer uses a probability of exceedance of the order of a few percent. While these numbers can be debated, it is relatively clear that these different fields of civil engineering operate at vastly different probability of exceedance levels. There is a need to document these different levels, agree on a target level, and then operate at that common level. Note that risk is associated with the product of the probability of occurrence and the value of the consequence. As such, the probability of exceedance target should vary with the consequence of the failure.

VERIFICATION

Although the SRICOS-EFA method was developed to predict the scour depth in fine-grained soil, it also can be used for coarse-grained soil due to the consideration of soil property and time effect. The maximum scour depth in coarse-grained soils can be reached in several days, while several days may generate only some portions of the maximum scour depth in fine-grained soil because of its slow erosion rate. Therefore calculation of the maximum scour depth without the consideration of the time effect may be reasonable in coarse-grained soils, meanwhile the effect of time should be considered in scour depth calculation in fine-grained soils.

Predictions by the SRICOS-EFA method are compared to measurements in other previous studies for the validation of the method. For scour depth calculations, the database should include hydraulic data (flow velocity and depth), channel and bridge data, and soil data (critical shear stress for coarse-grained soil, and both critical shear stress and erosion function for fine-grained soil). Many databases for coarse-grained soils are collected from literature review for pier scour, contraction scour and abutment scour, but no database for fine-grained soil with sufficient information could be found. For the comparison with databases for coarse-grained soils, the critical shear stresses of soil and Manning's coefficient *n* of channel bottom in Eq. (13) for the pier scour, in Eq. (16) for the contraction scour, and in Eq. (19) for the abutment scour were calculated by the Shields' relation (Shields, 1936) and Strikler's relation (Chow, 1959), respectively. The Shields' relation between the critical shear stress of the soil and the median soil particle size is given in equation (8), and Manning's coefficient in Stirikler's relation is given in equation (9).

$$\tau_c = \tau^* \left(\rho_s - \rho\right) g D_{50} \tag{31}$$

$$n = 0.013 D_{50}^{1/6} \geq 0.011 \tag{32}$$

where τ^* is Shields parameter, ρ_s is density of soil $\left(\approx 2650\ \mathrm{kg/m^3}\right)$, ρ is density of water at 20 ℃ $\left(=1000\ \mathrm{kg/m^3}\right)$, g is gravitational acceleration, D_{50} is median particle size of soil in the unit of m

PIER SCOUR

Predictions by Eq. (13) were also compared to full scale measurements from case histories. For scour depth calculations, the database should contain hydraulic data (water depth, flow velocity, and attack angle), pier data (pier width, pier length, and pier nose shape), and soil data (critical shear stress). Databases collected by Froehlich (Froehlich, 1988) and Muller and Lander (Muller and Landers, 1996) on coarse grained soils were obtained from literature reviews, but no fine grained soil database with sufficient information could be found. These two databases have very good pier data, average flow data, and very poor soil data including no critical shear stress and river bottom roughness.

The ranges of hydraulic and geotechnical characteristics in the two databases are summarized in Table 2, and Figure 15 shows the comparison of the predicted maximum pier scour depth to the field measurements in Froehlich (1988) and Muller and Lander (1996). Eq. (13) yields predictions once a factor of safety of 1.5 is applied which are conservative compared to the field measurements. These conservative predictions may result from the fact that the erosion rate may have been slow enough that the maximum scour depth was not reached.

Table 2 – Range of hydraulic and geotechnical characteristics in Froehlich (Froehlich, 1988) and (Muller and Landers, 1996).

Researched by	Range value	a (m)	L (m)	θ (^{o})	y_1 (m)	V_1 (m/s)	D_{50} (mm)	Measured $y_{s(Pier)}$ (m)
Froehlich (1988)	Minimum	*0.29*	*0.98*	*0*	*0.43*	*0.15*	*0.01*	*0.15*
	Median	*1.52*	*10.36*	*0*	*3*	*1.36*	*1.6*	*0.9*
	Maximum	*19.50*	*38*	*35*	*19.5*	*3.67*	*90*	*10.4*
	Average	*3.25*	*10.07*	*5.66*	*4.19*	*1.57*	*13.03*	*1.9*
Muller and Landers (1996)	Minimum	*0.29*	*2.44*	*0*	*0.12*	*0.15*	*0.17*	*0*
	Median	*0.98*	*10.36*	*0*	*3.40*	*1.13*	*0.97*	*0.59*
	Maximum	*4.27*	*27.43*	*43*	*12.62*	*4.08*	*108.00*	*7.65*
	Average	*1.15*	*10.46*	*4.29*	*4.09*	*1.31*	*14.2*	*0.81*

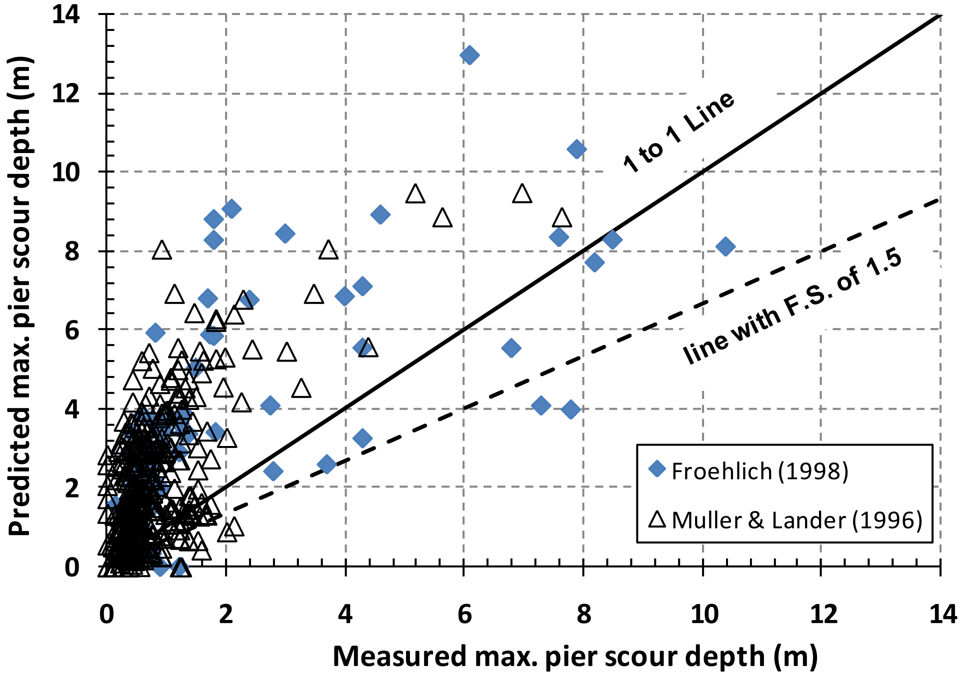

Figure 15 – Predicted maximum scour depth versus databases from Froehlich (1998) and Muller and Lander (1996).

CONTRACTION SCOUR

Databases for uniform contraction scour were obtained from flume test results in Komura (Komura, 1966), Gill (Gill, 1981), Webby (Webby, 1984) and Lim (Lim, 1993) through literature reviews. All flume tests were conducted in rectangular channels. The ranges of hydraulic and geotechnical characteristics in those databases are summarized in Table 3. The equation for uniform contraction scour depth (Eq. (16)) was used for the prediction because averaged contraction scour depths along the centerline of the channel were taken in those databases, and those are closed the uniform contraction scour depths rather than maximum contraction scour depths. The comparison with flume test measurements in these databases was made in Figure 16. In the figure, Eq. (16) yields good agreements, and a factor of safety of 1.5 ensures that all the measurements in these databases do not exceed the predictions.

Table 3 – Summary of hydraulic and geotechnical characteristics of previous flume test for contraction scour.

Researched by	D_{50} (mm)	V_1 (m/s)	y_1 (mm)	L_1 (m)	L_2 (m)	V_c (m/s)	Measured Scour Depth (mm)	Predicted Scour Depth (mm)
Komura (1966)	0.35 ~ 0.55	0.173 ~ 0.247	28 ~ 84	0.4	0.1 ~ 0.2	0.242 ~ 0.291	34 ~ 80	34 ~ 75
Gill (1981)	0.92 ~ 1.53	0.24 ~ 1.53	27 ~ 84	0.76	0.5	0.292 ~ 0.423	10 ~ 50	20 ~ 49
Webby (1984)	2.15	0.213 ~ 0.373	89 ~ 131	1.586	0.524	0.494 ~ 0.527	46 ~ 117	69 ~ 149
Lim (1993)	0.47	0.208 ~ 0.223	24 ~ 28	0.4	0.12 ~ 0.26	0.245 ~ 0.252	10 ~ 51	16 ~ 56

In Table 3, L_1 is channel width at approach section, L_2 is channel width at bridge section, V_1 is the average flow velocity at approach section, V_c is the critical velocity of riverbed material and equal to V_{mc} in rectangular channels, and y_1 is the water depth at approach section and equal to y_{m1} in rectangular channels

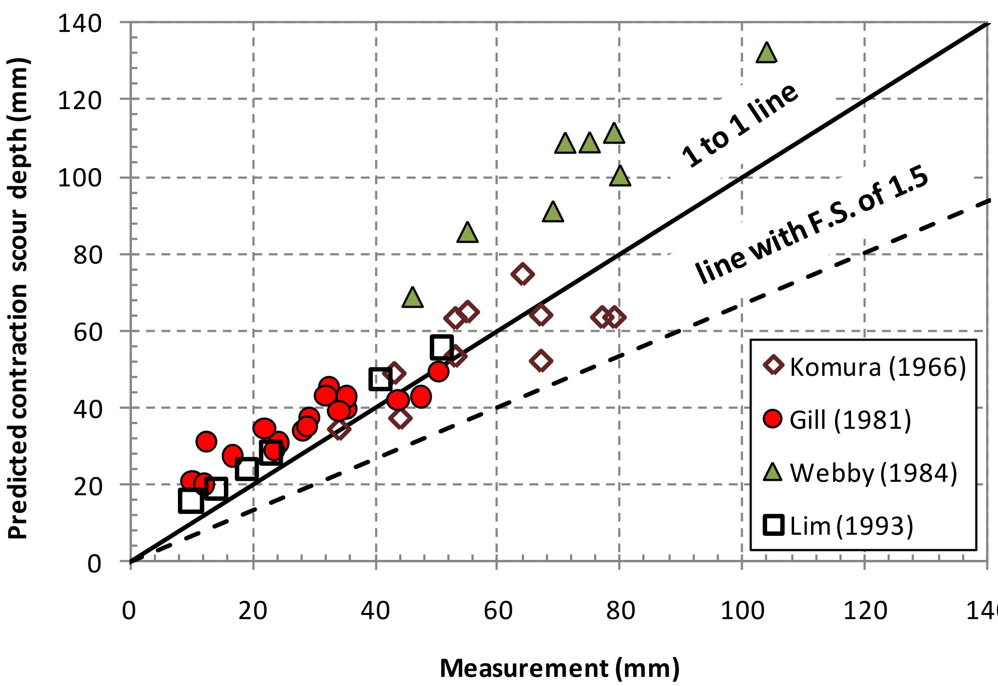

Figure 16 – Predicted uniform contraction scour depths vs. measured uniform contraction scour depths in previous researches.

ABUTMENT SCOUR

Three series of abutment scour databases from flume tests collected by Froehlich (Froehlich, 1989), Sturm (Sturm, 2004) and Ettema and his coworkers (Ettema *et al.*, 2008), and one series of field measurements in the Piedmont region of South Carolina by Benedict and Caldwell (Benedict and Caldwell, 2006) were obtained through literature review. Froehlich (Froehlich, 1989) collected and analyzed abutment scour measurements taken by other researchers in rectangular channels in different laboratory flumes. Sturm (Sturm, 2004) conducted flume tests in a compound channel using 3 different types of sand in 3 different setback conditions: three setback conditions are long setback $\left(L_f - L' > 5y_m\right)$, short setback $\left(L' \leq 0.25L_f\right)$ and intermediate setback. In Ettema *et al.* (Ettema *et al.*, 2008), eleven scour tests which have no erosion of embankment and erodible material in floodplain are selected among many flume measurements for the comparison because the test condition of the other tests is totally different with SRICOS-EFA method (e.g., floodplain made with concrete, embankment made with easily erodible material).

The ranges of hydraulic and geotechnical characteristics in those databases are summarized in Table 4. In order to find critical shear stress of riverbed materials, all types of soil were regarded as coarse-grained soils although some fine-grained soils were found in Benedict and Caldwell (2006). Note that the critical shear stress cannot be decided by D_{50} in fine-grained soils.

The measured scour depths in those databases are compared to the predicted scour depths by using the maximum abutment scour depth equation (Eq. (19)) in Figure 17 through Figure 20. Eq. (19) yields both under estimation and over estimation for databases in Froehlich (Froehlich, 1989) and Sturm (Sturm, 2004), mostly over estimation for field measurements in Benedict and Caldwell (Benedict and Caldwell, 2006), and good agreements with flume tests in Ettema *et al.* (Ettema *et al.*, 2008). The factor of safety of 1.5 seems to be required, and to be reasonable value by referring those comparisons although several measurements are underestimated.

In Figure 17, Figure 18 and Figure 19, S.T., W.W. and V.W represents spill-through abutment, wing-wall abutment and vertical-wall abutment, respectively. In Figure 18, Short, Inter and Long stands for short setback, intermediate setback and long setback, respectively. In Figure 20, Q_{100} represents the discharge in 100 year flood, and Historic data does the maximum historic discharge.

Table 4 – Summary of hydraulic and geotechnical characteristics of previous studies for abutment scour.

Researched by	Range Value	L' (m)	y_{f1} (m)	V_{f1} (m/s)	V_{f2} (m/s)	D_{50} (mm)	Measured $y_{s(Abut)}$ (m)	Predicted $y_{s(Abut)}$ (m)
Froehlich (1989)	Maximum	1.13	0.50	0.62	1.02	3.30	0.411	0.462
	Average	0.34	0.11	0.31	0.43	1.05	0.154	0.163
	Mininum	0.02	0.03	0.10	0.11	0.29	0.003	0.000
Sturm (2004)	Maximum	3.66	0.11	0.36	0.64	3.30	0.317	0.630
	Average	2.13	0.06	0.24	0.42	2.96	0.181	0.232
	Mininum	0.80	0.03	0.10	0.27	1.10	0.012	0.000
Benedict and Caldwell (2006)	Maximum	485.42	4.57	1.22	3.97	0.99	5.486	5.529
	Average	93.19	1.98	0.33	1.40	0.13	0.717	2.184
	Mininum	5.61	0.30	0.03	0.11	0.003	0.000	0.000
Ettema et al. (2008)	Maximum	2.76	0.15	0.33	1.03	0.45	0.370	0.616
	Average	1.68	0.15	0.33	0.61	0.45	0.282	0.298
	Mininum	0.56	0.15	0.33	0.38	0.45	0.170	0.136

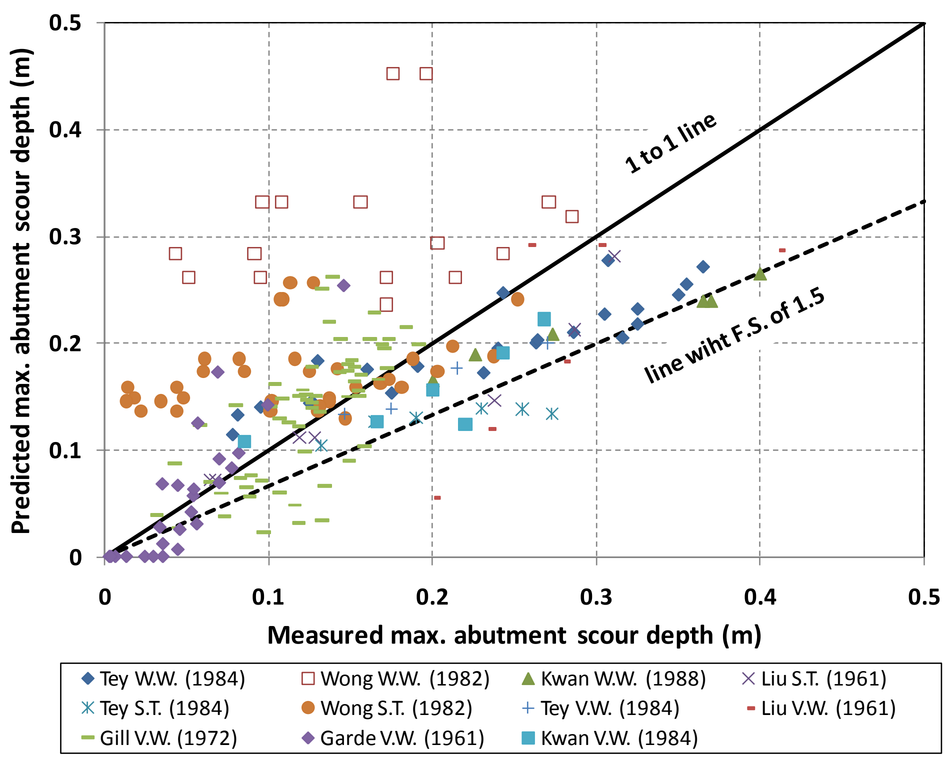

Figure 17 – Predicted maximum abutment scour depth vs. measured maximum abutment scour depth in Froehlich (1989).

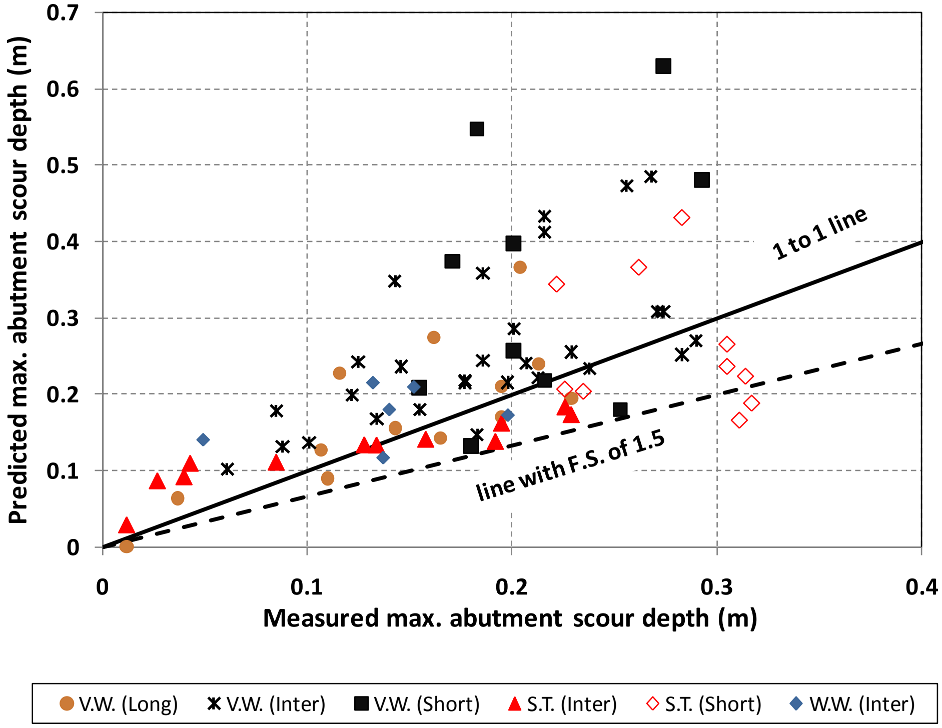

Figure 18 – Predicted maximum abutment scour depths vs. measured abutment scour depths in Sturm (2004).

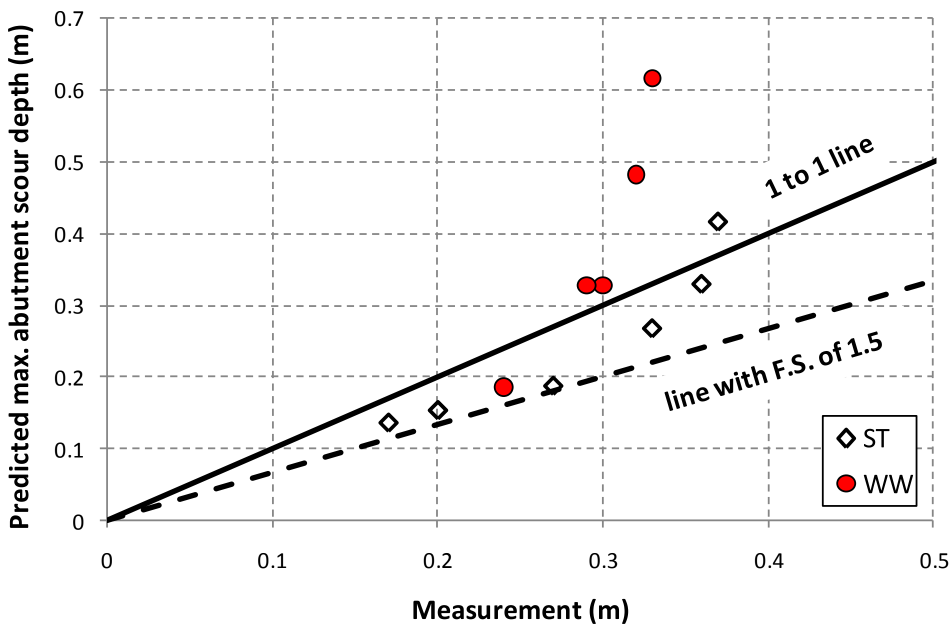

Figure 19 – Predicted maximum abutment scour depths vs. measured abutment scour depths in Ettema et al. (2008).

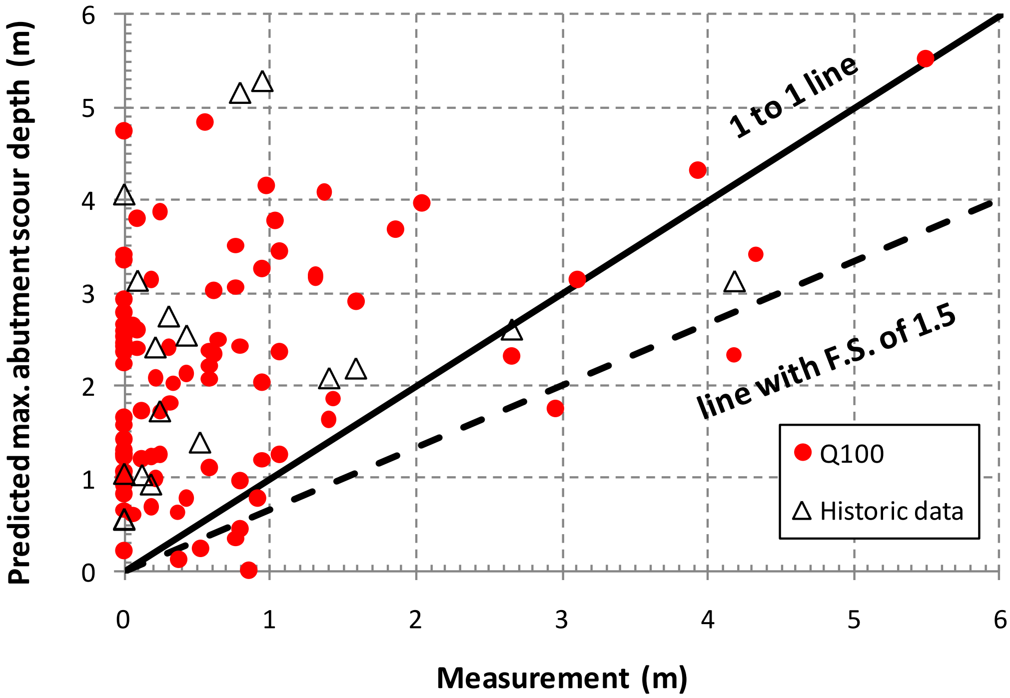

Figure 20 – Predicted maximum abutment scour depths vs. measured abutment scour depths in Benedict and Caldwell (2006).

Each prediction method was designed to makes the best agreement to the database which was used to develop the method, while it sometimes makes poor agreement to other databases. For the evaluation of each prediction method, 33 cases of imaginary full scale bridge conditions with geometries as shown in Figure 21 were made up to compare predictions by Eq. (19) to those by other previous methods. Three types of sand (D_{50} = 0.4 mm, 2.0 mm and 10 mm) were considered as riverbed material, and 1-D simulation results by HEC-RAS runs were used to obtain the flow velocities and water depths. The parameters in imaginary conditions are listed in Table 5, and comparisons with other previous methods are presented in Figure 22.

According to comparison in Figure 22, all prediction methods yield overestimated scour abutment scour depths compared to the scour depths by Eq. (19). The calculated abutment scour depths based on Maryland SHA Bridge Scour Program (ABSCOUR) (2007) agree well with those obtained by Eq. (19). Some prediction methods make big discrepancies with unreasonable abutment scour depths. From the comparison in Figure 22, it could be determined that Eq. (19)

yields reasonable abutment scour depths, although the predicted maximum abutment scour depths seem to be discrepant to measurements in Figure 17 through Figure 20.

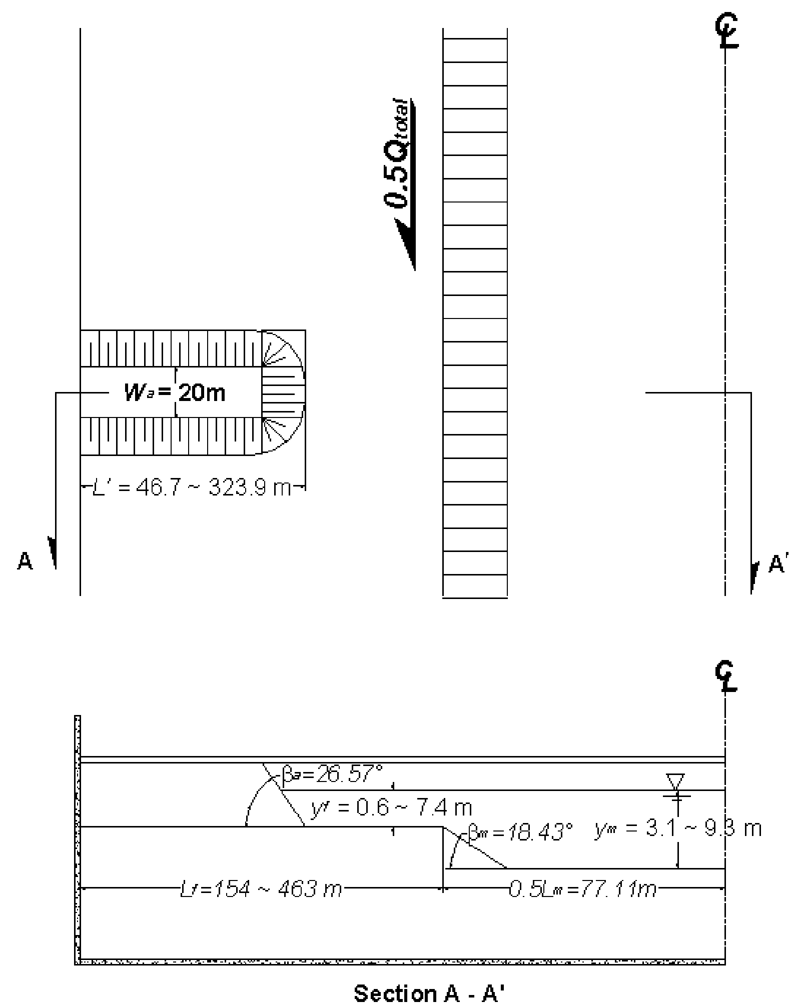

Figure 21 – Schematic diagram of imaginary full scale channel.

Table 5 – Summary of the imaginary condition for comparisons with other prediction methods for abutment scour depth.

Case No.	y_m (m)	y_f (m)	L_m (m)	L_f (m)	L' (m)	V_{f1} (m/s)	V_{m1} (m/s)	D_{50} (mm)	n	τ_c (Pa)	$0.5Q$ (m^3/s)	V_{fc} (m/s)	V_{max} (m/s)
1	3.08	0.62	77.11	154.23	46.69	0.17	0.46	0.4	0.011	0.364	122.29	0.51	0.48
2	3.08	0.62	77.11	154.23	46.69	0.21	0.58	2	0.015	1.006	155.51	0.65	0.61
3	3.08	0.62	77.11	154.23	46.69	0.41	1.10	10	0.019	6.164	294.42	1.22	1.15
4	9.25	1.85	77.11	154.23	46.69	0.23	0.56	0.4	0.011	0.364	415.74	0.60	0.59
5	9.25	1.85	77.11	154.23	46.69	0.29	0.71	2	0.015	1.006	528.67	0.77	0.75
6	9.25	1.85	77.11	154.23	46.69	0.54	1.35	10	0.019	6.164	1000.92	1.45	1.42
7	15.42	3.08	77.11	154.23	46.69	0.27	0.60	0.4	0.011	0.364	709.37	0.66	0.64
8	15.42	3.08	77.11	154.23	46.69	0.34	0.77	2	0.015	1.006	902.06	0.84	0.81
9	15.42	3.08	77.11	154.23	46.69	0.65	1.46	10	0.019	6.164	1707.86	1.58	1.55
10	3.08	0.62	77.11	154.23	107.96	0.17	0.47	0.4	0.011	0.364	122.29	0.50	0.51
11	3.08	0.62	77.11	154.23	107.96	0.21	0.58	2	0.015	1.006	155.51	0.64	0.64
12	3.08	0.62	77.11	154.23	107.96	0.40	1.13	10	0.019	6.164	294.42	1.21	1.25
13	9.25	1.85	77.11	154.23	107.96	0.23	0.56	0.4	0.011	0.364	415.74	0.60	0.63
14	9.25	1.85	77.11	154.23	107.96	0.29	0.71	2	0.015	1.006	528.67	0.77	0.8
15	9.25	1.85	77.11	154.23	107.96	0.54	1.35	10	0.019	6.164	1000.92	1.45	1.52
16	15.42	3.08	77.11	154.23	107.96	0.27	0.61	0.4	0.011	0.364	709.37	0.66	0.69
17	15.42	3.08	77.11	154.23	107.96	0.34	0.77	2	0.015	1.006	902.06	0.84	0.88
18	15.42	3.08	77.11	154.23	107.96	0.65	1.46	10	0.019	6.164	1707.86	1.58	1.67
19	9.25	1.85	77.11	154.23	154.23	0.23	0.56	0.4	0.011	0.364	415.74	0.60	0.66
20	9.25	1.85	77.11	154.23	154.23	0.29	0.71	2	0.015	1.006	528.67	0.77	0.84
21	9.25	1.85	77.11	154.23	154.23	0.54	1.35	10	0.019	6.164	1000.92	1.46	1.61
22	9.25	3.70	77.11	154.23	154.23	0.38	0.62	0.4	0.011	0.364	630.24	0.68	0.94
23	9.25	3.70	77.11	154.23	154.23	0.48	0.79	2	0.015	1.006	801.43	0.86	1.2
24	9.25	3.70	77.11	154.23	154.23	0.91	1.50	10	0.019	6.164	1517.34	1.63	2.31
25	9.25	7.40	77.11	154.23	154.23	0.55	0.61	0.4	0.011	0.364	1057.05	0.76	1.45
26	9.25	7.40	77.11	154.23	154.23	0.70	0.77	2	0.015	1.006	1344.18	0.97	1.85
27	9.25	7.40	77.11	154.23	154.23	1.32	1.46	10	0.019	6.164	2544.92	1.83	3.73
28	6.17	4.94	77.11	308.46	215.92	0.52	0.58	0.4	0.011	0.364	1065.71	0.71	1.21
29	6.17	4.94	77.11	308.46	215.92	0.66	0.74	2	0.015	1.006	1355.20	0.91	1.55
30	6.17	4.94	77.11	308.46	215.92	1.26	1.39	10	0.019	6.164	2565.77	1.71	3.11
31	9.25	7.40	77.11	462.69	323.88	0.56	0.61	0.4	0.011	0.364	2361.65	0.76	1.42
32	9.25	7.40	77.11	462.69	323.88	0.72	0.77	2	0.015	1.006	3003.16	0.97	1.82
33	9.25	7.40	77.11	462.69	323.88	1.36	1.46	10	0.019	6.164	5685.83	1.83	3.67

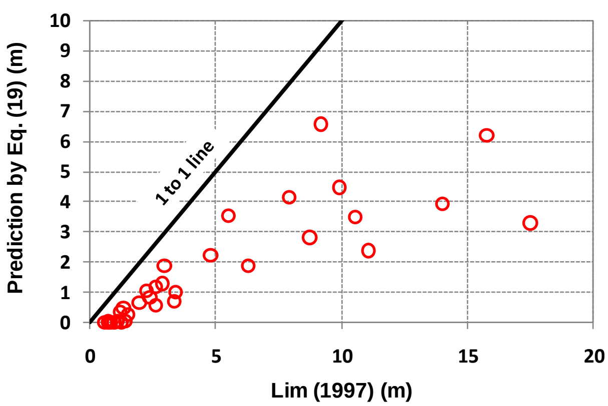

(a) Comparison with Lim's (1997) equation

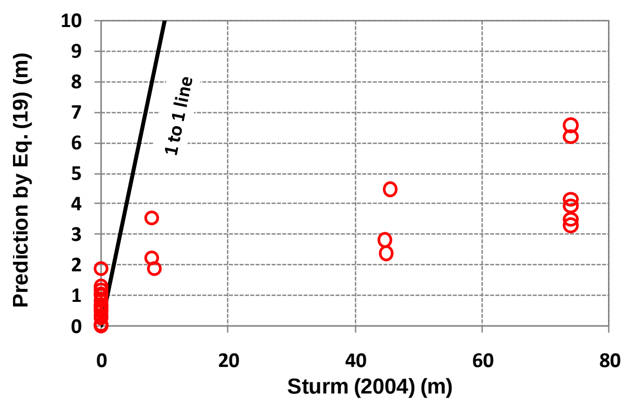

(b) Comparison with Sturm's (2004) equation

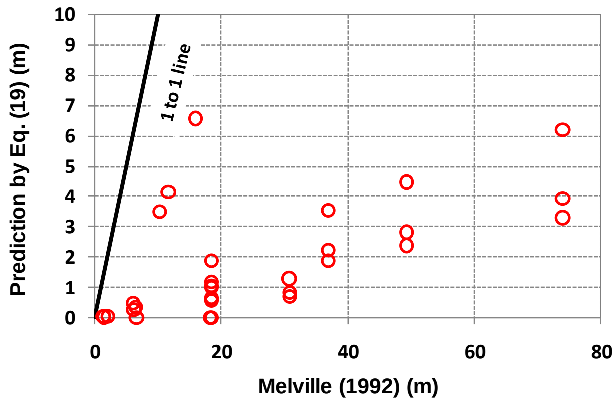

(c)Comparison with Melville's (1992) equation

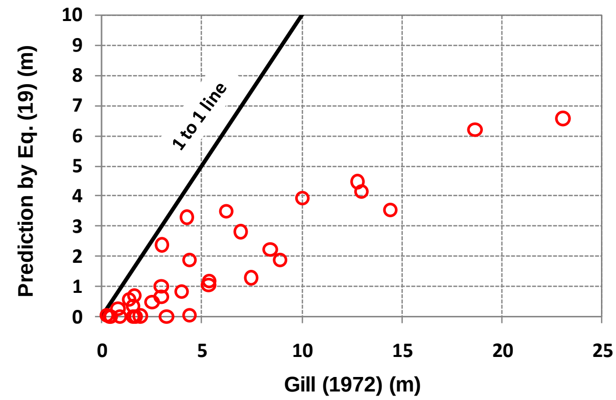

(d) Comparison with Gill's (1972) equation

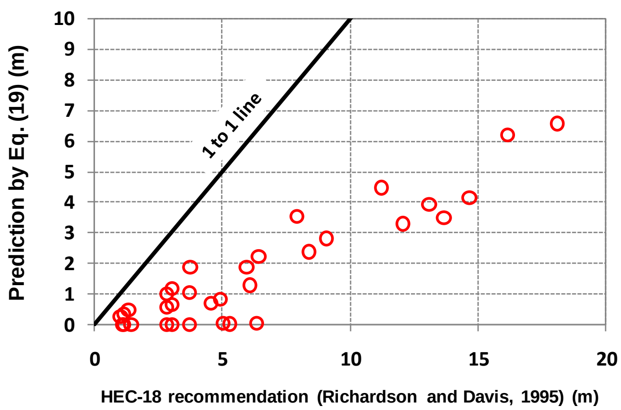

(e)Comparison with HEC-18 recommendation (Richardson and Davis, 1995)

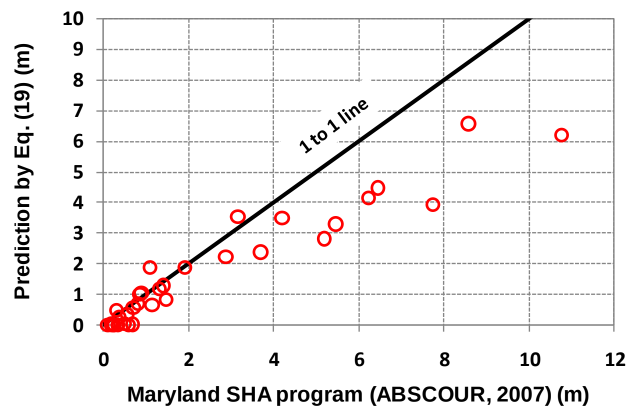

(f) Comparison with method in Maryland SHA program (ABSCOUR,2007)

Figure 22 – Comparisons with other prediction equations for full scale bridge.

The SRICOS-EFA method is primarily designed to predict scour depths in fine-grained soils. For the evaluation of SRICOS-EFA method in fine-grained soil, flume test measurements conducted by Briaud *et al.* (2009) were used. The Porcelain clay was used as riverbed material, and the erosion function and critical shear stress of Porcelain clay after 11 EFA tests was $\dot{z}(mm/hr) = 0.135 \cdot \tau^{1.325}$ and $\tau_c = 0.8(Pa)$, respectively. The abutment scour depths measured at different time during can be expressed by the hyperbolic model as shown in Figure 23, and the model satisfying measurements can be expressed as:

$$y_{s(Abut)}(t) = \frac{t}{a \cdot t + b} \tag{33}$$

where $y_{s(Abut)}$ is the abutment scour depth, t is time in hour, a is the inverse of the asymptotive scour depth , and b is the inverse of the initial tangent to the scour depth versus time curve

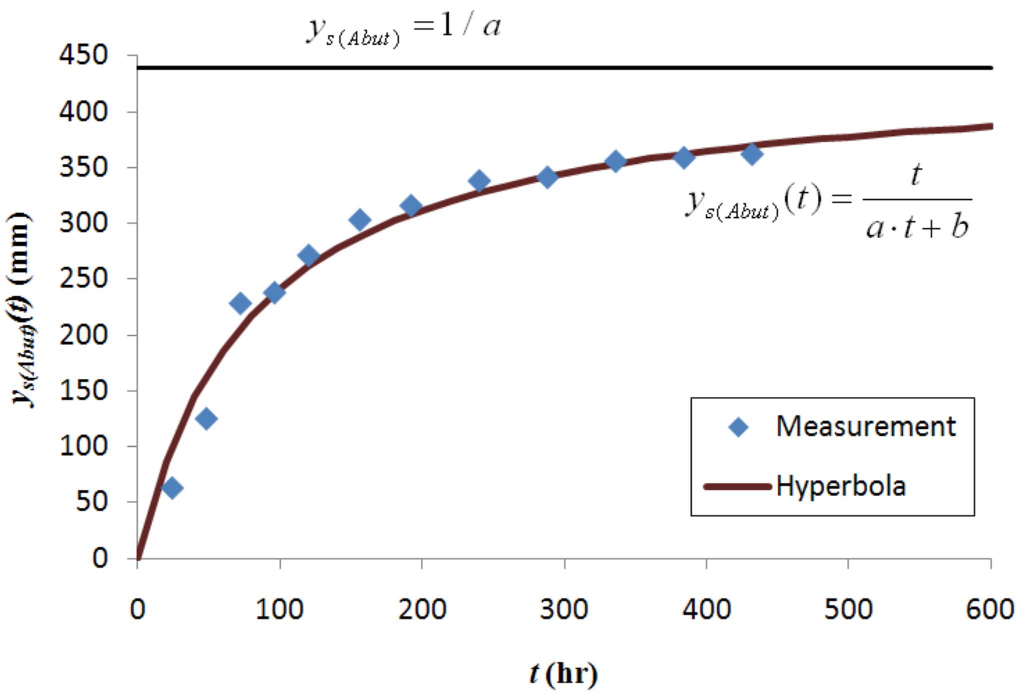

Figure 23 – Abutment scour measurement and hyperbolic fit.

Test conditions and values of a and b for abutment scour in Briaud *et al.* (2009) are summarized in Table 6. The abutment scour depths at 50 hours, 200 hours and 1000 hours are compared to the predicted abutment scour depth by the SRICOS-EFA method, and the comparison is shown in Figure 24; it shows that the SRICOS-EFA method yields good agreements with measurements revealing mostly slightly conservative prediction.

Table 6 – Test condition of abutment scour in fine-grained soil and the hyperbolic characteristics *a* and *b* values.

Test No.	Abutment Shape	Channel Type	V_{f1} (m/s)	V_{avg1} (m/s)	y_{f1} (m)	y_{m1} (m)	L (m)	L_f (m)	L_a (m)	θ (°)	a (mm^{-1})	b (mm/hr)
1	ST (2:1)	Comp.	0.442	0.448	0.293	0.496	3.658	2.438	1.829	90	0.0023	0.1861
2	ST (2:1)	Comp.	0.410	0.439	0.293	0.497	3.658	2.438	1.829	90	0.0020	0.1623
3	ST (2:1)	Comp.	0.356	0.363	0.183	0.386	3.658	2.438	1.829	90	0.0035	1.3509
4	ST (2:1)	Comp.	0.475	0.485	0.400	0.603	3.658	2.438	1.829	90	0.0017	0.9482
5	ST (2:1)	Comp.	0.340	0.347	0.291	0.494	3.658	2.438	1.829	90	0.0033	0.8745
6	ST (2:1)	Comp.	0.504	0.518	0.295	0.499	3.658	2.438	1.829	90	0.0012	0.6025
7	ST (2:1)	Comp.	0.409	0.432	0.293	0.496	3.658	2.438	1.219	90	0.0028	0.7976
8	ST (2:1)	Comp.	0.417	0.447	0.291	0.494	3.658	2.438	2.438	90	0.0008	0.2198
9	ST (3:1)	Comp.	0.422	0.446	0.290	0.493	3.658	2.438	1.829	90	0.0024	0.4541
10	WW	Comp.	0.412	0.441	0.294	0.497	3.658	2.438	1.829	90	0.0015	0.5542
11	ST (2:1)	Comp.	0.414	0.433	0.292	0.496	3.658	2.438	1.829	60	0.0024	0.4201
12	ST (2:1)	Comp.	0.417	0.442	0.292	0.495	3.658	2.438	1.829	120	0.0023	0.4269
13	WW	Rect.	0.322	0.322	0.366	0.366	3.658	3.658	1.015	90	0.0151	2.3458
14	WW	Rect.	0.320	0.320	0.371	0.371	3.658	3.658	1.625	90	0.0033	0.4165
15	WW	Rect.	0.302	0.302	0.384	0.384	3.658	3.658	2.234	90	0.0030	0.5693
16	WW	Rect.	0.208	0.208	0.373	0.373	3.658	3.658	2.743	90	0.0022	0.3112
17	WW	Rect.	0.364	0.364	0.364	0.364	3.658	3.658	1.320	90	0.0038	0.5103

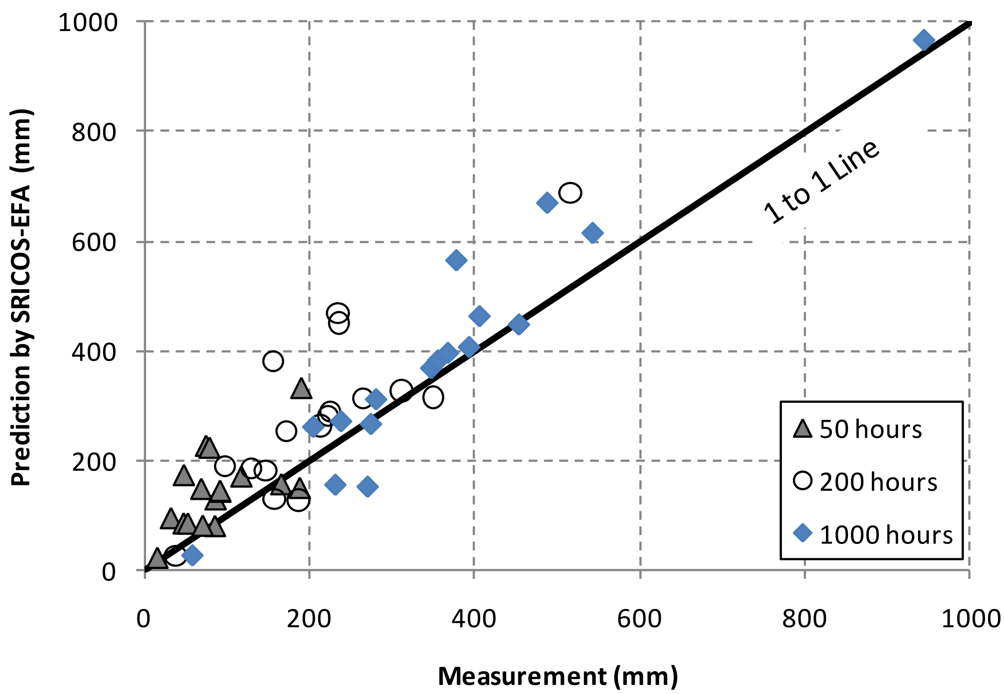

Figure 24 – Comparison of abutment scour depth in Porcelain clay between prediction by SRICOS-EFA and measurement.

STEP BY STEP PROCEDURE IN SRICOS-EFA METHOD

Once the soil erodibility is classified, HEC-RAS is used to obtain hydraulic information including the unit discharge, the velocity, and the water depth near the abutment. Knowing the soil erosion function and the velocity, one can proceed with equations generated from the flume tests and the numerical simulations that we conducted. The equations give two parameters: the maximum scour depth and the initial maximum shear stress on the riverbed before the scour starts. If only the maximum depth of scour is needed, one just uses the maximum depth of scour equation (Method A). To take advantage of the slow erosion process of an erosion resistant soil, one can use the time rate of erosion method proposed (Method B). This method consists of calculating the scour depth accumulated each day during the design life or remaining life of the bridge. This requires a hydrograph or the knowledge of Q_{100} and Q_{500}, whichever is available at the site. A short cut to that method is to use a time compression concept to regroup the effect of the whole hydrograph into one time step called the final equivalent time (Method C). The final equivalent time is the time necessary for the highest velocity in the hydrograph to create the same scour depth as the entire hydrograph. In this case, the time rate calculations are significantly reduced and can be done on the back of an envelope.

The steps for Methods A, B, and C are shown below. The SRICOS-EFA computer program which is available free of charge on the web automates the steps of Method B.

METHOD A

1. Collect samples at the site.
2. Test the samples in the EFA to get the erodibility curves $(\dot{z}\text{ vs. }\tau)$ or use the proposed soil erosion charts (Figure 3 and Figure 4).
3. Describe the geometry of bridge structure.
4. Describe the geometry of the river (main channel width, flood plain width left, flood plain width right, main channel to flood plain transition slope, flood plain bank slope, Manning coefficient and longitudinal slope of the river).
5. Run HEC-RAS to obtain the water depth and the velocity corresponding to the design

flood.

6. Use the maximum scour equation - Eq.(13) for pier scour, Eq.(15) and (16) for contraction scour, and Eq. (19) for abutment scour – to calculate the maximum scour depth.

METHOD B

1. Collect samples at the site.
2. Test the samples in the EFA to get the erodibility curves $(\dot{z} \text{ vs. } \tau)$ or use the proposed soil erosion charts (Figure 3 and Figure 4).
3. Describe the geometry of bridge structure.
4. Describe the geometry of the river (main channel width, flood plain width left, flood plain width right, main channel to flood plain transition slope, flood plain bank slope, Manning coefficient and longitudinal slope of the river)
5. Input the flow hydrograph.
6. Run HEC-RAS to obtain the relationship between the flow and velocity at bridge section, and the flow and water depth immediately upstream of the bridge.
7. Transform the flow hydrograph into a bridge section velocity hydrograph and a water depth hydrograph for immediately upstream of the bridge.
8. Calculate the maximum scour depth for the i^{th} velocity on the hydrograph using Eq.(13) for pier scour, Eq.(15) for contraction scour, and Eq.(19) for abutment scour.
9. Calculate the initial maximum shear stress τ_{max} around the abutment for the i^{th} velocity (before the scour hole development) using Eq.(14) for pier scour, Eq.(17) for contraction scour, and Eq.(19) for abutment scour .
10. Read the initial scour rate corresponding to the initial maximum shear stress τ_{max} on the appropriate EFA curve.
11. Use the results of steps 8 and 10 to construct the scour depth versus time curve for the i^{th} velocity.
12. Calculate the equivalent time for the i^{th} velocity and the curve of step 11. The equivalent time for the i^{th} velocity is the time necessary for the highest velocity in the hydrograph up to the i^{th} time step to create the same scour depth as the hydrograph from start to the i^{th}

time step.

13. Read the additional scour depth contributed by the ith velocity during the ith time step.
14. Repeat steps 8 to 13 for the entire hydrograph.
15. Output the scour depth versus time and read the final scour depth at the end of the hydrograph period.

METHOD C

1. Collect samples at the site.
2. Test the samples in the EFA to get the erodibility curves $(\dot{z} \text{ vs. } \tau)$ or use the proposed soil erosion charts (Figure 3 and Figure 4).
3. Describe the geometry of the bridge structure.
4. Describe the geometry of the river (main channel width, flood plain width left, flood plain width right, main channel to flood plain transition slope, flood plain bank slope, Manning coefficient and longitudinal slope of the river.
5. Obtain the flow hydrograph.
6. Run HEC-RAS to determine the relationship between the flow and velocity at bridge section, and the flow and water depth immediately upstream of the bridge.
7. Transform the flow hydrograph into a bridge section velocity hydrograph and a water depth hydrograph for immediately upstream of the toe of the abutment.
8. Obtain the maximum velocity and corresponding water depth in the hydrograph.
9. Calculate the initial maximum shear stress $\tau_{\max}$ around the abutment for the ith velocity (before the scour hole development) using Eq.(14) for pier scour, Eq.(17) for contraction scour, and Eq.(19) for abutment scour
10. Read the initial scour rate corresponding to the initial maximum shear stress $\tau_{\max}$ on the EFA curve for the soil.
11. Calculate the maximum scour depth for the maximum velocity in the hydrograph using Eq.(13) for pier scour, Eq.(15) for contraction scour, and Eq.(19) for abutment scour
12. Use the results of steps 10 and 11 to construct the scour depth versus time curve for the maximum velocity in the hydrograph (Eq. (1))

13. Calculate the final equivalent time for the entire hydrograph. The final equivalent time for the entire hydrograph is the time necessary for the highest velocity in the hydrograph to create the same scour depth as the entire hydrograph (Eq. (21) for pier scour and Eq. (22) for contraction scour).

14. Read the final scour depth corresponding to the final equivalent time on the scour depth versus time curve of step12

PROCEDURE OF SRICOS-EFA PROGRAM

Fine grained soils may be scoured so much more slowly than coarse grained soils, thus the scour rate should be included for scour prediction. The SRICOS-EFA method has been developed for this reason with consideration of the time effect, the soil properties and the hydraulic parameters, and the SRICOS-EFA computer program is programmed to calculate three types of scour depth simultaneously. The procedure of the SRICOS-EFA method is outlined in Figure 25, and it is simply summarized as:

1. Collect samples at the site.

2. Test the samples in the EFA to get the erodibility curves or use the proposed soil erosion charts.

3. Describe the geometry of the abutment (length, width, shape and alignment angle), and pier (nose shape, width, length, skew angle).

4. Describe the geometry of the river (main channel width, floodplain width left, floodplain width right, main channel to floodplain transition slope, floodplain bank slope, Manning coefficient and longitudinal slope of the river).

5. Input the flow hydrograph.

6. Run HEC-RAS to obtain the relationship between the flow and velocity at bridge section, and the flow and water depth.

7. Transform the flow hydrograph into a bridge section velocity hydrograph and a water depth hydrograph.

8. Calculate the maximum scour depth for the i^{th} velocity on the hydrograph (Eq.(13) for pier scour, Eq.(15) for contraction scour, and Eq.(19) for abutment scour).

9. Calculate the initial maximum shear stress for the i^{th} velocity (before the scour hole development) (Eq.(14) for pier scour, Eq.(17) for contraction scour, and Eq.(19) for abutment scour).

10. Read the initial scour rate corresponding to the initial maximum shear stress on the appropriate EFA curve.

11. Use the results of steps 8 and 10 to construct the scour depth versus time curve for the i^{th} velocity.

12. Calculate the equivalent time for the i^{th} velocity and the curve of step 11. The equivalent time for the i^{th} velocity is the time necessary for the highest velocity in the hydrograph up to the i^{th} time step to create the same scour depth as the hydrograph from start to the i^{th} time step.

13. Read the additional scour depth contributed by the i^{th} velocity during the i^{th} time step.

14. Repeat steps 8 to 13 for the entire hydrograph.

15. Output the scour depth versus time and read the final scour depth at the end of the hydrograph period.

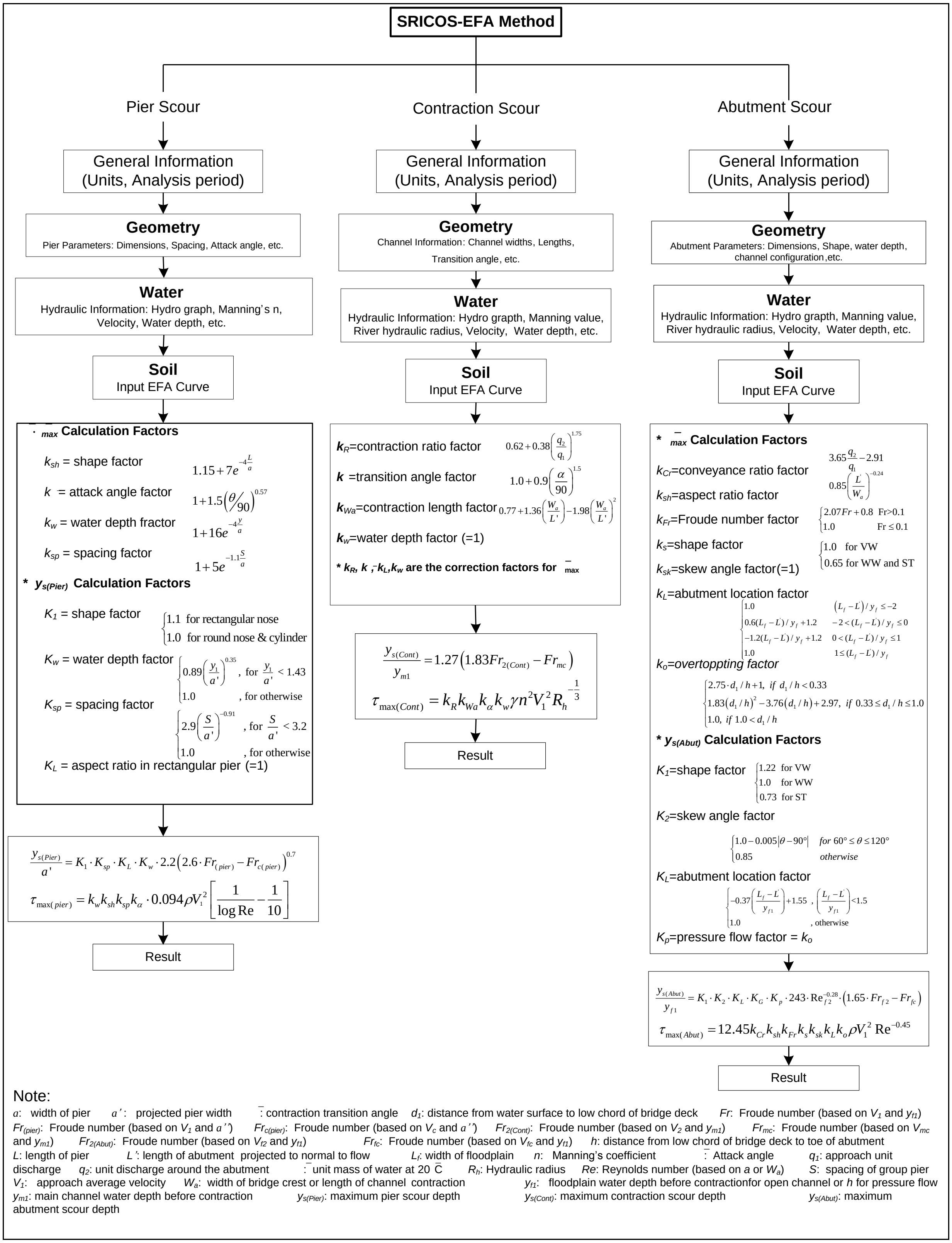

Figure 25 – Procedure of SRICOS-EFA method.

USING SRICOS-EFA PROGRAM

Using SRICOS-EFA program involves the following steps:

1. Create the general project information, choose the **Scour Type** and the applicable **Unit System**

2. Enter **Geometry Data**

3. Enter **Water Data**

4. Enter **Soil Data**

5. Run the analysis to perform SRICOS-EFA calculations

6. Review the analysis results (tables, plots)

To start SRICOS-EFA, please double-click on the SRICOS-EFA icon on the desktop. If you do not have an SRICOS-EFA shortcut on the desktop, please go to **Start** menu and select **Programs**, and then select **SRICOS-EFA**.

When SRICOS-EFA program started, you will see the main SRICOS-EFA window as shown in Figure 26. Each icon in Figure 26 is explained in Table 7.

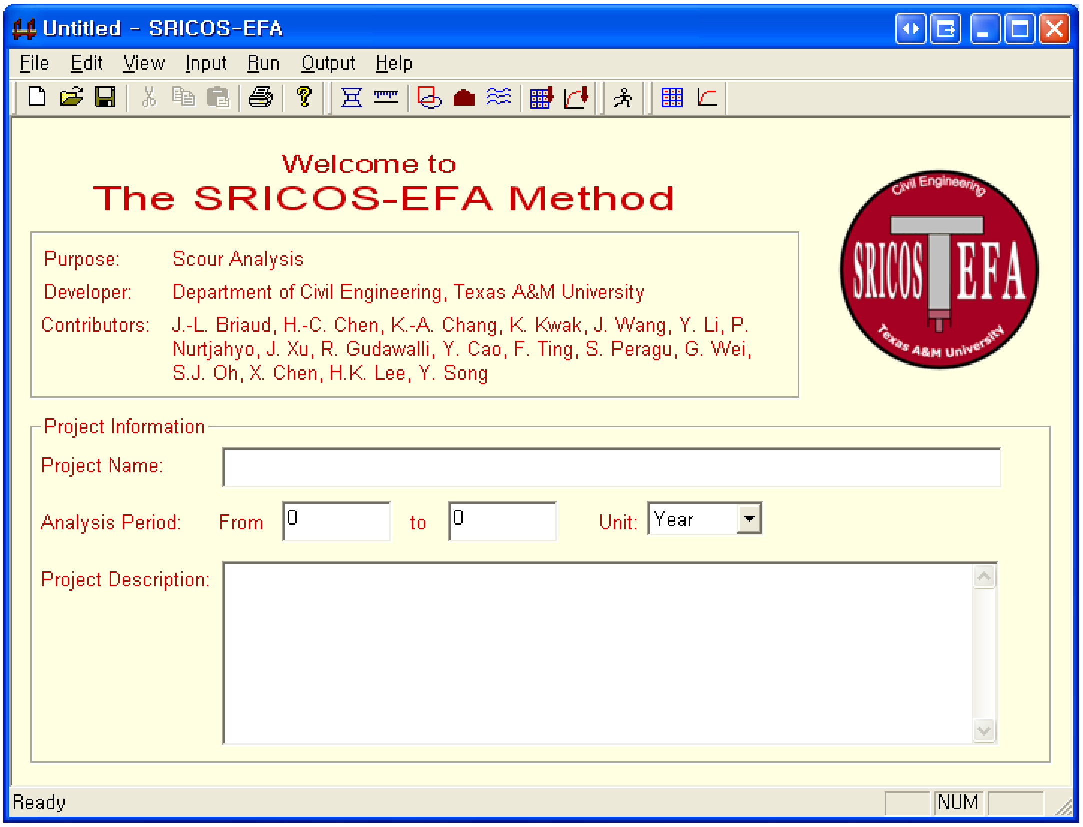

Figure 26 - The SRICOS-EFA main window.

Table 7 – Icons and commands.

Icon	Command	Icon	Command
	Create a new document		Open an existing project
	Save the active document		Print current project
	Display program information		Select proper scour type to calculate
	Select unit system		Edit or enter geometric data
	Edit or enter soil data		Edit or enter water data
	Display the input tables		Display the input plots
	Perform a scour calculation		Display the result in tables
	Display the result in plots		

EVALUATION OF SCOUR DEPTH USING HYDROGRAPH

DATA INPUT

In order to start a new project, go to the File menu and select New on the top of main SRICOS-EFA program window or click the New Project icon in the tool bar menu on the main SRICOS-EFA program window. The documental information can be entered in the main window.

Pier scour

1) Scour type selection

Choose the scour type by selecting **Scour Type** option under **Input** menu or click the **Scour Type** icon in the tools bar menu on the top of main program window. In this case, **Pier scour** is selected as shown in Figure 27.

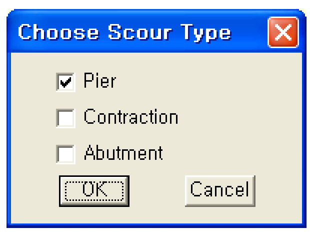

Figure 27 – Scour type selection window.

2) Unit system selection

Choose the Unit system by selecting **Units** option under **Input** menu or click the **Units** icon in the tool bar menu on the top of main window. The SI unit is the default unit system of the program.

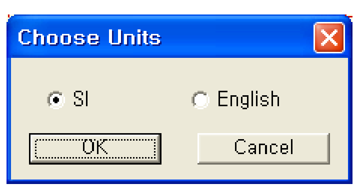

Figure 28 – Unit system selection window.

3) Geometry data input

Geometry Data window is open by selecting **Geometry** from the **Input** menu or **Geometry** icon on the tools bar menu in the main program window. All geometry input data should be entered in activated boxes. Click the button of Help for Pier for more information, and then the schematics of all pier parameters will be shown as Figure 30. (Note: only several input boxes are activated in Figure 29 because only they are required for pier scour.)

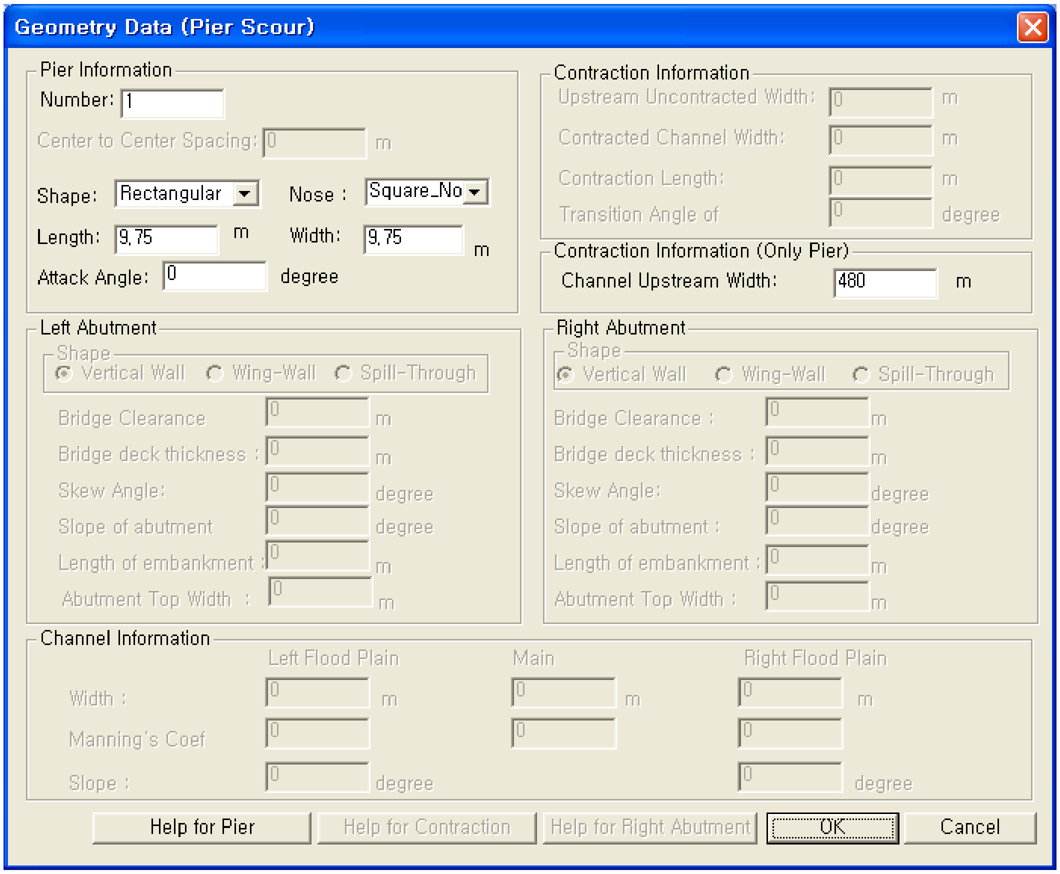

Figure 29 – Geometry data input window for pier scour.

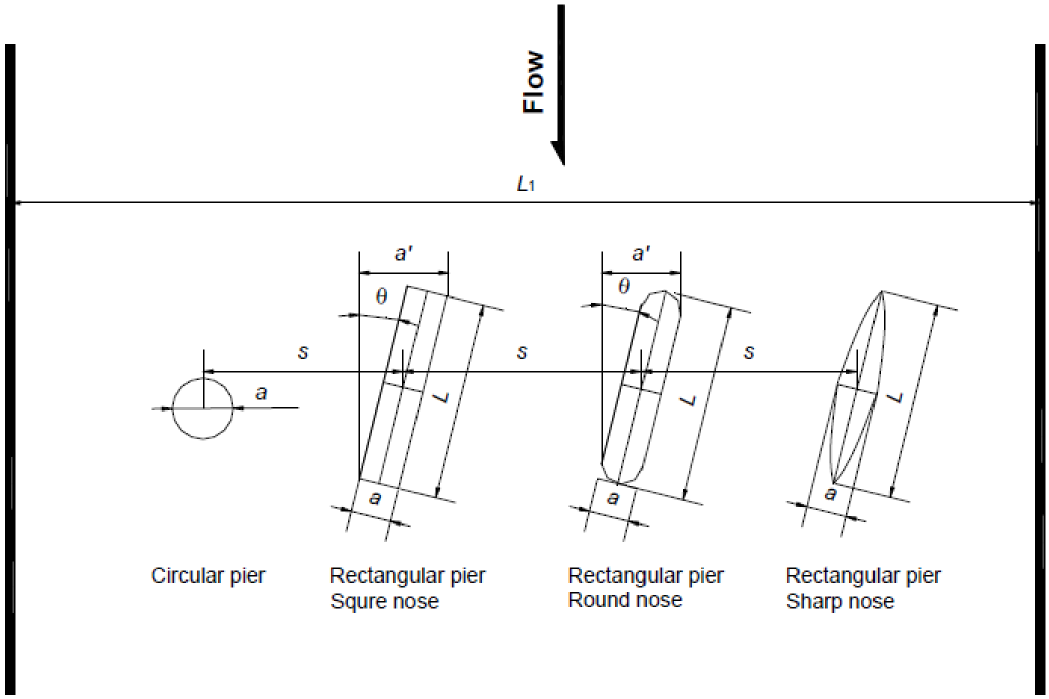

a	: pier width	L_1	: channel upstream width
a'	: projected pier width	s	: center to center spacing
L	: pier length	θ	: attack angle

Definition of symbol.

Figure 30 – Schematics of pier parameters.

4) Soil data input

Soil Data window is popped up by selecting **Soil** option from the **Input** menu or **Soil** icon on the tools bar menu in the main program window (Figure 31). As shown, the detail of Soil Data input includes:

A. Number of Soil Layers

User needs to enter the number of soil layers involved in the scour calculation. If the soil layers are more than one layer, user can push the button under Number of Layers to change the layer numbers. The maximum number of soil layers can be 100. Users need to roughly estimate the potential scour depth in the field and make sure the total soil depth of different layers is larger than the estimated potential scour depth.

B. Current Layer

The layers displaying in the **Current Layer** box are corresponding to the number of soil layers the user entered. The soil properties will be entered by one layer by one layer. For example, when you select Layer 1 as the current layer, you can enter the soil data for this layer. After finishing Layer 1 soil data input, select Layer 2 to start the input for Layer 2.

C. Layer Thickness

User needs to enter the thicknesses of each soil layer.

D. Critical Shear Stress

In SRICOS-EFA program, the critical shear stress is corresponding to an erosion rate of 1mm/hr in the EFA curve. User needs to enter the critical shear stress for each soil layer.

E. Number of Points on the EFA Curve and the Values

EFA curve describes the erosion properties of soil. Figure 7 shows a typical EFA curve from the EFA test. User should decide how many regression points on EFA curve need to be entered in the program. These data points will be entered into the SRICOS-EFA program to represent the entire curve. Then user needs to enter the values of regression points for the relationship between the scour rate $\dot{z}$ (mm/hr) and the hydraulic shear stresses τ. EFA curve needs to be entered into program for each soil layer. It is important to make sure that the EFA curve covers the range of the shear stresses in the calculation. For this purpose, it is recommended to enter some large values by using the regression equation for the EFA curve. For example, Figure 32, the maximum shear stress is 46 N/m^2 in the EFA test. In some case the value of the maximum shear stress in the scour calculation probably will beyond the 46 N/m^2. In this case, you need to find the regression equation for this EFA curve. Then you can use the regression equation to extend the data range of the EFA curve.

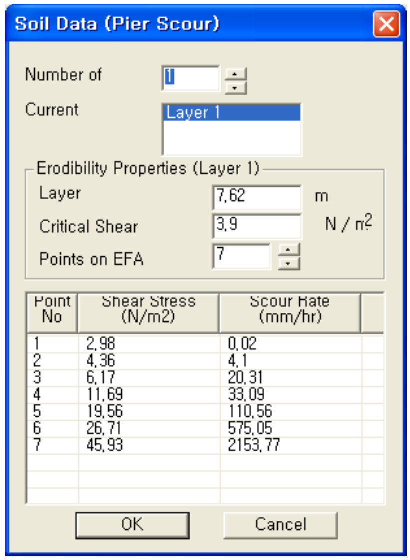

Figure 31 – Soil data input window for pier scour.

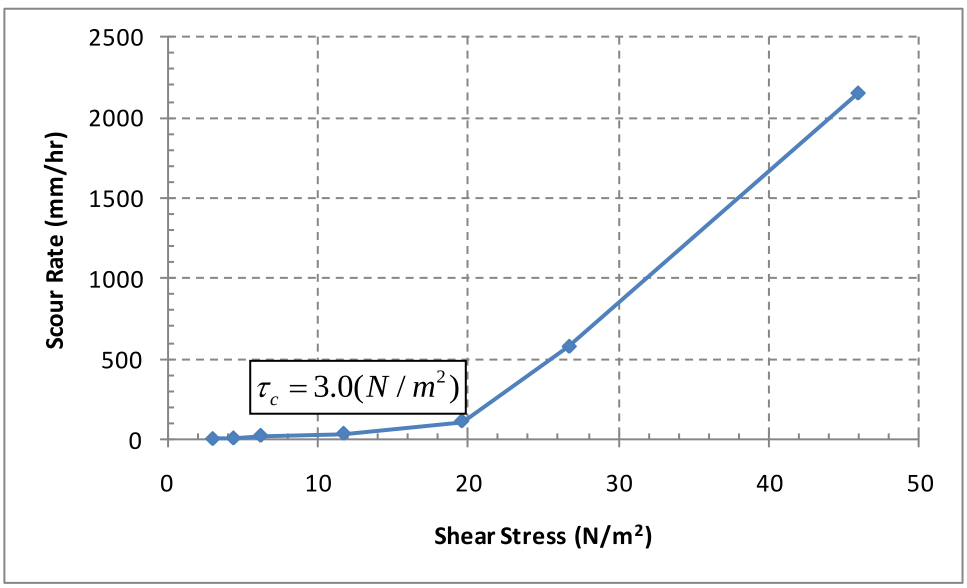

Figure 32 – Typical EFA test result.

5) Water data input

Water Data window is popped up by selecting **Water** option from the **Input** menu or **Water** icon on the tools bar menu in the main program window (Figure 33).

A. Manning's Coefficient

Manning's coefficient (s/m^3) is used to describe the friction characteristics of channel and it is an empirical value and usually obtained from experiments. Young (1997) summarized the value of Manning's coefficient in different conditions (Table 8)

B. Time Step

The time step is the interval time between two continuous hydrograph data. If you download the hydrograph from the USGS website (www.usgs.gov), usually the time step of the data is 24 hours.

C. Input Hydrologic Data

Two kinds of hydrograph data can be used in the SRICOS-EFA program: Discharge vs. Time or Velocity vs. Time. You need to click the type of hydrograph data that you have.

SRICOS-EFA program has the function to compute the constant hydrograph data and the multi-flood hydrograph.

1) If the hydrograph is constant, the user needs to enter the discharge value or velocity value, which depends on what kind of data you have and then enter the Time (analysis period) as the scouring time.

2) If the hydrograph is a multi-flood hydrograph, the velocity vs. time or discharge vs. time data should be prepared and saved as a text document with one line one value format before running the program. Click the **Browse** button, and then the window appears. User can choose the prepared hydrograph file and **Open** it. The program will read the values in the file automatically in the calculation.

3) SRICOS-EFA program has another function that the user can input the 100-year flood and 500 year flood into the normal hydrograph file. Users can accomplish it by click the **Flood Insert** button under the **Browse button** in the Water Data input window. When it is clicked, the window will appear as it is shown in Figure 33. Users have the options to choose to insert the flood only 100-year flood or 500-year flood. In this case, user clicks the corresponding 100-year and 500-year flood box, and then enters the value for 100-year or 500-year flood. The 100-year flood or 500-year flood will be inserted at the middle of the hydrograph. For example, if the duration of the hydrograph lasts 70 years, the flood is inserted at 35 year. In the case, user wants to insert the 100-year flood and 500-year flood both, user needs to click the 100-year Flood and 500-year Flood boxes and enter the values for both. Then the 100 year flood will be inserted in the one third of the hydrograph file and 500 year flood will be inserted in the two third of the hydrograph file. For example, if the duration of the hydrograph is 60 years, then the 100 year flood will be inserted in 20 year and the 500 year flood will be inserted in the 40 year. After inserting the floods, the Status will show Inserted. If you want to use the normal hydrograph file not

the inserted hydrograph, you just need to Browse and Open the prepared hydrograph file without one more time. The Status will show Not Inserted again.

D. Entering Relationships between the Hydrologic Parameters

Water depth and velocity are two parameters that directly used in the SRICOS-EFA program. Usually the hydrograph types are **Discharge vs. Time** or **Velocity vs. Time**. For discharge vs. time, it is necessary to have the relationships discharge vs. velocity and discharge vs. water depth. For velocity vs. time, the relationship between velocity and water depth need to be entered. The computer program called Hydrologic Engineering Center - River Analysis System (HEC-RAS), which was developed by United States Army Corps of Engineers, is used for flood analysis to obtain the different hydrologic relationships. Different with previous version of SRICOS-EFA, the water data at both two sides of floodplain in the relationship between hydrologic parameters are required in current version. The data for floodplains are required when **Abutment** Scour is selected in **Scour Type.** In this case, only the pier scour is selected. Thus the hydrologic parameters for floodplains are not required, and you need to enter the parameters only in 2nd and 4th columns (the sections with red square in Figure 33).

Following Figure 34and Figure 35 are the examples of the calculation results from HEC-RAS.

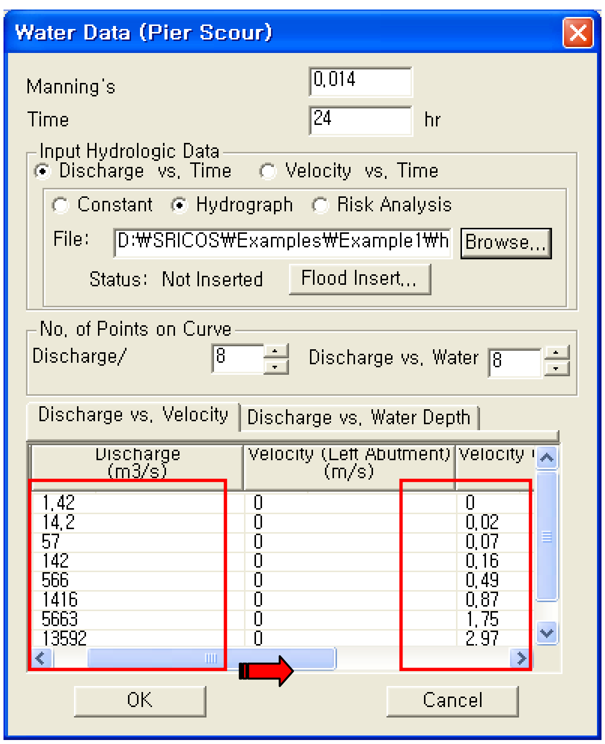

Figure 33 – Water data input window for pier scour.

Table 8 – Manning's coefficient in different conditions (Young, 1997)

Categories		Manning's Coefficient	Categories		Manning's Coefficient
Natural Channel	Clean and straight	0.030	Artificially lined channel	Glass	0.010
	Sluggish with deep pools	0.040		Brass	0.011
	Major rivers	0.035		Steel, smooth	0.012
Floodplains	Pasture, farmland	0.035		Steel, painted	0.014
	Light brush	0.050		Steel, riveted	0.015
	Heavy brush	0.075		Cast, iron	0.013
	Trees	0.15		Concrete, finished	0.012
Excavated earth channels	Clean	0.022		Concrete, unfinished	0.014
	Gravelly	0.025		Planned wood	0.012
	Weedy	0.030		Clay tile	0.014
	Stony, cobbles	0.035		Brickwork	0.015
				Asphalt	0.016
				Corrugated metal	0.022
				Rubble masonry	0.025

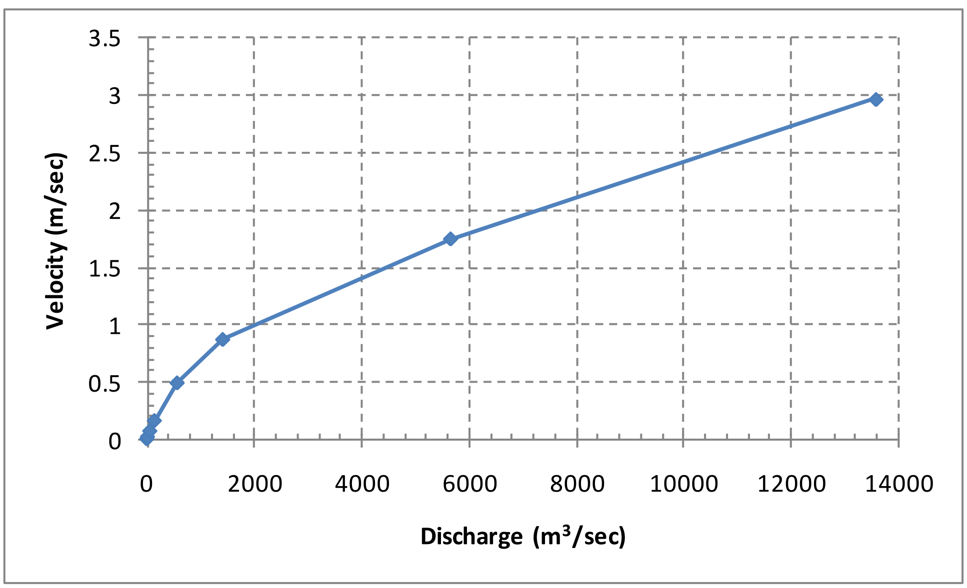

Figure 34 – Relationship between Discharge versus Velocity from HEC-RAS results.

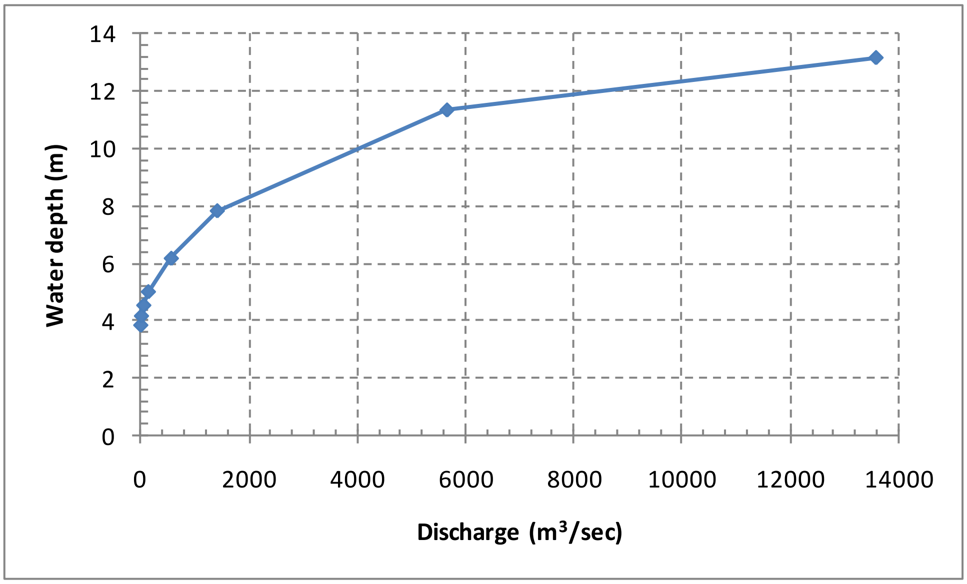

Figure 35 – Relationship between Discharge versus Water depth from HEC-RAS results.

Contraction scour

1) Scour type selection

Choose the scour type by selecting **Scour Type** option under **Input** menu or click the **Scour Type** icon in the tools bar menu on the top of main program window. In this case, **Contractions scour** is selected as shown in Figure 36.

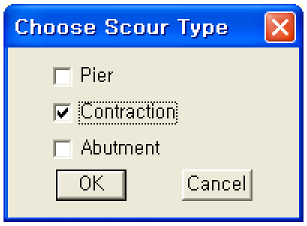

Figure 36 – Scour type selection for contraction scour.

2) Unit system selection

Choose the Unit system by selecting **Units** option under **Input** menu or click the **Units** icon in the tool bar menu on the top of main window. The SI unit is the default unit system of the program.

3) Geometry data input

Geometry Data window is open by selecting **Geometry** from the **Input** menu or **Geometry** icon on the tools bar menu in the main program window. All geometry input data should be entered in activated boxes. Click the button of Help for Contraction for more information, and then the schematics of all contraction parameters will be shown as Figure 38 (Note: some input boxes are activated in Figure 37 because only they are required for contraction scour.)

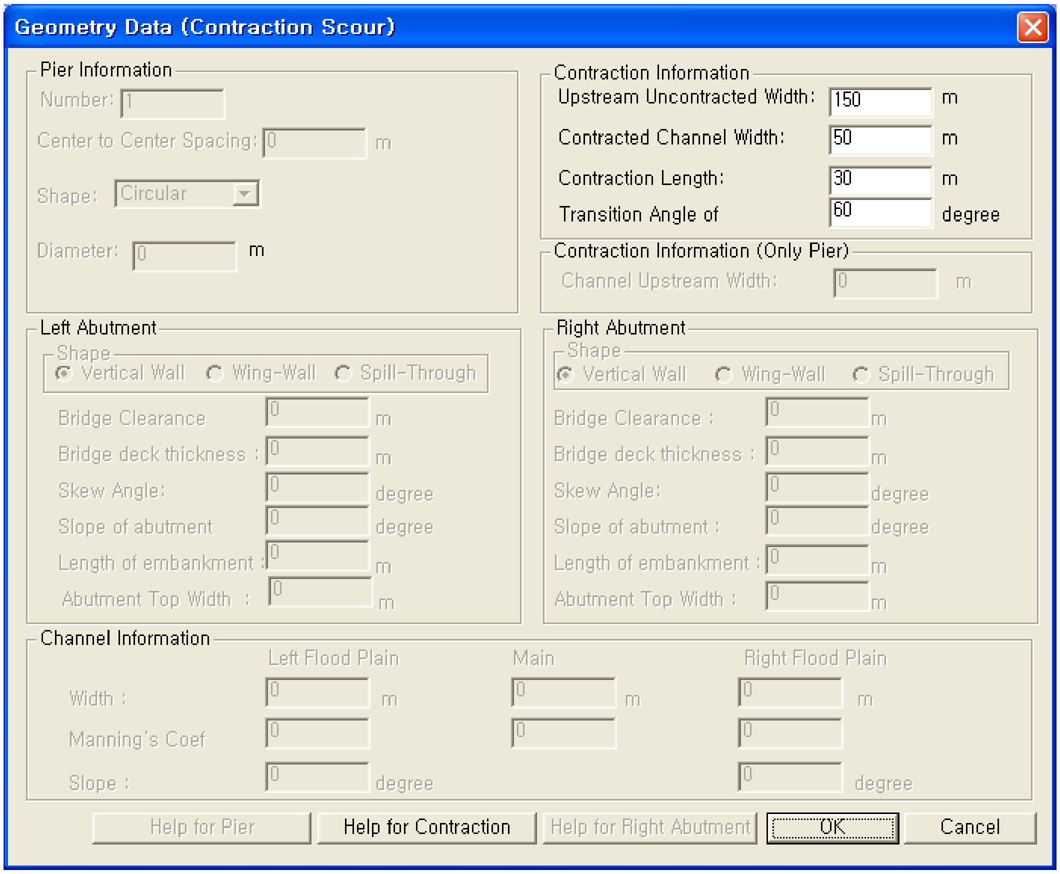

Figure 37 – Geometry data input window for contraction scour.

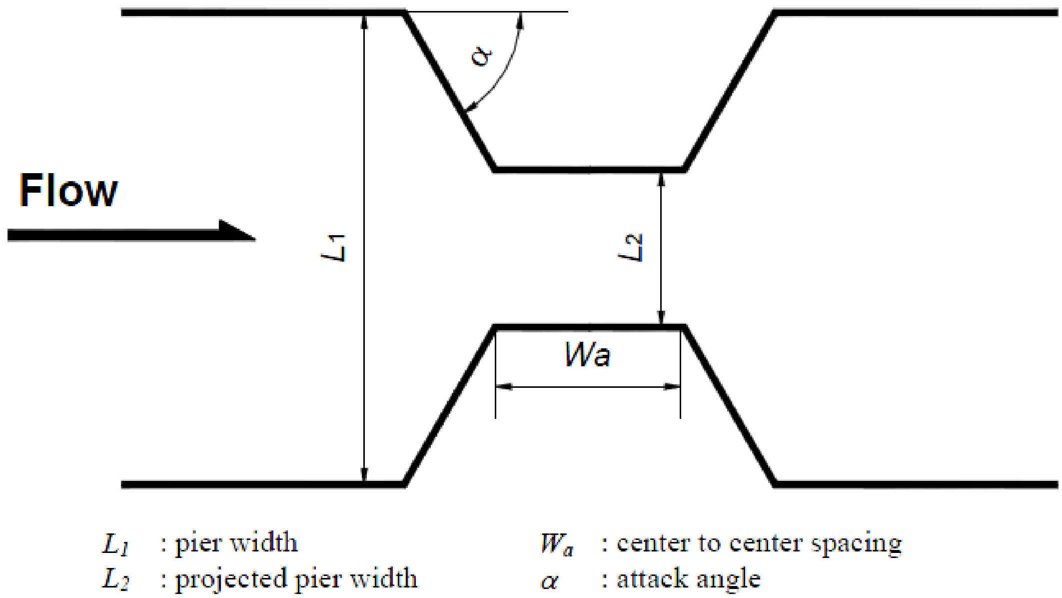

Figure 38 – Schematics of contraction scour parameters.

4) Soil data input

The procedures of entering soil data for contraction scour are same to the procedures in pier scour. For detailed information, please refer to the section of Soil Data input in Pier Scour.

5) Water data input

The procedures of entering soil data for contraction scour are same to the procedures in pier scour. For detailed information, please refer to the section of Water Data input in Pier Scour.

Pier + Contraction scour

1) Geometry data input

The **Geometry Data** for the combined scour (Pier Scour + Contraction Scour) consists of the geometry data of pier scour and the geometry data of contraction scour. Figure 39 shows **Geometry Data** input window for pier + contraction scour. For the information of entering Geometry Data in pier + contraction scour, please refer to the sections of Entering Geometry Data (Pier Scour) and Entering Geometry Data (Contraction Scour).

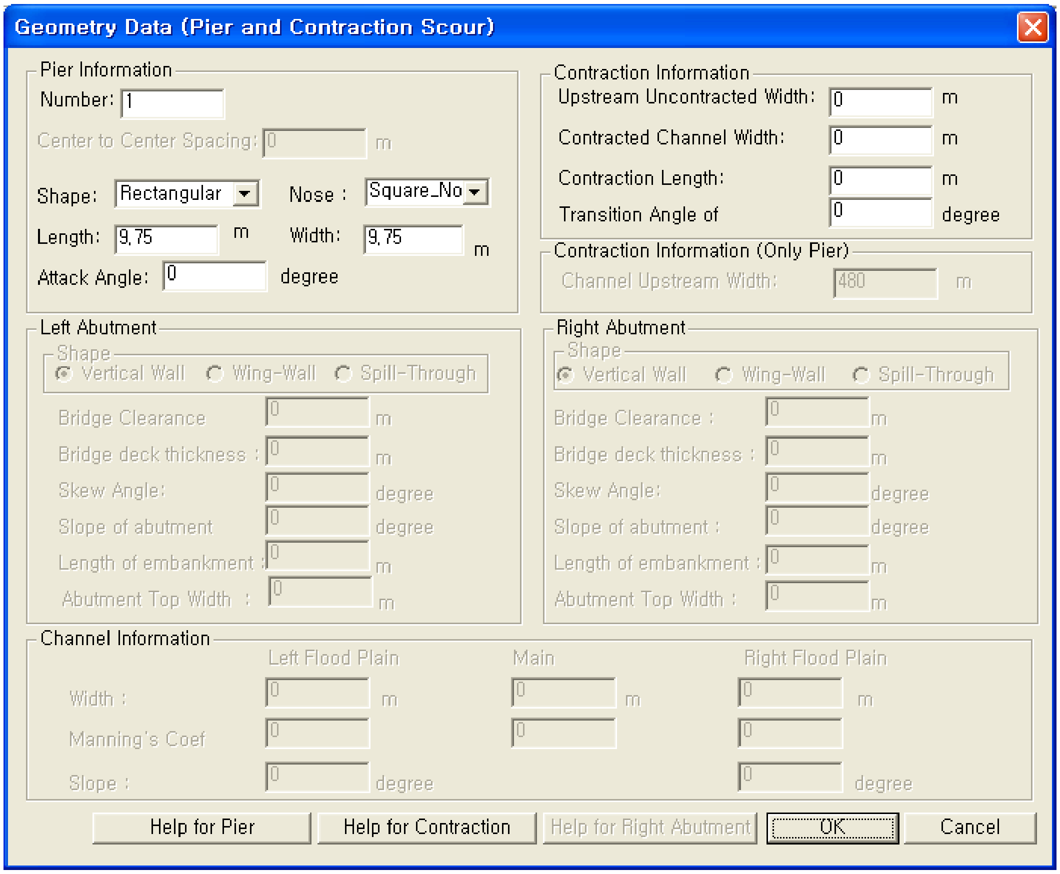

Figure 39 – Geometry data input window for pier + contraction scour.

2) Soil data input

The procedures of entering soil data for pier + contraction scour are same to the procedures in pier scour. For the details information, please refer to the Section of Soil Data input in Pier Scour.

3) Water data input

The procedures of entering Water Data for pier + contraction scour is same to the Water Data entering procedures in pier scour. For the information of entering Water Data in pier + contraction scour, please refer to the Section of Water Data input in Pier Scour.

Abutment + Contraction scour

1) Scour type selection

Both contraction scour and abutment scour happen when channels are constricted by bridge embankments. Thus SRICOS-EFA is programmed to consider both contraction and abutment scour. If only abutment scour is selected, an error message like Figure 40 will appear. As shown in Figure 40, SRICOS-EFA can handle five combinations of scour. Please check scour type combination correctly.

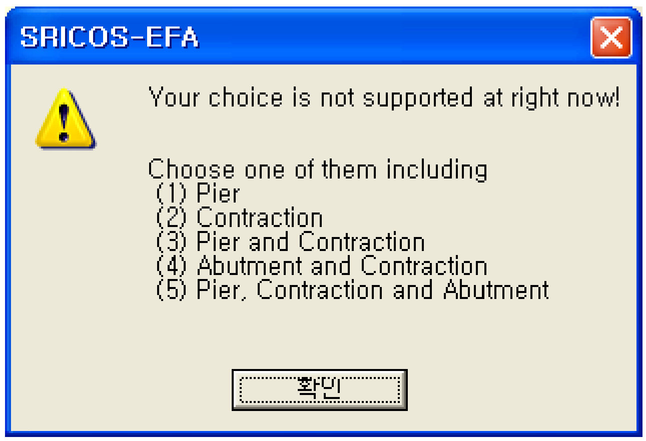

Figure 40 – Error message for the wrong selection of scour type combination.

2) Geometry data input

Geometry Data window is open by selecting **Geometry** from the **Input** menu or **Geometry** icon on the tools bar menu in the main program window. All geometry input data should be entered in activated boxes. The SRICOS-EFA program automatically calculates the area at the bridge section by using the Channel Information and water depths, so Upstream Uncontracted Width and Contracted Channel Width in Contraction Information section are not required and not activated.

Click the button of Help for Contraction for more information, and then the schematics of all contraction parameters will be shown as Figure 42. Different with pier scour and contraction scour, three Manning's coefficients are required to be entered in Geometry data input window because left floodplain, right floodplain and main channel should be clearly divided to calculate the abutment scour depth. To enter Manning's coefficient, please refer Table 8 for the appropriate selection of Manning's coefficient.

(Note: some input boxes are not activated in Figure 41 because they are not required for abutment and contraction scour.)

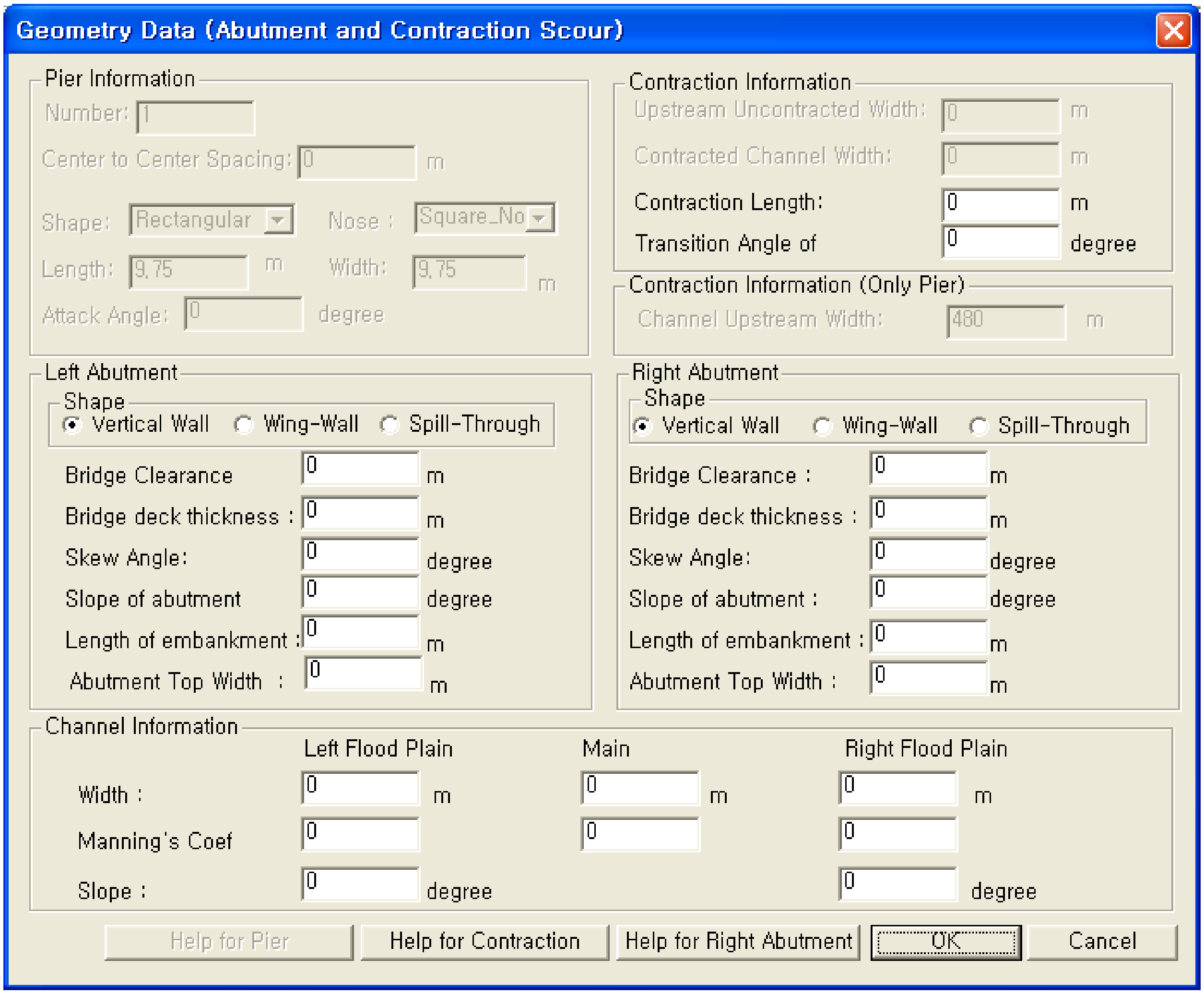

Figure 41 – Geometry data input window for abutment and contraction scour.

Shape of abutment.

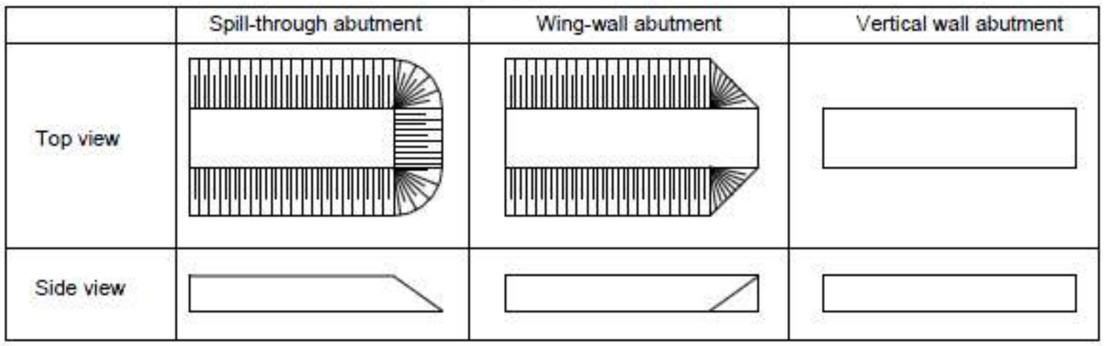

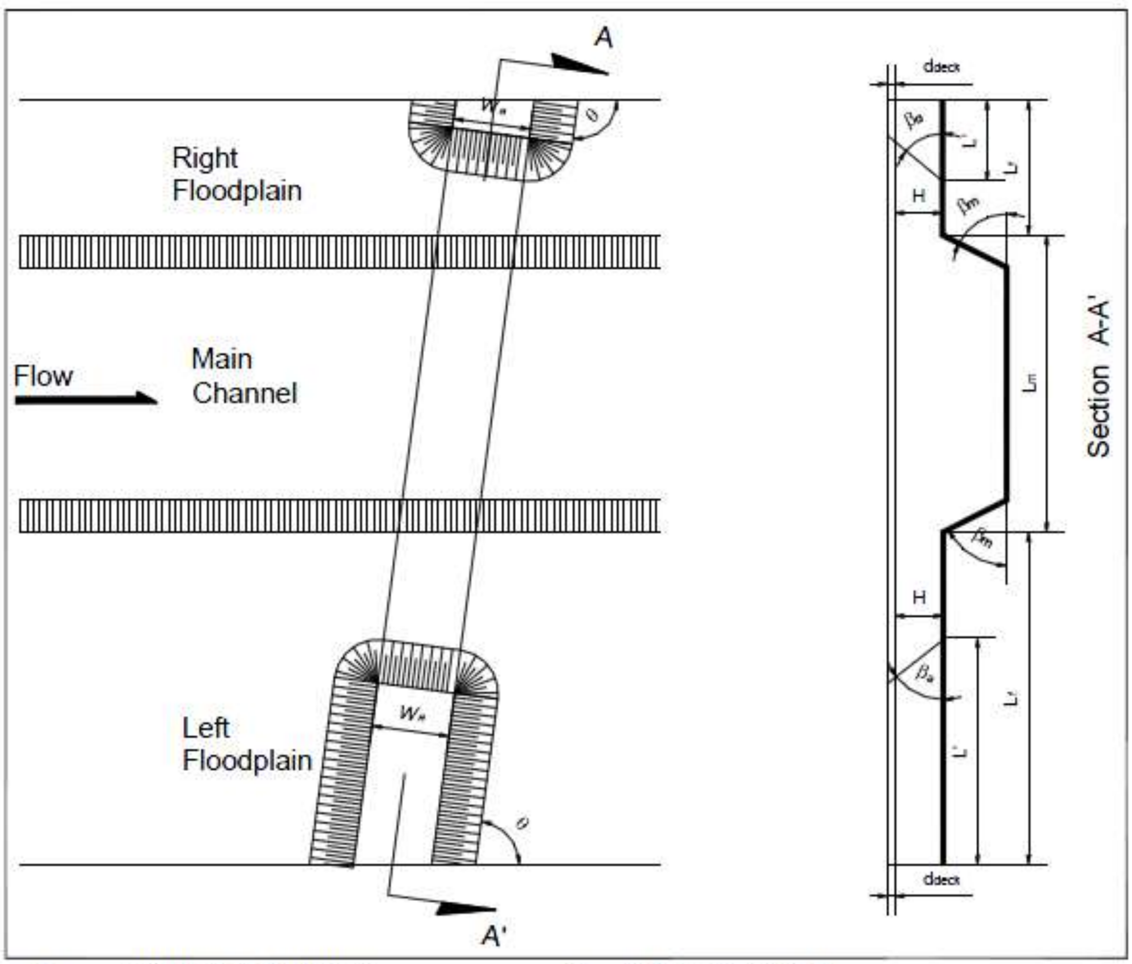

d_{deck}	: thickness of bridge deck	W_a	:abutment tip width
H	: bridge clearance	β_a	:slope of abutment
L_f	: width of floodplain	β_m	: slope of main channel
L'	: length of embankment projected to flow	θ	: skew angle of approach embankment
L_m	: width of main-channel		

Figure 42 – Schematics of abutment scour parameters.

3) Soil data input

The procedures of entering soil data for abutment + contraction scour are same to the procedures in pier scour. For the details information, please refer to the Section of Soil Data input in Pier Scour.

4) Water data input

Different with previous Water data inputs, the water data at both two sides of floodplain in the relationship between hydrologic parameters are required if **Abutment** Scour is selected in **Scour Type**. So you need to enter the parameters in all columns. Whereas Manning's coefficient is not required in this input window because it was already entered in **Geometry Data** input window.

Following Figure 44 and Figure 45 are the examples of the calculation results from HEC-RAS.

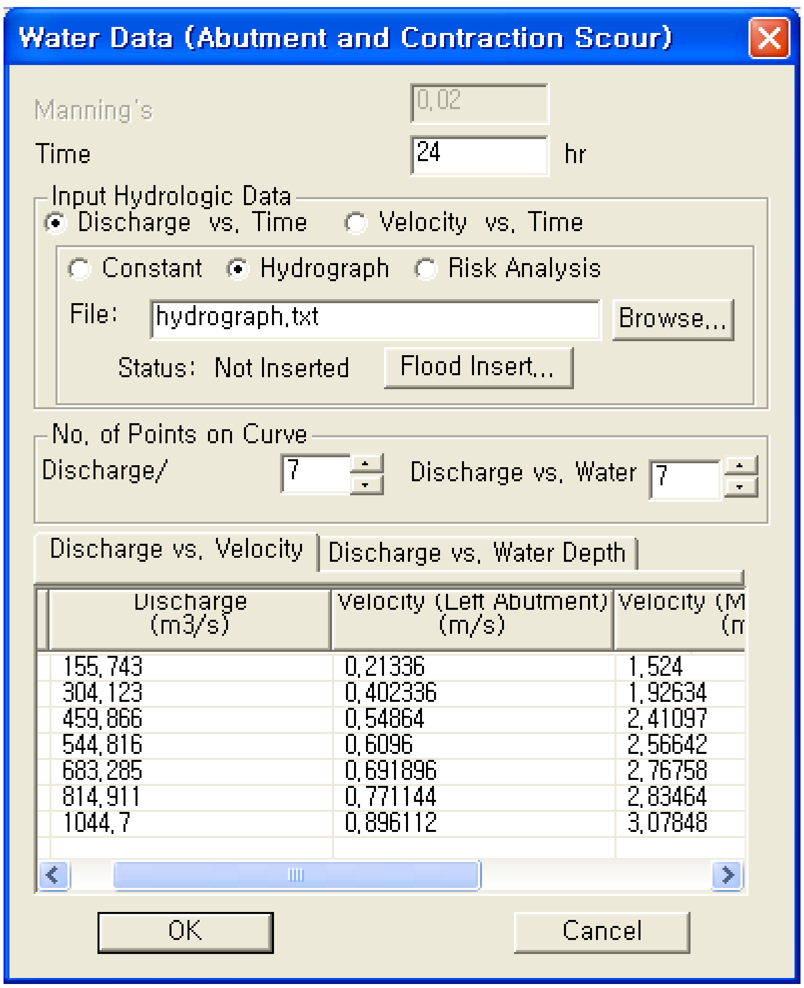

Figure 43 – Water data input window for abutment and contraction scour.

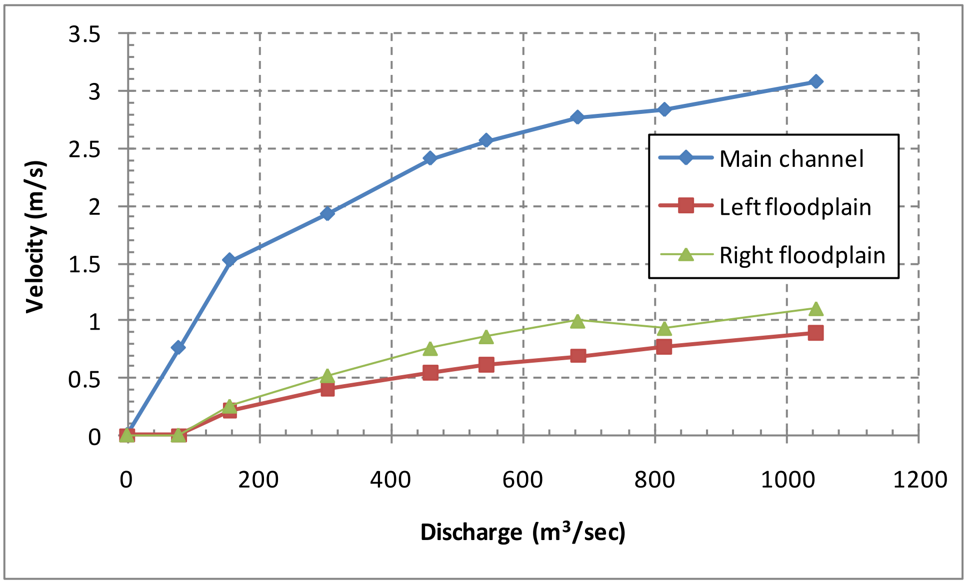

Figure 44 – Relationship between Discharge and Velocity.

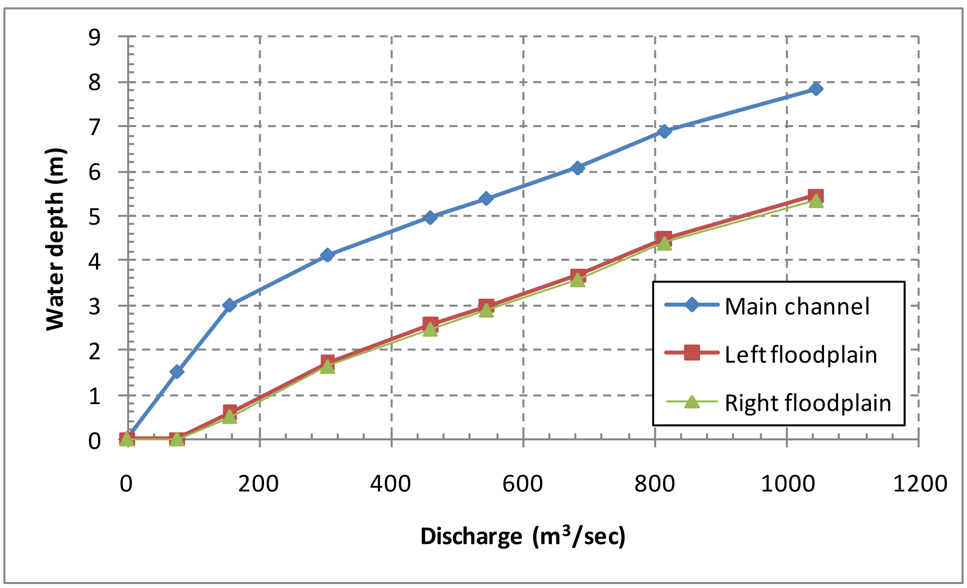

Figure 45 – Relationship between Discharge and Water depth.

Abutment + Contraction + Pier scour

1) Geometry data input

The pier information is required if all three types of scour were selected. The procedures to enter Pier Information are same as those in Pier Scour, and the procedures to enter Abutment and Contraction and scour are same as those in Abutment + Contraction Scour. For the detail information, please refer to the Section of Soil Data input in Pier Scour and in Abutment + Contraction Scour.

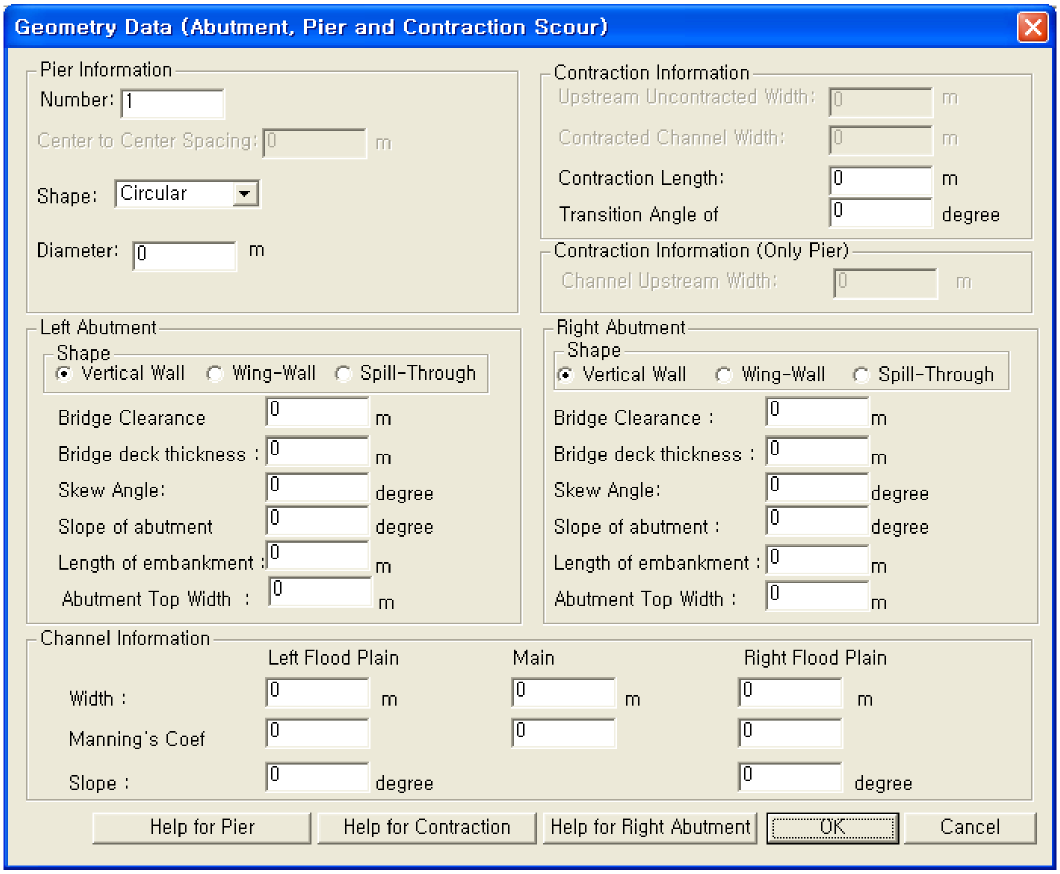

2) Soil data input

The procedures of entering soil data for abutment + pier + contraction scour are same to the procedures in pier scour. For the detail information, please refer to the Section of Soil Data input in Pier Scour.

3) Water data input

The procedures of entering water data for abutment + pier + contraction scour are same to the procedures in abutment + contraction scour. For the detail information, please refer to the Section of Soil Data input in Abutment + Contraction scour.

REVIEW OF INPUT TABLES AND PLOTS

After finishing input, all input values can be reviewed through **Input Tables** and **Input Plots**. The window of **Input Tables** will be popped up by selecting **Tables** in **Input** menu or clicking **Input Tables** icon. Figure 46 and Figure 47 show examples of input tables. (Note: all input values will be shown by changing options using radio button.) The window of **Input Plots** will be popped up by selecting **Plots** in **Input** menu or clicking **Input Plots** icon. (Note: all input values will be plotted by checking a radio button, a focused plain and clicking **Show Graph**.) Figure 48 shows an example of **Input Plots.**

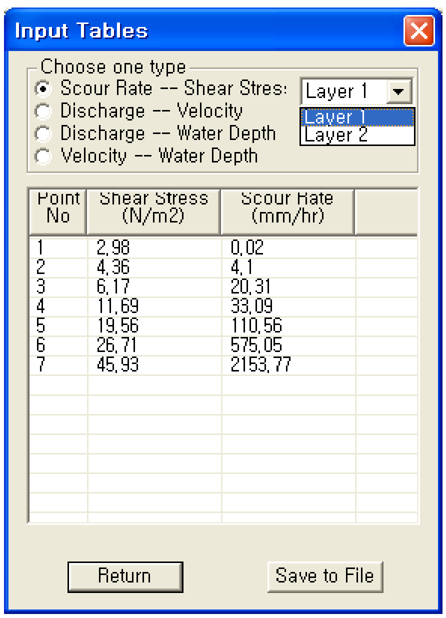

Figure 46 – Example of Input Tables (Scour Rate vs. Shear Stress).

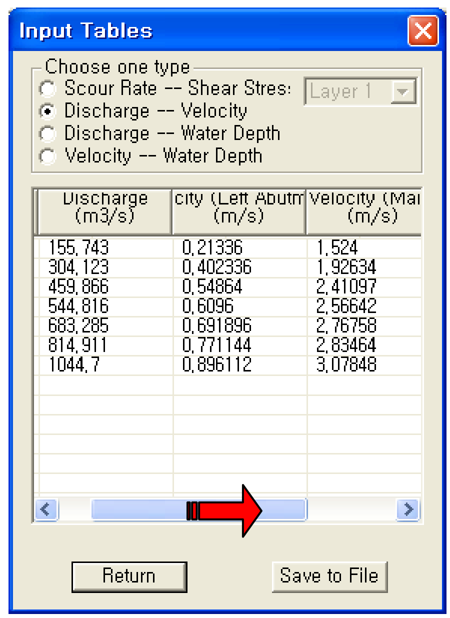

Figure 47 – Example of Input Tables (Discharge vs. Velocity).

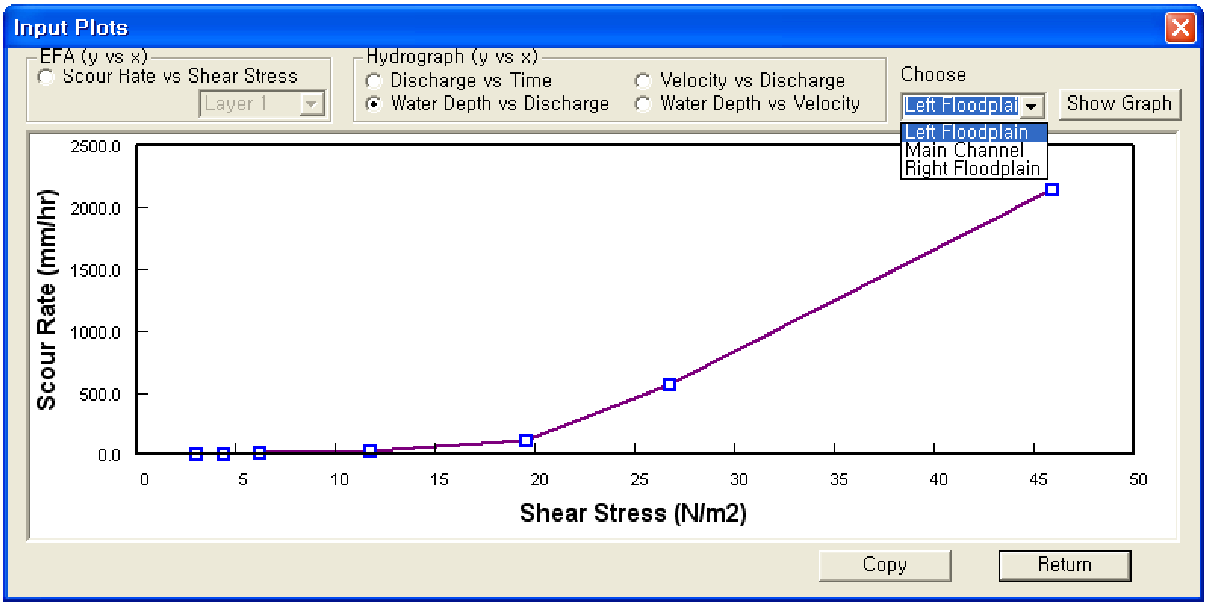

Figure 48 – Example of Input Plots (Water Depth vs. Discharge on Left Floodplain).

Perform the scour analysis

To perform the pier scour analysis, select **Run** option from **Run** menu or the **Run** icon in the tools bar menu in the main program window.

Viewing results

After finishing the computation, all computation results can be reviewed. The output options include **Output Table** and **Output Plots**. The **Output Table** and **Output Plots** are available from the **Output** menu and the **Output Table** and **Output Plots** icons on the tools bar menu in the SRICOS-EFA main program window. You can save the Output Table as an Excel file for better review of all calculated results by clicking **Save** button below the table. In the **Output Table**, the 1st column shows the point number of data in hydrograph, and the 2nd column shows the elapsed days from the first day of analysis. The other columns show the calculated value. More details are:

1) Columns from the 3rd through the 5th show the calculated velocities using the relationship of discharge vs. velocity for each discharge for the left floodplain, the right floodplain and the main channel.

2) Columns from the 6th through the 8th show the calculated water depth using the relationship of discharge vs. water depth for each discharge for the left floodplain, the right floodplain and the main channel.

3) Columns from the 9th through the 10th show the calculated shear stress around the toe of the left and right abutments using the equation (12).

4) The 11th column shows the maximum shear stress around the pier using the equation (6), and the 12th column shows the maximum contraction shear stress in the middle line of channel using the equation (9).

5) The 13th and the 14th column show the maximum scour depth around the toe of left and right abutment, respectively, using equation (11).

6) Columns from the 15th through 18th show the time dependent abutment scour depth, contraction scour depth and pier scour depth using equation (1) through (4).

7) Columns from the 19th through 25th show the combined summation of each scour depth.

Figure 49 shows the **Output Table**. (Note: mostly values on the left and right floodplain are zero because the water level in normal condition is lower than the elevation of floodplains.)

Figure 50 through Figure 53 show examples of **Output Plots** for left floodplain and abutment scour.

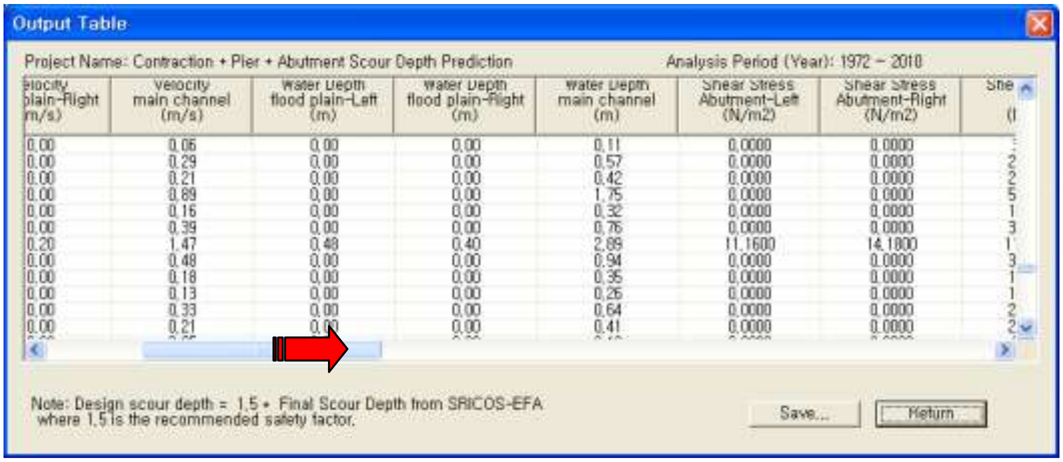

Velocity flood plain-Right (m/s)	Velocity main channel (m/s)	Water Depth flood plain-Left (m)	Water Depth flood plain-Right (m)	Water Depth main channel (m)	Shear Stress Abutment-Left (N/m2)	Shear Stress Abutment-Right (N/m2)
0.00	0.06	0.00	0.00	0.11	0.0000	0.0000
0.00	0.29	0.00	0.00	0.57	0.0000	0.0000
0.00	0.21	0.00	0.00	0.42	0.0000	0.0000
0.00	0.89	0.00	0.00	1.75	0.0000	0.0000
0.00	0.16	0.00	0.00	0.32	0.0000	0.0000
0.00	0.39	0.00	0.00	0.76	0.0000	0.0000
0.20	1.47	0.48	0.40	2.89	11.1600	14.1800
0.00	0.48	0.00	0.00	0.94	0.0000	0.0000
0.00	0.18	0.00	0.00	0.35	0.0000	0.0000
0.00	0.13	0.00	0.00	0.26	0.0000	0.0000
0.00	0.33	0.00	0.00	0.64	0.0000	0.0000
0.00	0.21	0.00	0.00	0.41	0.0000	0.0000

Figure 49 – Output Table.

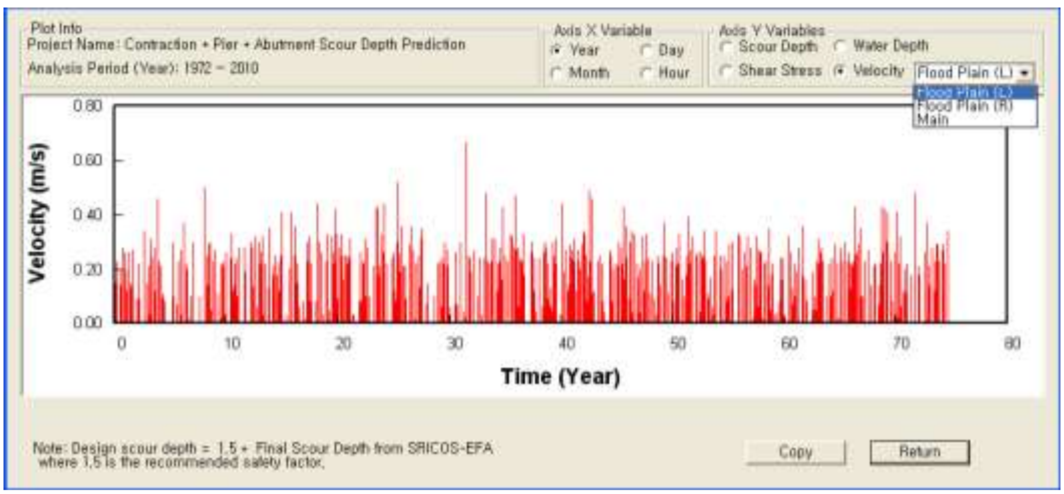

Figure 50 – Example of Output Plots (flow Velocity on Left Floodplain vs. Time).

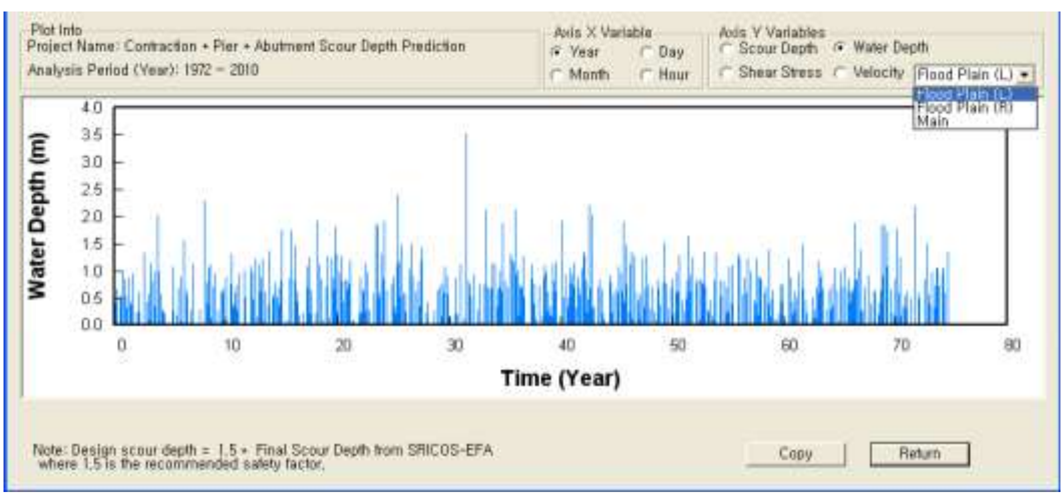

Figure 51 – Example of Output Plots (Water Depth on Left Floodplain vs. Time).

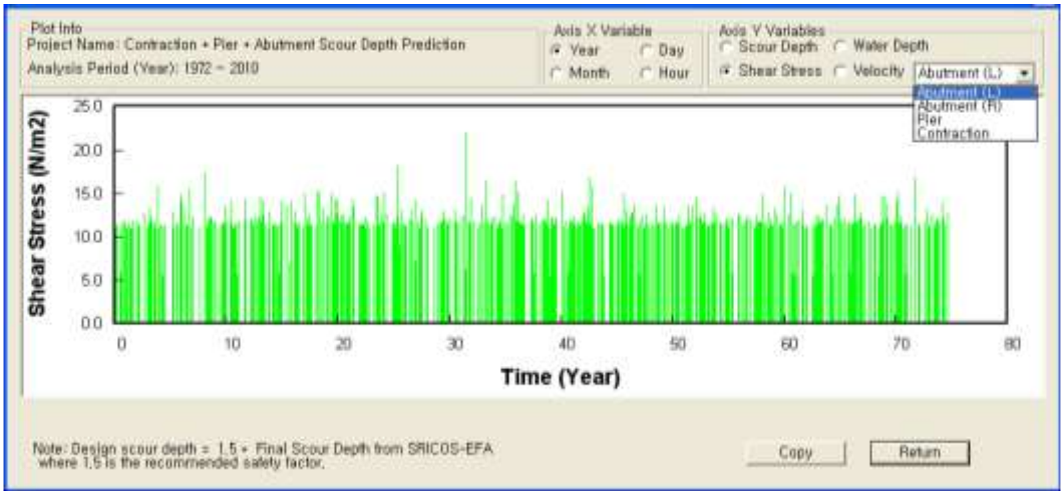

Figure 52 – Example of Output Plots (Shear Stress around the toe of Left Abutment vs. Time).

Figure 53 – Example of Output Plots (Scour Depth around the toe of Left Abutment vs. Time).

RISK ANALYSIS I – PREDICTION OF FUTURE SCOUR DEPTH USING EXISTING HYROGRAPH

The SRICOS-EFA can generate future hydrographs using existing hydrograph. The method is mentioned in the section of ***Existing hydrograph method*** in **FUTURE HYDROGRAPHS AND SCOUR RISK ANALYSIS**. For more detail, please refer that section.

DATA INPUT:

Following procedures (step 1 through step 5) are same with the procedures in the section of EVALUATION OF SCOUR DEPTH USING HYDROGRAPH.

1) General information
2) Scour type selection
3) Unit system selection
4) Geometry data input
5) Soil data input

Same as section of EVALUATION OF SCOUR DEPTH USING HYDROGRAPH

6) Water data input: every sub step is same with previous section except following
   a) Check the option of Risk Analysis and File.
   b) Enter the number of iteration in No. of Runs.
   c) Enter Hydrograph Time for the bridge design

   The red square in Figure 54 shows the difference in Water Data input window compared to EVALUATION OF SCOUR DEPTH USING HYDROGRAPH.

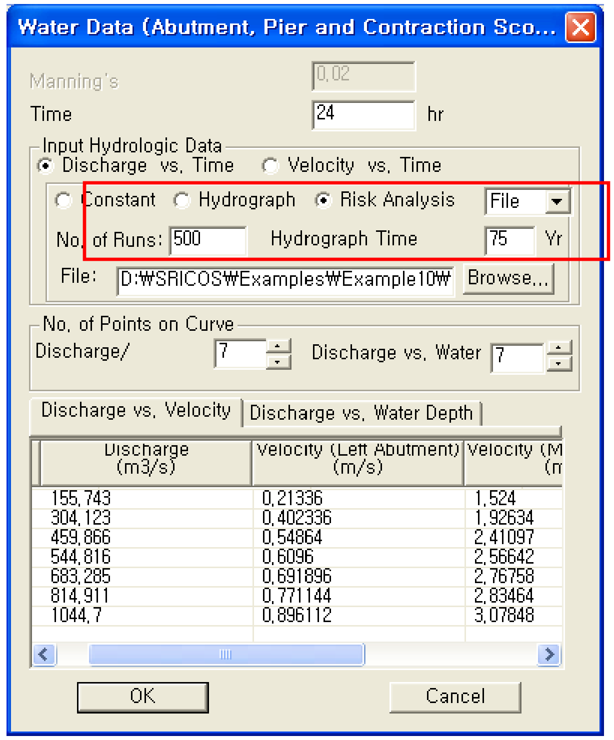

Figure 54 – Water Data input window for Risk Analysis using existing hydrograph.

REVIEW OF INPUT TABLES AND PLOTS

The procedures are same as section of EVALUATION OF SCOUR DEPTH USING HYDROGRAPH. For the information of Review of Input Tables and Plots, please refer to the Section of EVALUATION OF SCOUR DEPTH USING HYDROGRAPH.

PERFORM THE SCOUR ANALYSIS

The Risk Analysis method requires you to be patient because this method generates hydrographs and iterates as many as **No. of Runs** to get the results. The progress bar as shown at the bottom of Figure 55 (red rectangular) indicates the state of Risk Analysis calculation. Since it is a method of statistics, the more **No. of Runs** make the better results.

VIEWING RESULTS

After finishing the computation, all computation results can be reviewed. The output options include **Output Table** and **Output Plots**. The **Output Table** and **Output Plots** are available from the **Output** menu and the **Output Table** and **Output Plots** icons on the tools bar menu in the SRICOS-EFA main program window. You can save the Output Table as an Excel file for better review of all calculated results by clicking **Save** button below the table.

Different with the results in EVALUATION OF SCOUR DEPTH USING HYDROGRAPH, the result of each line in the **Output Table** is the final scour depth of all possible scour type using virtually made hydrograph. Thus if the **No. of Runs** is 100, the length of output table will be 100 lines. Figure 56 shows the example of the **Output Table** of the risk analysis. Figure 57 shows the example of **Output Plot** for the frequency of occurrence, and Figure 58 shows the example of **Output Plot** for the probability of exceedance.

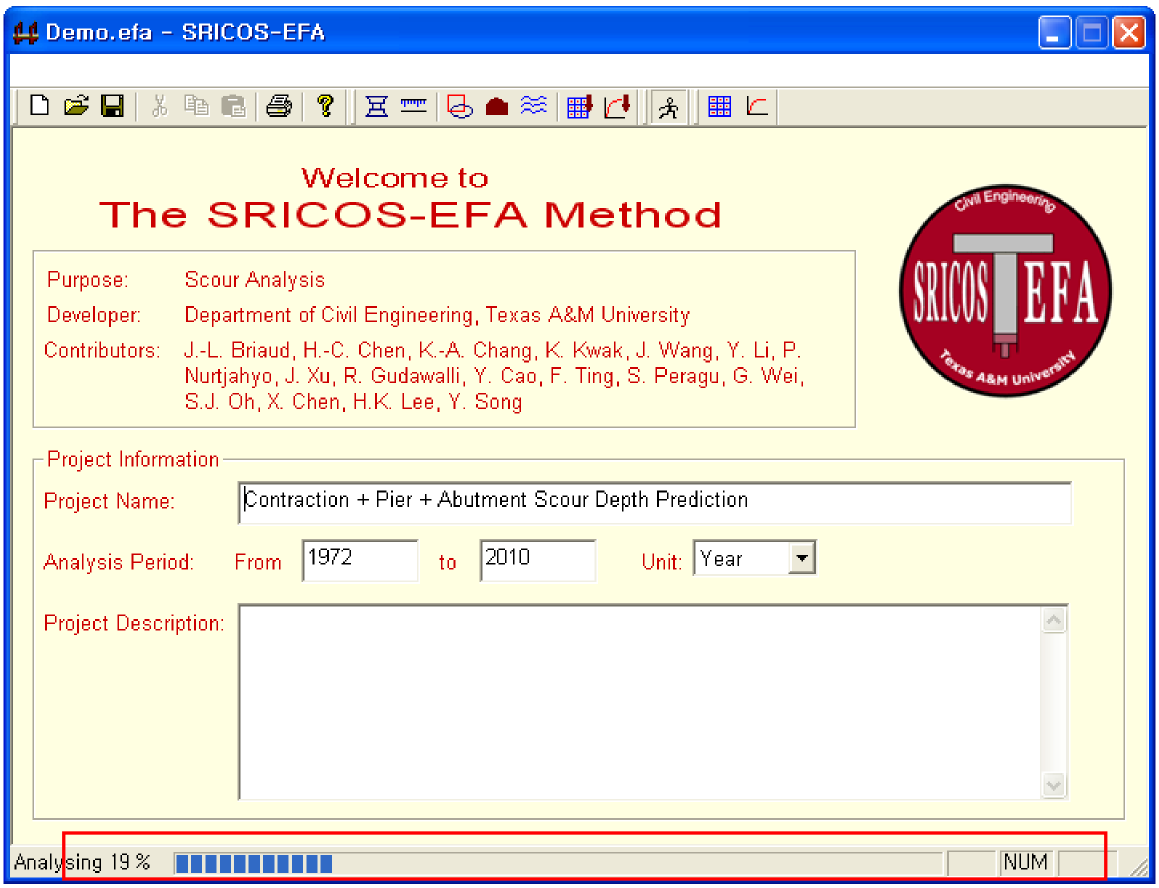

Figure 55 – Main window of program during risk analysis calculation.

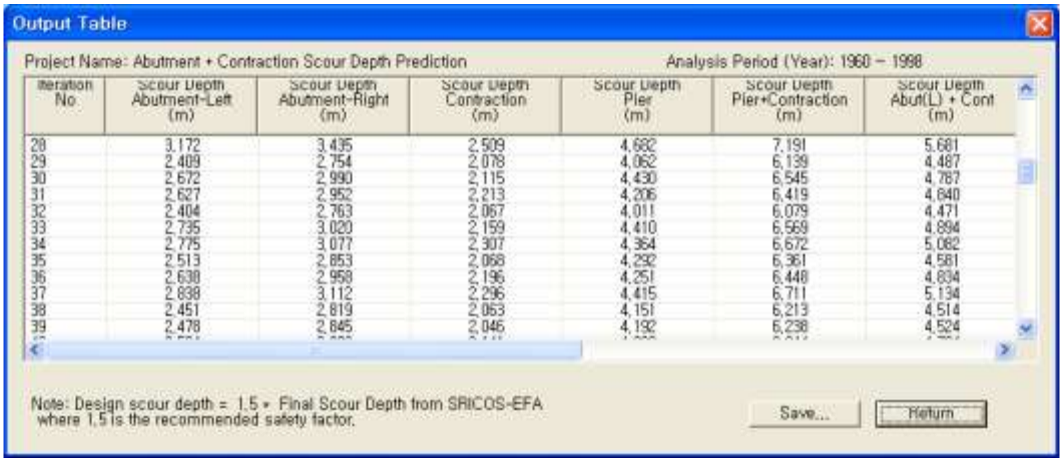

Output Table

Project Name: Abutment + Contraction Scour Depth Prediction — Analysis Period (Year): 1960 – 1998

Iteration No.	Scour Depth Abutment-Left (m)	Scour Depth Abutment-Right (m)	Scour Depth Contraction (m)	Scour Depth Pier (m)	Scour Depth Pier+Contraction (m)	Scour Depth Abut(L) + Cont (m)
28	3.172	3.435	2.509	4.682	7.191	5.681
29	2.409	2.754	2.078	4.062	6.139	4.487
30	2.672	2.990	2.115	4.430	6.545	4.787
31	2.627	2.952	2.213	4.206	6.419	4.840
32	2.404	2.763	2.067	4.011	6.079	4.471
33	2.735	3.020	2.159	4.410	6.569	4.894
34	2.775	3.077	2.307	4.364	6.672	5.082
35	2.513	2.853	2.068	4.292	6.361	4.581
36	2.638	2.958	2.196	4.251	6.448	4.834
37	2.838	3.112	2.296	4.415	6.711	5.134
38	2.451	2.819	2.063	4.151	6.213	4.514
39	2.478	2.845	2.046	4.192	6.238	4.524

Note: Design scour depth = 1.5 * Final Scour Depth from SRICOS-EFA
where 1.5 is the recommended safety factor.

Save... Return

Figure 56 – Example of the Output Table for risk analysis.

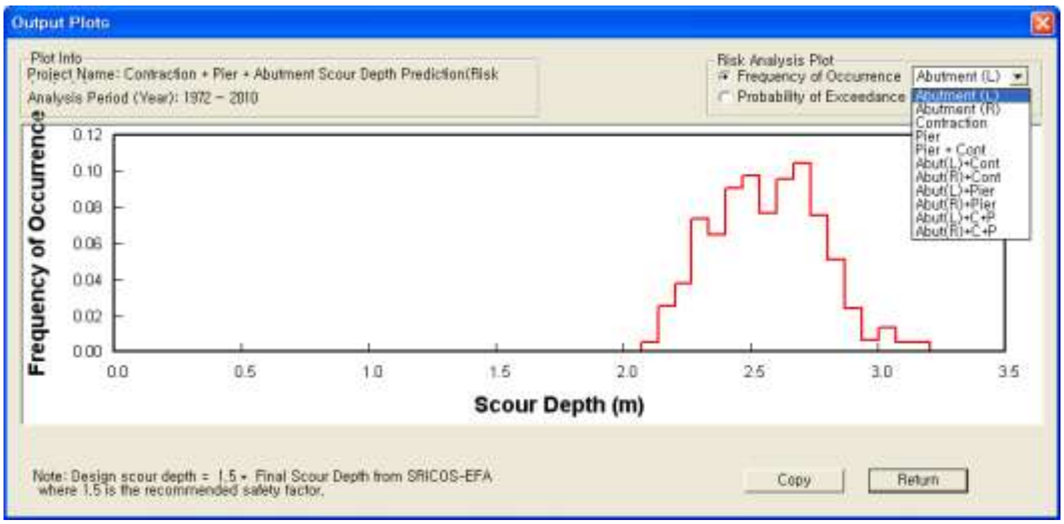

Figure 57 – Example of Frequency of Occurrence.

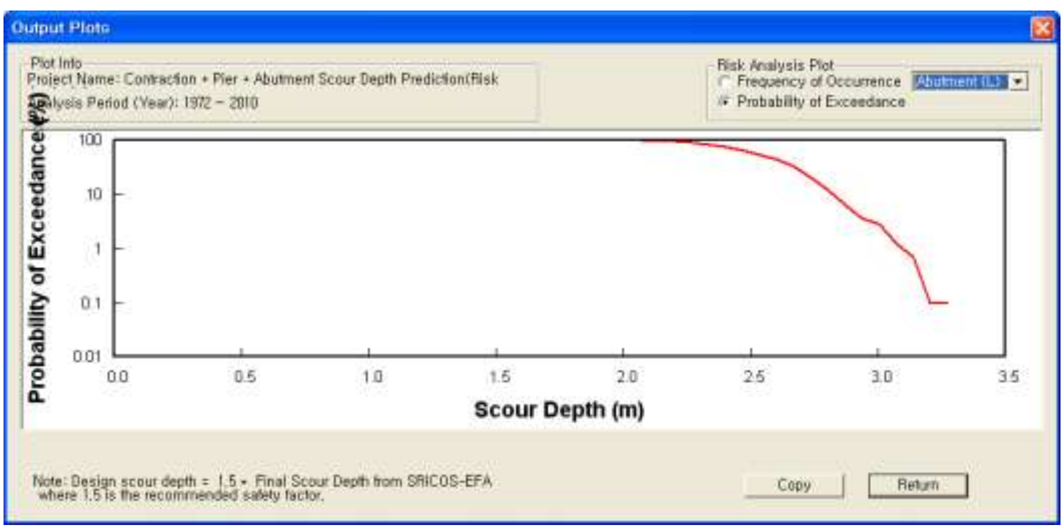

Figure 58 – Example of Probability of Exceedance.

RISK ANALYSIS II – PREDCITION OF FUTURE SCOUR DEPTH USING Q_{100} AND Q_{500} METHOD

The SRICOS-EFA can generate future hydrographs using existing hydrograph. The method is mentioned in the section of ***Q_{100} and Q_{500} method*** in **FUTURE HYDROGRAPHS AND SCOUR RISK ANALYSIS**. For more detail, please refer that section.

DATA INPUT:

Following procedures (step 1 through step 5) are same with the procedures in the section of EVALUATION OF SCOUR DEPTH USING HYDROGRAPH.

1) General information
2) Scour type selection
3) Unit system selection
4) Geometry data input
5) Soil data input

Same as section of EVALUATION OF SCOUR DEPTH USING HYDROGRAPH

6) Water data input: every sub step is same with previous section except following
   a) Check the option of Risk Analysis and Value.
   b) Enter the number of iteration in No. of Runs.
   c) Enter discharges for 100 year flood and 500 year flood.

The red square in Figure 59 shows the difference in Water Data input window compared to EVALUATION OF SCOUR DEPTH USING HYDROGRAPH.

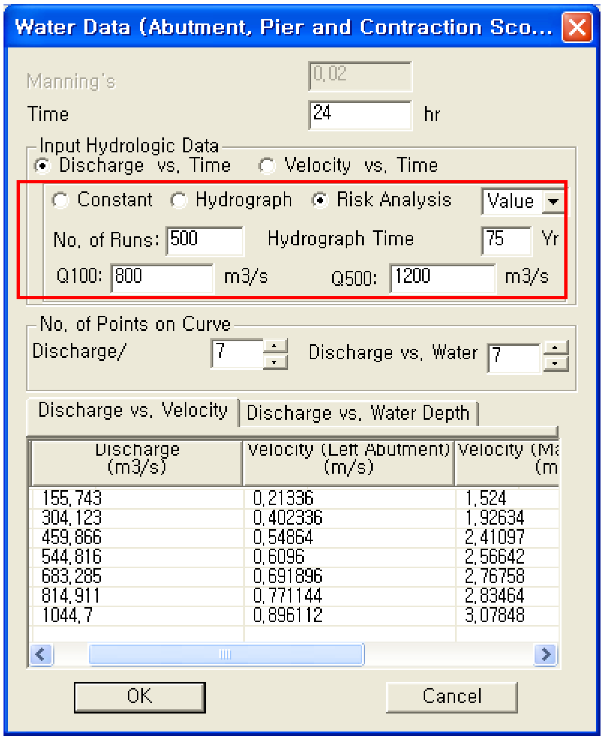

Figure 59 – Water Data input window for Risk Analysis using Q_{100} and Q_{500} method.

REVIEW OF INPUT TABLES AND PLOTS

The procedures are same as the section of EVALUATION OF SCOUR DEPTH USING HYDROGRAPH. For the information of Review of Input Tables and Plots, please refer to the Section of EVALUATION OF SCOUR DEPTH USING HYDROGRAPH.

PERFORM THE SCOUR ANALYSIS

The procedures are same as the section of Risk analysis I – prediction of future scour depth using existing hydrograph. For details, please refer to the Section of Risk analysis I – prediction of future scour depth using existing hydrograph.

VIEWING RESULTS

The procedures are same as the section of Risk analysis I – prediction of future scour depth using existing hydrograph. For details, please refer to the Section of Risk analysis I – prediction of future scour depth using existing hydrograph.

EXAMPLE 1 (METHOD A)

Problem A round nose pier, with 2 m in width and 6 m in length, is located in 7.89 m deep water with an approach flow velocity of 1.4 m/s and the attack angle is 0^{o}, as shown in Figure EX. 1. The EFA test was conducted using the soil sample obtained around pier and abutment, and the erosion function of soil is given in Figure EX. 2. The critical shear stress of soil is 3.96 Pa. The Manning's roughness coefficient is 0.018, and the duration of flood is 48 hour. Find the pier scour depth after 48 hour of flood.

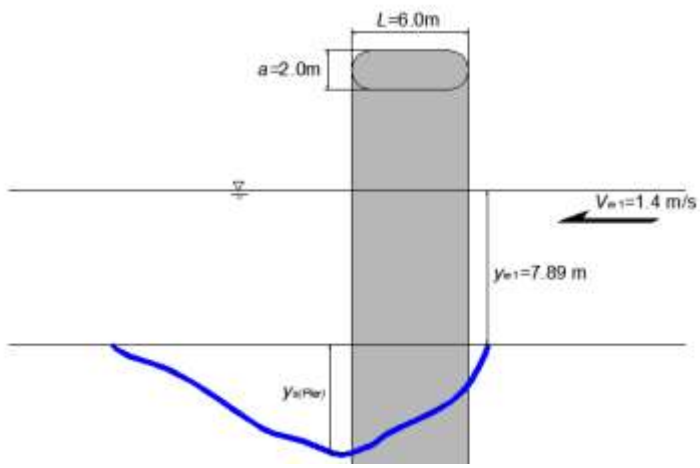

Figure EX. 1 – Pier scour example.

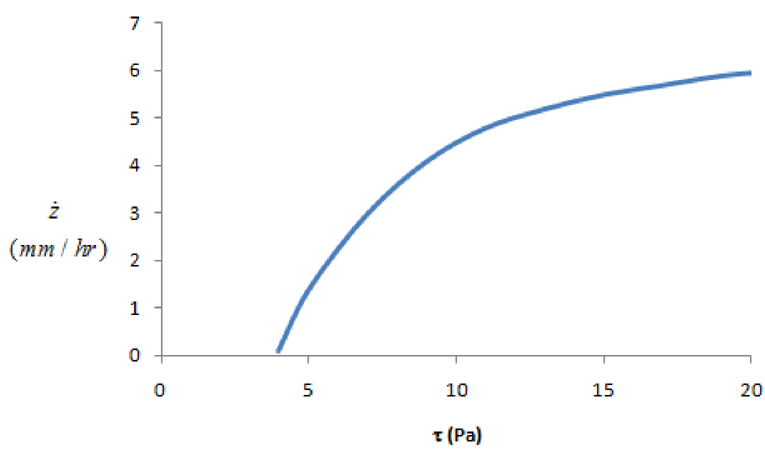

Figure EX. 2 – Erosion function of soil.

Solution. The maximum scour depth and the maximum shear stress around pier in given condition can be calculated according to Eq.(13) and (14), respectively. The step by step calculation is:

Maximum scour depth:

The correction factors for water depth (K_w), pier shape (K_1), pier aspect ratio (K_L) and pier spacing (K_{sp}) is 1.0. Froude number calculated with the approach velocity and pier width is $Fr_{(pier)} = \frac{V_1}{\sqrt{g \cdot a'}} = \frac{1.4}{\sqrt{9.81 \cdot 2}} = 0.316$, and the critical pier Froude number is

$$Fr_{c(pier)} = \frac{V_c}{\sqrt{g \cdot a}} = \sqrt{\frac{\tau_c \cdot y_1^{1/3}}{\rho \cdot g \cdot n^2}} / \sqrt{g \cdot a} = \sqrt{\frac{3.96 \times 7.89^{1/3}}{9.81 \times 1000 \times 0.018^2}} / \sqrt{9.81 \times 2} = 0.356$$

Therefore the maximum pier scour depth in given condition is:

$$\begin{aligned} y_{s(Pier)} &= 2.2 \cdot K_w \cdot K_1 \cdot K_L \cdot K_{sp} \cdot a'\left(2.6 \cdot Fr_{(pier)} - Fr_{c(pier)}\right)^{0.7} \\ &= 2.2 \cdot 1.0 \cdot 1.0 \cdot 1.0 \cdot 1.0 \cdot 2.0 \cdot (2.6 \cdot 0.316\text{-}0.356)^{0.7} \\ &= 2.58\text{m}=2{,}580\text{mm} \end{aligned}$$

Maximum shear stress around pier:

The correction factors for water depth (k_w) is 1.0, pier spacing (k_{sp}) is 1.0, attack angle (k_α) is 1.0, and pier shape $\left(k_{sh} = 1.15 + 7e^{-4\frac{L}{a}} = 1.15 + 7e^{-4 \cdot 3}\right)$ is 1.15. The Reynolds number defined with pier width is $\left(\text{Re} = \frac{1.4 \times 2}{10^{-6}}\right)$ is 2,800,000.

Therefore the maximum shear stress around pier in given condition is:

$$\begin{aligned} \tau_{\max(pier)} &= k_w k_{sh} k_{sp} k_\theta \cdot 0.094 \rho V_1^2 \left[\frac{1}{\log \text{Re}} - \frac{1}{10}\right] \\ &= 1.0 \times 1.15 \times 1.0 \times 1.0 \times 0.094 \times 1000 \times 1.4^2 \left[1/\log 2800000 - 1/10\right] \\ &= 11.676 \text{ Pa} \end{aligned}$$

The initial rate of scour:

$\dot{z}_i$ pier is read on the EFA curve at $\tau = \tau_{\max}$, and it is 4.8 mm/hr, as shown in Figure EX. 3 :

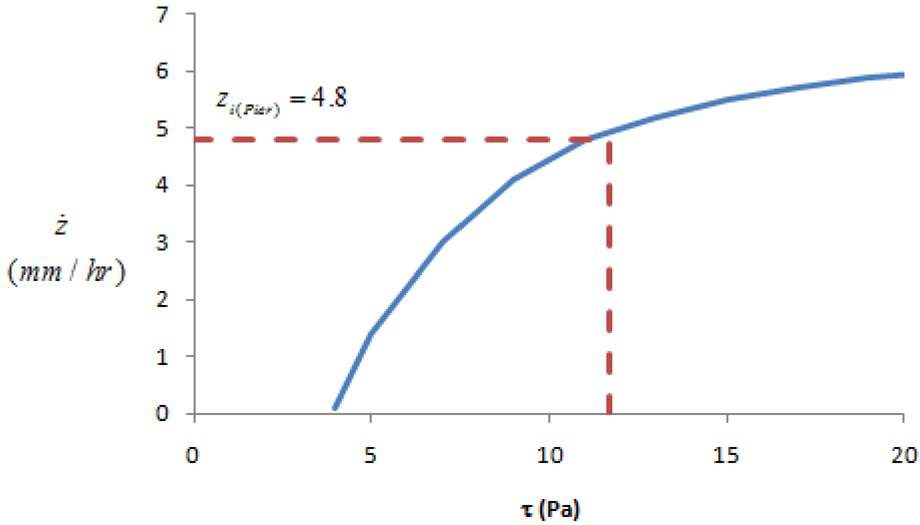

Figure EX. 3 – Erosion function and the initial erosion rate of pier.

The depth of pier scour after 48 hour flood can be calculated using Eq.(1), and it is:

$$y_s(t) = \frac{t(hrs)}{\frac{1}{\dot{z}_i} + \frac{t(hrs)}{y_s}} = \frac{48}{\frac{1}{4.8} + \frac{48}{2580}} = 211.5mm$$

Therefore the pier scour depth generated by 48 hour flood is 8.2 % of the maximum pier scour depth

EXAMPLE 2 (METHOD A)

Problem Geometries of channel and bridge are given as Figure EX. 4. The compound channel is symmetrical, and The discharge during flood is $Q = 2,000 m^3 / s$. The Manning's roughness coefficient is 0.018. The erosion function of soil in both floodplain and main-channel is obtained after EFA test, and it is given in Figure EX. 2. The duration of flood is 48 hours, and the hydraulic data after HEC-RAS run are obtained as following

$V_1 = 1.13 m/s, V_{f1} = 0.78 m/s, V_{m1} = 1.40 m/s,\ R_{h_1} = 3.65 m,\ y_{f1} = 2.55 m,\ y_{m1} = 7.89 m,$

$V_2 = 1.75 m/s\ , V_{m2} = 1.83 m/s$

Find the abutment scour depth and contraction scour after 48 hour of flood.

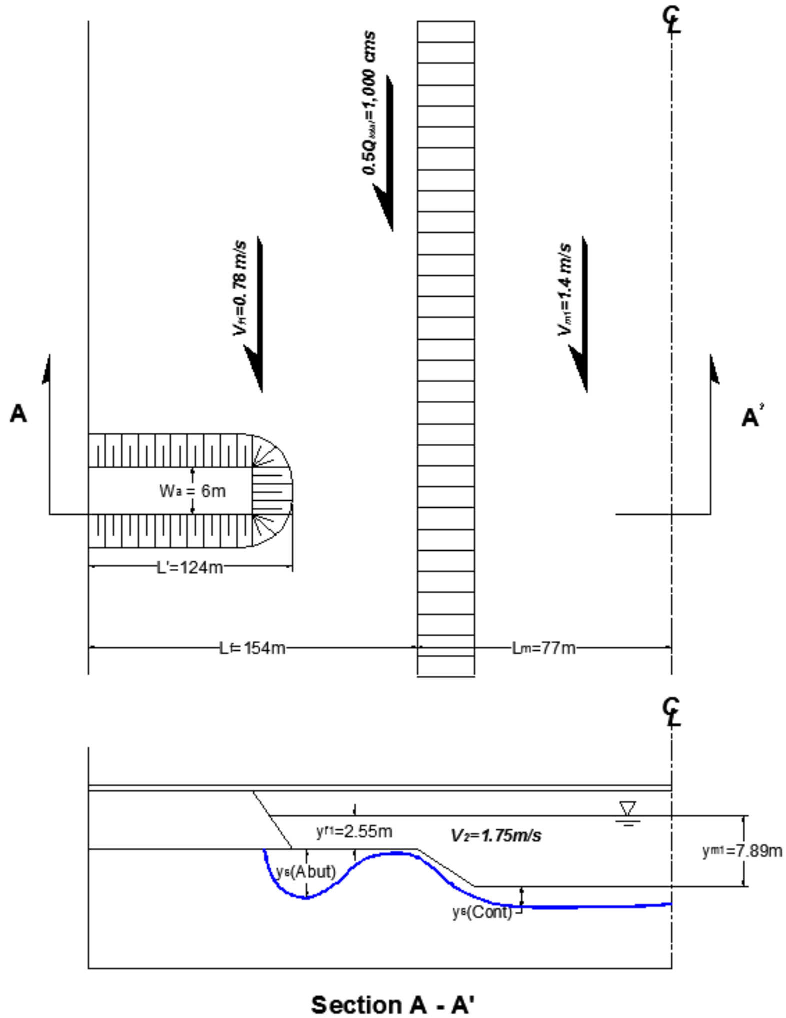

Figure EX. 4 – Channel geometry.

Solution. The maximum shear stress in the middle of channel and around abutment can be calculated according to Eq. (17) and (20), respectively. The maximum shear stresses in this flow condition are:

$$\begin{aligned}\tau_{\max(Cont)} &= k_R \cdot k_L \cdot k_\theta \cdot k_W \cdot \gamma \cdot n^2 \cdot V_1^2 \, \mathrm{R}_h^{-1/3} \\ &= 1.44 \times 0.83 \times 1.9 \times 1 \times 9810 \times 0.018^2 \times 1.4^2 \times 3.65^{-1/3} \\ &= 5.98 Pa\end{aligned}$$

$$\begin{aligned}\tau_{\max(Abut)} &= 12.45 \cdot k_c \cdot k_{sh} \cdot k_{Fr} \cdot k_s \cdot k_L \cdot \rho \cdot V_1^2 \, \mathrm{Re}^{-0.45} \\ &= 12.45 \times 2.74 \times 0.41 \times 1.27 \times 0.65 \times 1000 \times 1.13^2 \times \left(6.78 \times 10^6\right)^{-0.45} \\ &= 12.45 Pa\end{aligned}$$

The initial rate of scour $\dot{z}_i$ for contraction scour and abutment scour are read on the EFA curve at $\tau = \tau_{\max}$, and it is 2.15 and 5.1, respectively as shown in Figure EX. 5.

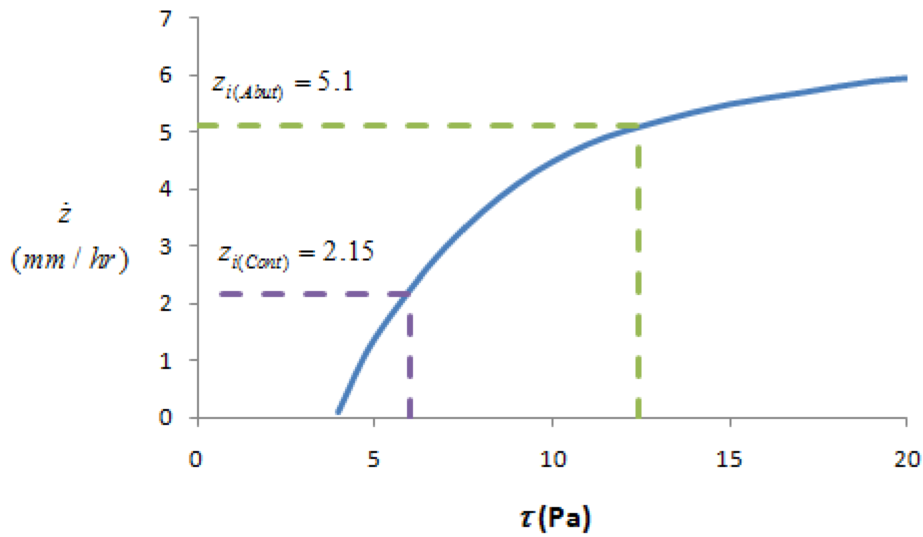

Figure EX. 5 – Erosion function and initial erosion rate for contraction scour and abutment scour.

The maximum contraction scour depth $y_{s(Cont)}$, and the maximum abutment scour depth $y_{s(Abutment)}$ can be calculated according to Eq. (15) and (19). Since the distance of setback is 30 m and the water depth in main-channel is 7.89 m, the degree of setback for this condition is short setback. The local velocity for short setback is the average velocity at bridge section $\left(V_2 = 1.75 m/s\right)$. The Froude number in the main-channel is $Fr_{(Cont)} = \dfrac{V_2}{\sqrt{g \cdot y_{m1}}} = \dfrac{1.75}{\sqrt{9.81 \times 7.89}} = 0.199$, the Froude number around the toe of abutment is $Fr_{(Abut)} = \dfrac{V_2}{\sqrt{g \cdot y_{f1}}} = \dfrac{1.75}{\sqrt{9.81 \times 2.55}} = 0.35$, the critical Froude number in main-channel is

$$Fr_{c(Cont)} = \frac{V_c}{\sqrt{g \cdot y_{m1}}} = \frac{\sqrt{\tau_c / \rho}}{gny_{m1}^{1/3}} = \frac{\sqrt{3.96/1000}}{9.81 \times 0.018 \times 7.89^{1/3}} = 0.179$$, the critical Froude number around the toe of abutment is

$$Fr_{c(Abut)} = \frac{V_c}{\sqrt{g \cdot y_{f1}}} = \frac{\sqrt{\tau_c / \rho}}{gny_{f1}^{1/3}} = \frac{\sqrt{3.96/1000}}{9.81 \times 0.018 \times 2.55^{1/3}} = 0.261$$, and the Reynolds number around the toe of abutment is $\mathrm{Re}_{f2} = \dfrac{V_{f2} \times y_{f1}}{\nu} = \dfrac{1.75 \times 2.55}{10^{-6}} = 4,462,500$.

The maximum scour depths in this flow condition are:

$$\begin{aligned}
y_{s(Cont)} &= 2.21\left(1.31 \cdot Fr_{(Cont)} - Fr_{c(Cont)}\right) \cdot y_{m1} \\
&= 2.21 \times \left(1.31 \times \frac{1.75}{\sqrt{9.81 \times 7.89}} - 0.179\right) \times 7.89 \\
&= 1.42 m
\end{aligned}$$

$$\begin{aligned}
y_{s(Abut)} &= K_1 \cdot K_2 \cdot K_L \cdot K_G \cdot K_p \cdot 243 \cdot \mathrm{Re}_{f2}^{-0.28} \cdot \left(1.65 \cdot Fr_{f2} - Fr_{fc}\right) \cdot y_{f1} \\
&= 0.73 \times 1.0 \times 1.0 \times 1.0 \times 1.0 \times 243 \times 4462500^{-0.28} \times \left(1.65 \times 0.35 - 0.261\right) \cdot 2.55 \\
&= 1.97 m
\end{aligned}$$

The depth of pier scour after 48 hour flood can be calculated using Eq.(1), and it is:

$$y_{s(Cont)}(t) = \frac{t(hrs)}{\dfrac{1}{\dot{z}_i} + \dfrac{t(hrs)}{y_s}} = \frac{48}{\dfrac{1}{2.15} + \dfrac{48}{1420}} = 96.2 mm$$

$$y_{s(Abut)}(t) = \frac{t(hrs)}{\dfrac{1}{\dot{z}_i} + \dfrac{t(hrs)}{y_s}} = \frac{48}{\dfrac{1}{5.1} + \dfrac{48}{1970}} = 217.7 mm$$

Therefore the contraction scour depth generated by 48 hour flood is 6.8 % of the maximum contraction scour depth, while the abutment scour depth generated by same flood is 11.1 % of the maximum abutment scour depth.

EXAMPLE 3 (METHOD B)

Problem: The channel upstream width is 480 m, and a rectangular pier width 9.75 m width and 9.75 m length in the middle of channel (Figure EX. 6). The hydrograph in the terms of discharge is given in Figure EX. 7. The soil layer is 57.65 m thick and the critical shear stress is $3.9 N/m^2$. The EFA results are given in Figure EX. 8. Manning's n value of the channel bed material is 0.014. What is the magnitude of final pier scour depth after 39 years?

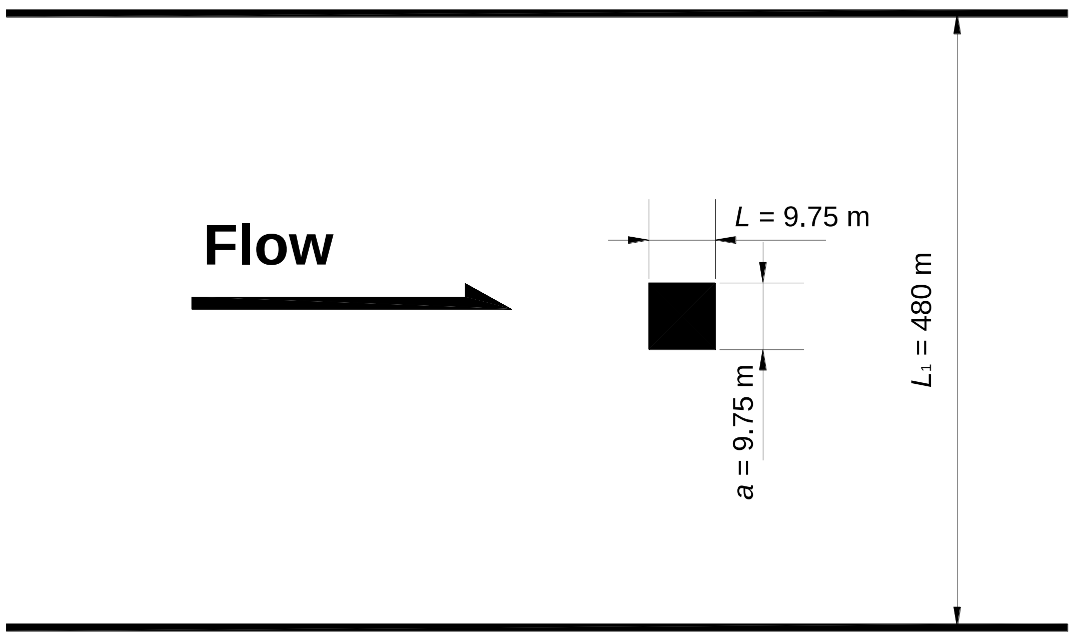

Figure EX. 6 – Channel and pier geometry.

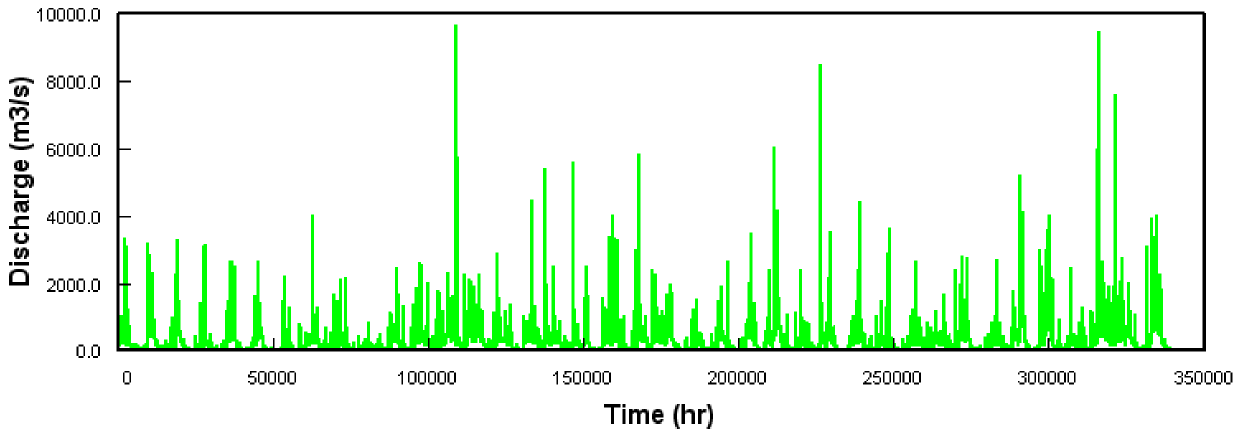

Figure EX. 7 – Hydrograph from 1960 to 1998 (341,640 hours).

Shear Stress (N/m2)	Scour Rate (mm/hr)
2.98	0.02
4.36	4.1
6.17	20.31
11.69	33.09
19.56	110.56
26.71	575.05
45.93	2153.77

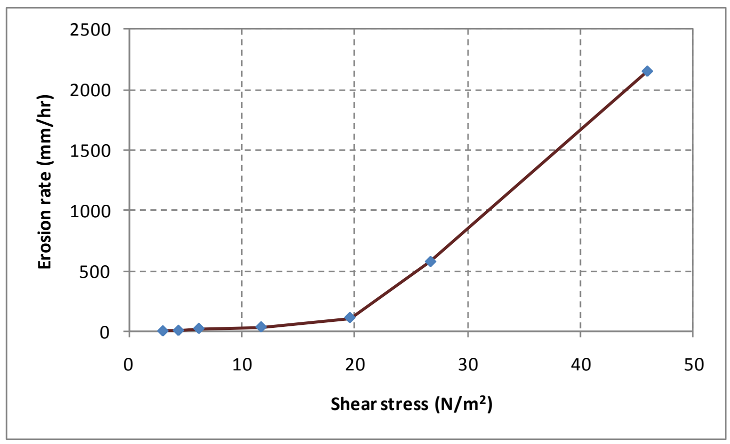

Figure EX. 8 – EFA results of soil layer.

Solution:

1. Define hydrologic relationships:

The relationships between the discharge and velocity, and between the discharge and water depth are required in order to convert the hydrograph in terms of discharge and time (Figure EX. 9) to hydrographs in terms of water depth and time, and of velocity and time. HEC-RAS can be the one of the good tool to find the relationships. The followings (Figure EX. 9 and Figure EX. 10) are the results obtained from HEC-RAS for this case.

Discharge (m^3/s)	Velocity (Main channel) (m/s)
1.42	0
14.2	0.02
57	0.07
142	0.16
566	0.49
1416	0.87
5663	1.75
13592	2.97

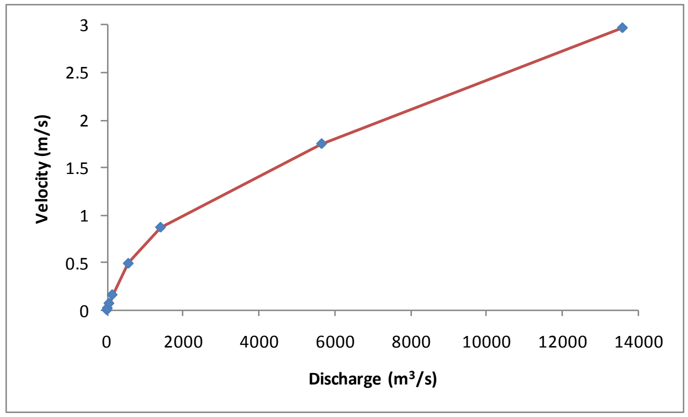

Figure EX. 9 – Relationship Discharge vs. Velocity (by HEC-RAS run).

Discharge (m^3/s)	Water Depth (Main Channel) (m)
1.42	0.18
14.2	3.86
57	4.55
142	5.02
566	6.18
1416	7.83
5663	11.33
13592	13.15

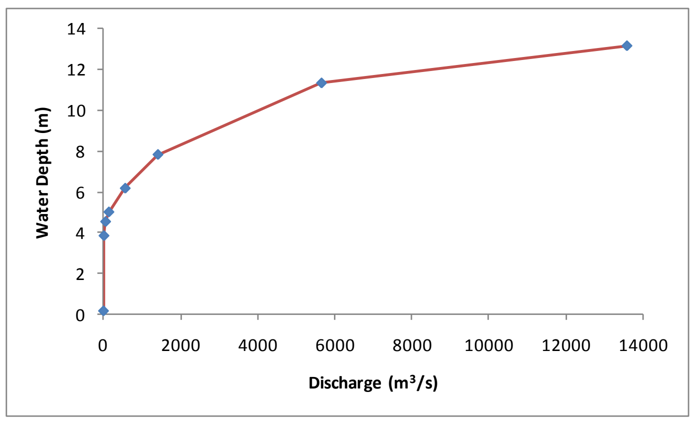

Figure EX. 10 – Relationship of Discharge vs. Water depth (by HEC-RAS run).

2. Data input

After inputting all information required for pier scour depth calculation in SRICOS-EFA program, the program will calculate the pier scour depth and the number of iteration equals to the number of data in hydrograph.

3. Data output

The calculated scour depth for floods in 39 years is plotted in Figure EX. 11, and the final pier scour depth is 9.35 m.

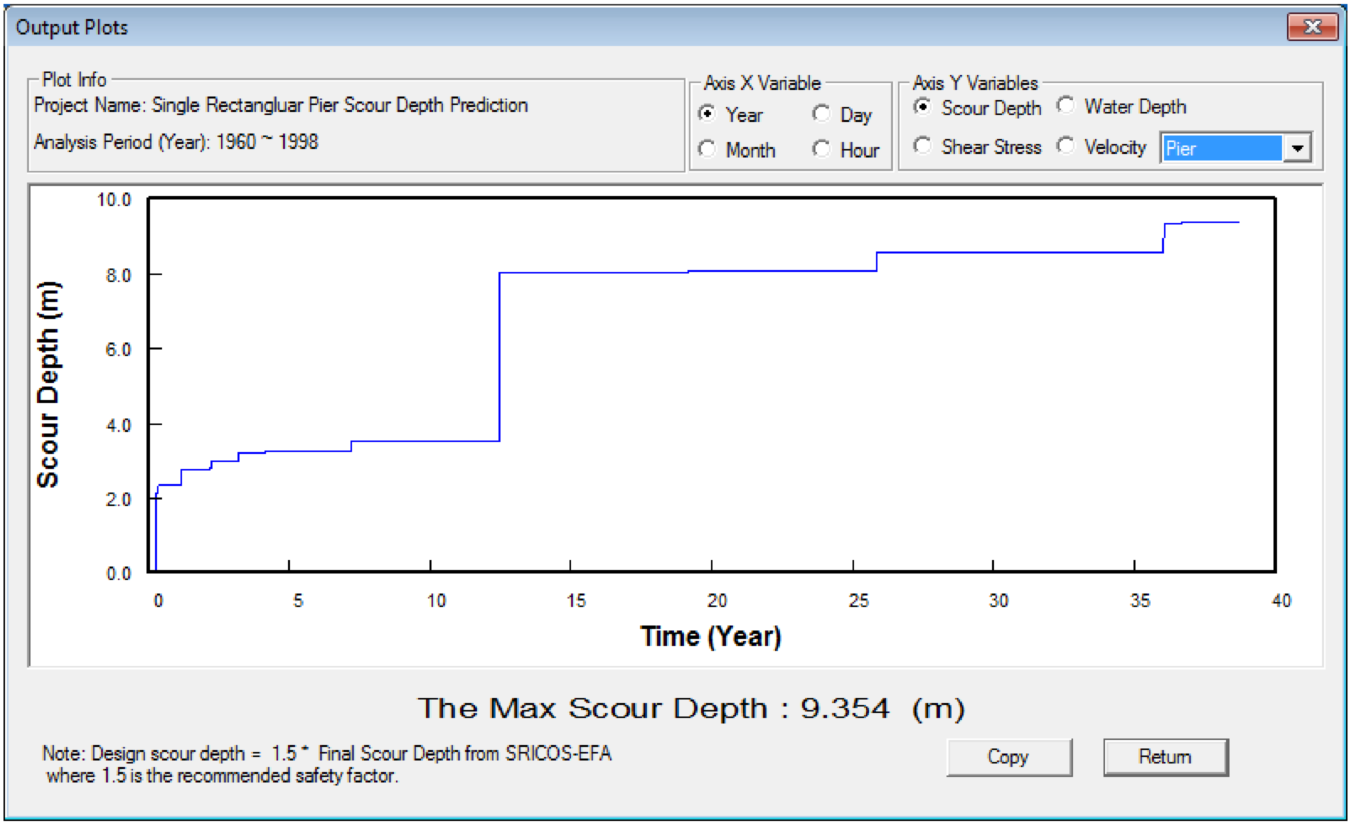

Figure EX. 11 – Development of pier scour depth for 39 years (Example 3).

EXAMPLE 4 (METHOD B)

Problem: The geometry of channel is given in Figure EX. 12. The hydrograph in the terms of discharge is given in Figure EX. 13. The bridge is 6 m wide. The soil layer is 57.65 m thick and the critical shear stress is $3.9 N/m^2$. The EFA results are given in Figure EX. 14, and the Manning's n value for both main-channel and floodplain is 0.02. What is the magnitude of final pier scour depth after 75 years?

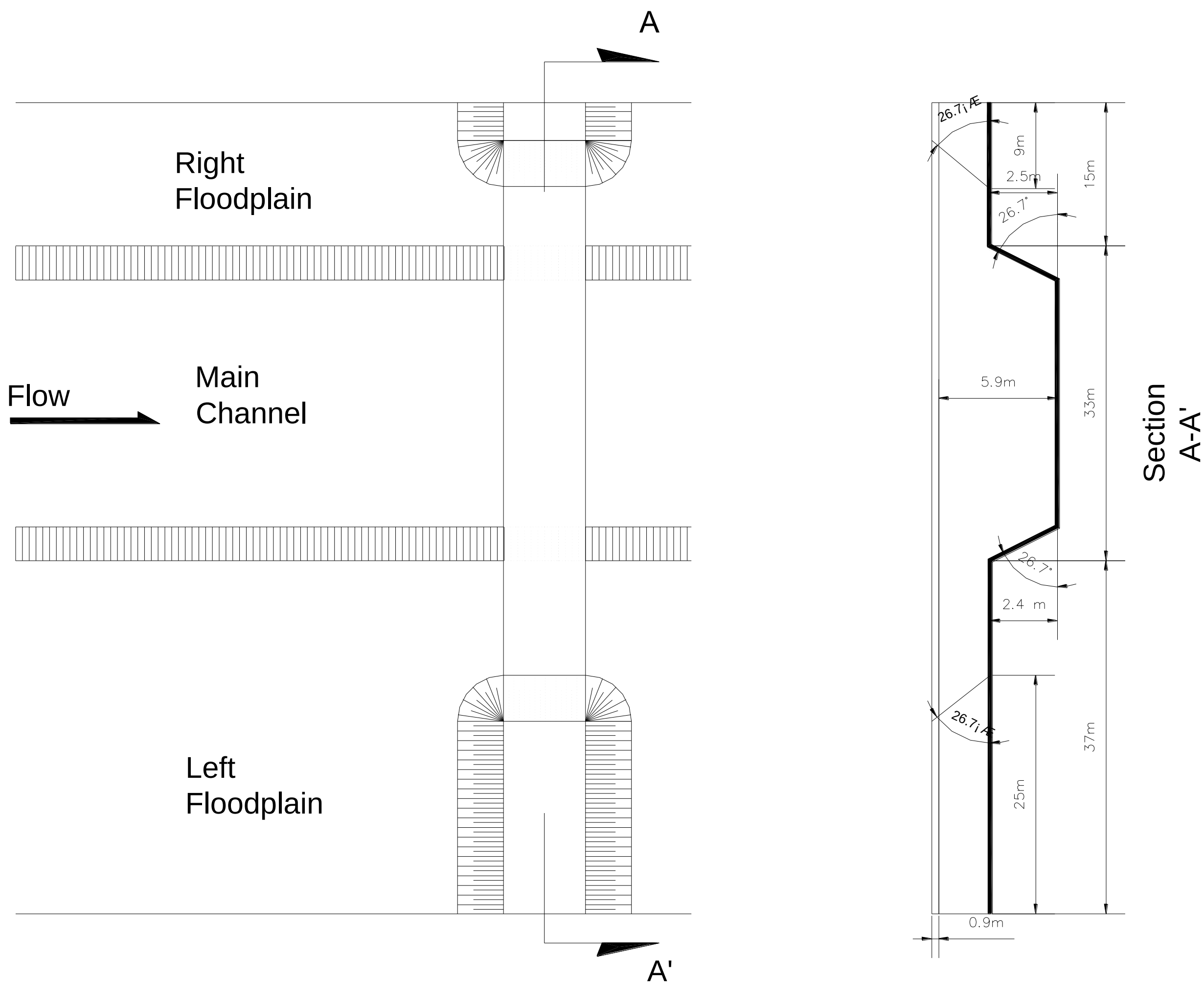

Figure EX. 12 – Channel geometry (Example 4).

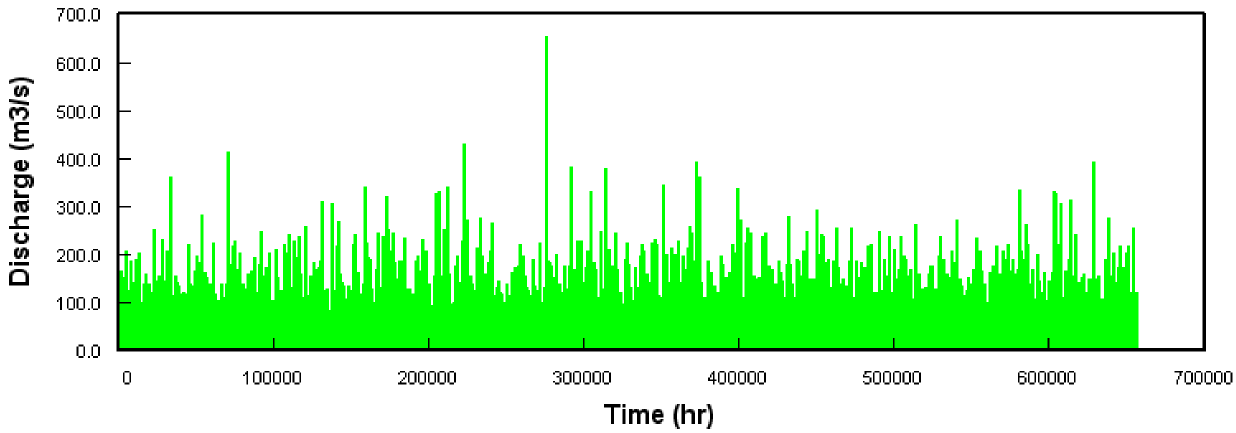

Figure EX. 13 – Hydrograph from 1932 to 2006 (657,000 hours).

Shear Stress (N/m2)	Scour Rate (mm/hr)
2.98	0.02
4.36	4.1
6.17	20.31
11.69	33.09
19.56	110.56
26.71	575.05
45.93	2153.77

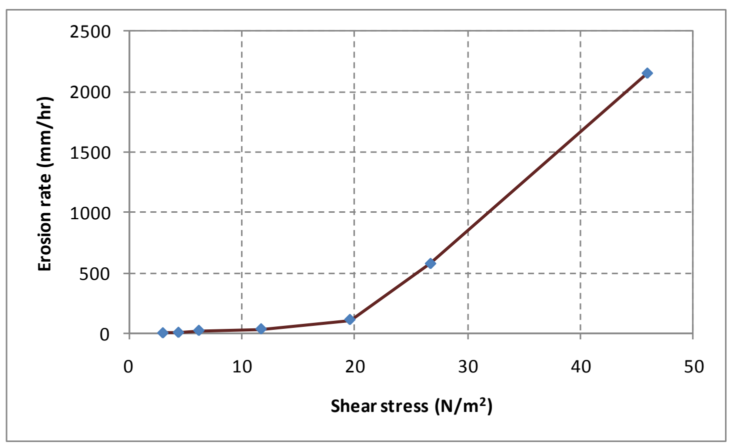

Figure EX. 14 – EFA results for soil layer (Example 4).

Solution:

1. Define hydrologic relationships:

The relationships between the discharge and velocity, and between the discharge and water depth are required in order to convert the hydrograph in terms of discharge and time (Figure EX. 14) to hydrographs in terms of water depth and time, and of velocity and time. HEC-RAS can be the one of the good tool to find the relationships. The followings (Figure EX. 15 and Figure EX. 16) are the results obtained from HEC-RAS for this case.

Discharge (m^3/s)	Velocity Left Abut. (m/s)	Main Channel (m/s)	Right Abut. (m/s)
75.28	0.00	0.75	0.00
155.74	0.21	1.52	0.25
304.12	0.40	1.93	0.52
459.87	0.55	2.41	0.76
544.82	0.61	2.57	0.86
683.28	0.69	2.77	1.00
814.91	0.77	2.83	0.94
1044.7	0.90	3.08	1.11

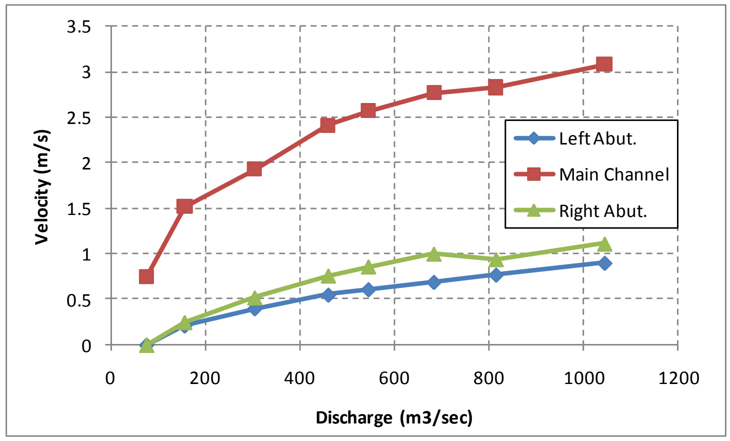

Figure EX. 15 – Relationship of Discharge vs. Velocity (by HEC-RAS run).

Discharge (m^3/s)	Water depth Left Abut. (m/s)	Main Channel (m/s)	Right Abut. (m/s)
75.28	0.00	1.45	0.00
155.74	0.59	2.99	0.50
304.12	1.71	4.12	1.63
459.87	2.55	4.96	2.47
544.82	2.98	5.39	2.90
683.28	3.66	6.07	3.58
814.91	4.48	6.89	4.40
1044.7	5.44	7.85	5.36

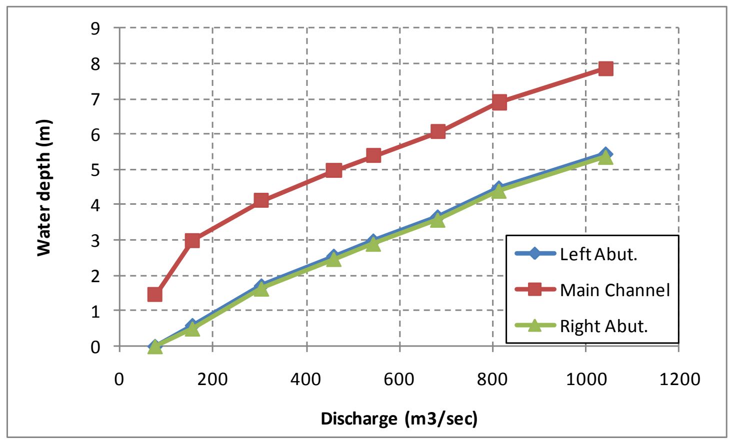

Figure EX. 16 – Relationship of Discharge vs. Water depth (by HEC-RAS run).

2. Data input

After inputting all information required for pier scour depth calculation in SRICOS-EFA program, the program will calculate the pier scour depth and the number of iteration equals to the number of data in hydrograph (657,000).

3. Data output

The calculated scour depth for floods in 75 years is plotted in Figure EX. 17, and the final scour depth of left abutment is 2.531 m, of right abutment is 2.9 m, and of contraction scour depth in the main-channel is 1.999 m.

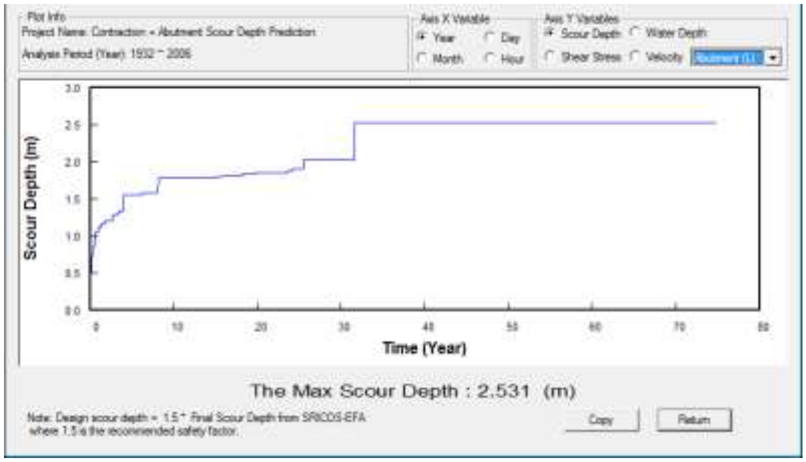

(a) At left abutment.

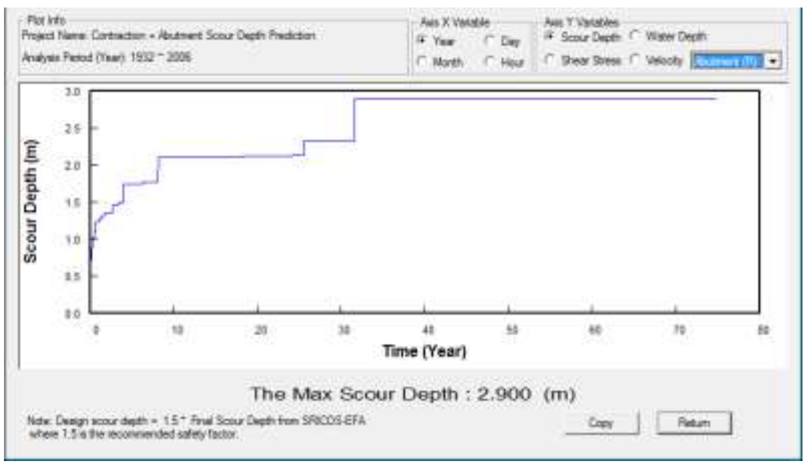

(b) At right abutment.

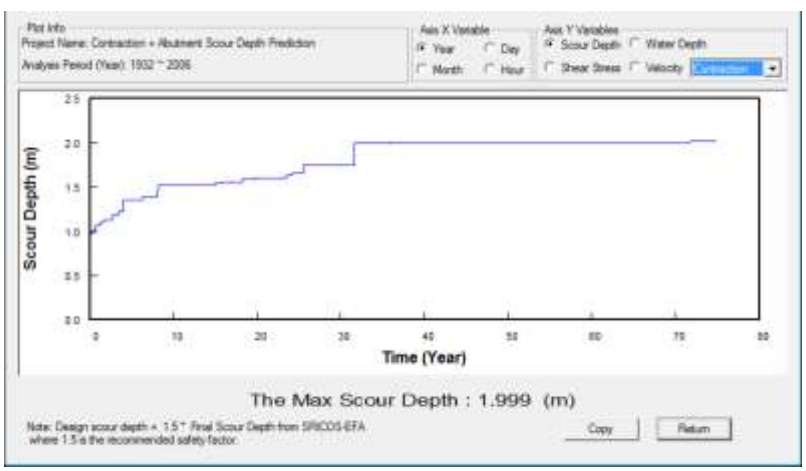

(c) Contraction scour in main-channel.

Figure EX. 17 – Development of Scour depth for 75 years.

EXAMPLE 5 (METHOD C)

Problem: Find the equivalent time for pier scour in Example 3. The recorded maximum velocity is 2.42 m/sec, and the maximum water depth is 12.3m. The duration of hydrograph is 39 years.

Solution:

Calculate of the maximum shear stress around pier for $V_1 = 2.42m/s$, and $y_{m1} = 12.3m$

The correction factors for water depth $\left(k_w = 1 + 16e^{\frac{-4y_1}{a}} = 1 + 16e^{\frac{-4\times12.3}{9.75}}\right)$ is 1.1, pier spacing $\left(k_{sp}\right)$ is 1.0, attack angle $\left(k_\alpha\right)$ is 1.0, and pier shape $\left(k_{sh} = 1.15 + 7e^{-4\frac{L}{a}} = 1.15 + 7e^{-4}\right)$ is 1.28. The Reynolds number defined with pier width is $\left(\mathrm{Re} = \frac{2.42\times9.75}{10^{-6}}\right)$ is 23,595,000.

Therefore the maximum shear stress around pier in given condition is:

$$\tau_{\max(pier)} = k_w k_{sh} k_{sp} k_\theta \cdot 0.094 \rho V_1^2 \left[\frac{1}{\log \mathrm{Re}} - \frac{1}{10}\right]$$
$$= 1.1\times1.28\times1.0\times1.0\times0.094\times1000\times2.42^2\left[1/\log 23595000 - 1/10\right]$$
$$= 27.65 \text{ Pa}$$

Find $\dot{z}_i$ (the initial rate of scour corresponding to the maximum velocity)

$\dot{z}_i$ (the initial rate of scour corresponding to the maximum velocity) is 600 mm/hr, as shown in Figure EX. 18.

The equivalent time of pier scour for this condition can be obtained by Eq. (21), and it is:

$$t_{equiv}\left(\text{hrs}\right) = 73\left(t_{hydro}\left(\text{years}\right)\right)^{0.126}\left(V_{\max}\left(\text{m/s}\right)\right)^{1.706}\left(\dot{z}_i\left(\text{mm/hr}\right)\right)^{-0.20}$$
$$= 73\times39^{0.126}\times2.42^{1.706}\times600^{-0.2}$$
$$= 145.5$$

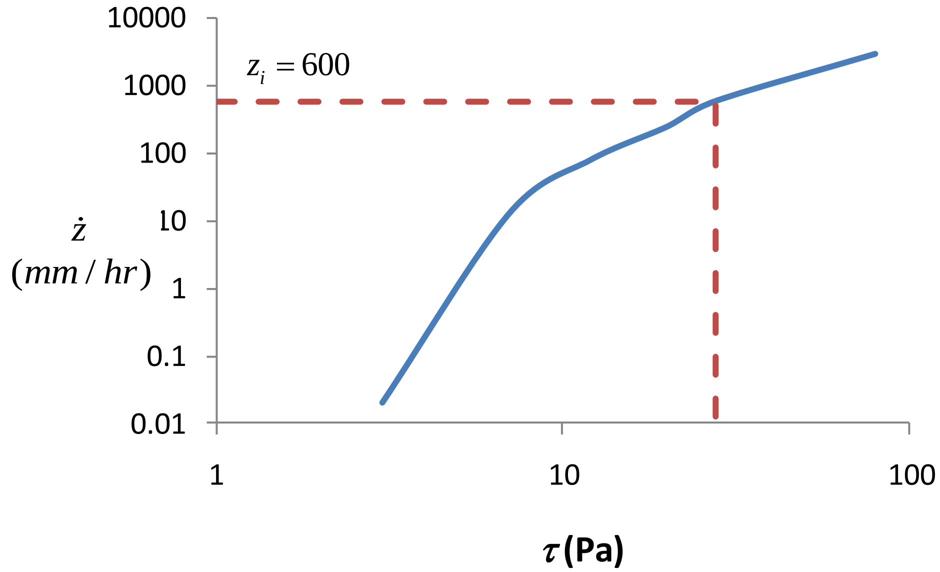

Figure EX. 18 – Erosion function and initial erosion rate corresponding to the maximum velocity. (Example 5)

EXAMPLE 6 (METHOD C)

Problem: Find the equivalent time for contraction scour in Example 4. The recorded maximum velocity is 2.82 m/sec, and the maximum hydraulic radius is 4.8 m. The duration of hydrograph is 75 years. The area ratio between the approach section and the bridge section is 1.52.

Solution:

Calculate the maximum shear stress in the main-channel for $V_1 = 2.82 m/s$, and $y_{m1} = 5.9m$.

The correction factor for contraction ratio $\left(k_R = 0.62 + 0.38 \left(A_1 / A_2 \right)^{1.75} = 0.62 + 0.38 \times 1.52^{1.75} \right)$ is 1.41, the correction factor for the transition angle $\left(k_\theta = 1.0 + 0.9 \left(90/90 \right)^{1.5} \right)$ is 1.9, the correction factor for the contraction length $\left(k_{Wa} = 0.77 + 1.36 \left(\frac{W_a}{L_1 - L_2} \right) - 1.98 \left(\frac{W_a}{L_1 - L_2} \right)^2 \right)$ is 0.95.

$$\tau_{\max(Cont)} = k_R k_{Wa} k_\theta k_w \rho g n^2 V_1^2 R_h^{-\frac{1}{3}}$$
$$= 1.41 \times 0.95 \times 1.9 \times 1.0 \times 1000 \times 9.81 \times 0.02^2 \times 2.82^2 \times 4.8^{-\frac{1}{3}}$$
$$= 20.67 \text{ Pa}$$

Find $\dot{z}_i$ (the initial rate of scour corresponding to the maximum velocity).

$\dot{z}_i$ (the initial rate of scour corresponding to the maximum velocity) is 145 mm/hr, as shown in Figure EX. 19.

The equivalent time of pier scour for this condition can be obtained by Eq.(22), and it is:

$$t_{equiv}(\text{hrs}) = 644.32 \cdot \left(t_{hydr}(\text{yrs}) \right)^{0.4242} \cdot \left(V_{\max} \left(\text{m}/\text{s} \right) \right)^{1.648} \cdot \left(\dot{z}_{i,mean} \left(\text{mm}/\text{hr} \right) \right)^{-0.605}$$
$$= 644.32 \times 75^{0.4242} \times 2.82^{1.648} \times 250^{-0.605} = 787$$

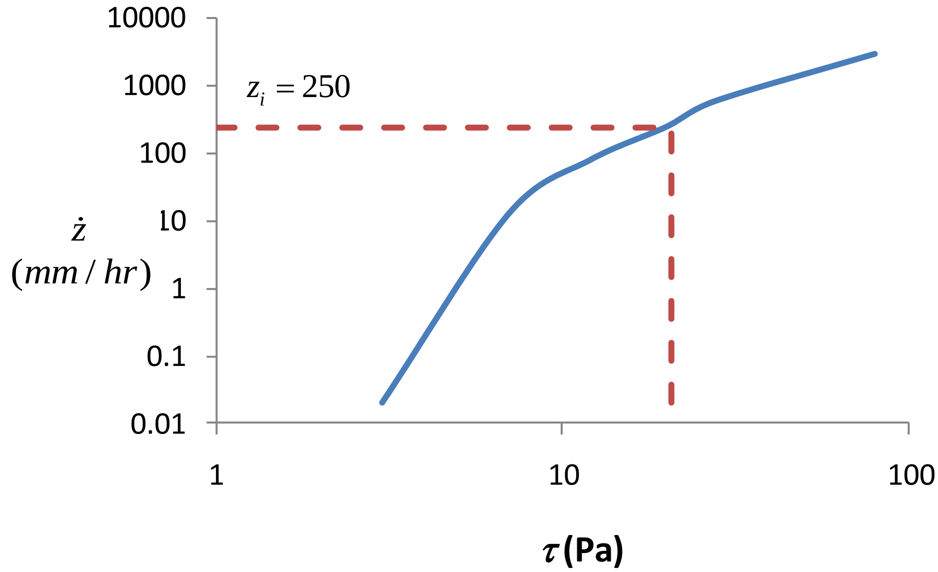

Figure EX. 19 – Erosion function and initial erosion rate corresponding to the maximum velocity (Example 6).

NOMENCLATURE

a	Pier width
a'	Projected pier width
A_1	Total flow area in the approach section immediately upstream of the abutment
A_2	Total flow area in the contracted section
A_{f1}	Flow area on the floodplain in the approach section immediately upstream of the abutment
A_{f2}	Flow area on the floodplain in the contracted section
β_a	Slope of abutment
β_m	Slope of main channel
C_r	Unit discharge ratio $C_r = Q_{total} / (Q_{total} - Q_{blocked})$
d_1	Distance from water surface to the low chord of the bridge at upstream face of the bridge
d_{deck}	Thickness of bridge deck
D	Hydraulic diameter
D_{50}	Median diameter of sediment
ε	Average height of the roughness elements
f	Friction factor obtained from Moody chart
Fr	Froude number based on V_1 and y_{f1}
$Fr_{(Pier)}$	Froude number based on V_1 and a
$Fr_{c(Pier)}$	Critical Froude number based on V_c and a
Fr_{f2}	Froude number based on V_{f2} and y_{f1}
Fr_{m2}	Froude number based on V_2 and y_{m1}
Fr_{fc}	Froude number based on V_c and y_{f1}
Fr_{mc}	Critical Froude number based on V_{mc} and y_{m1}
g	Gravitational acceleration
γ	Unit weight of water
Gs	Specific gravity of cohesionless soil
h	Distance from the low chord of the bridge to the river bottom before scour starts
k_α	Correction factor of the contraction transition angle for τ_{max}
k_c	Correction factor of channel conveyance ratio for τ_{max}
k_{Fr}	Correction factor of Froude number for τ_{max}
k_L	Correction factor of the abutment location for τ_{max}
k_o	Correction factor of overtopping for τ_{max}
k_θ	Correction factor of attack angle for τ_{max}

k_R	Correction factor of contraction ratio for τ_{max}
k_s	Correction factor of abutment shape for τ_{max}
k_{sh}	Correction factor of aspect ratio for τ_{max}
k_{Wa}	Correction factor of the contraction length for τ_{max}
K_1	Correction factor of pier or abutment shape for maximum abutment or pier scour depth
K_2	Correction factor of attack angle for maximum abutment or pier scour depth
K_I	Correction factor for flow intensity
K_f	Correction factor for spiral flow at the abutment toe
K_G	Correction factor for channel geometry
K_L	Correction factor of the abutment location for maximum abutment scour depth
K_{sp}	Correction factor of the pier spacing for maximum pier scour depth
K_p	Correction factor of pressure flow for maximum abutment scour depth
K_w	Correction factor of water depth for maximum abutment or pier scour depth
L'	Length of embankment projected normal to flow
L_1	Width of channel at approach section
L_2	Width of channel at contracted section
L_f	Width of floodplain
L_m	Half width of main channel
M	Discharge contraction ratio $\left(M = \frac{Q_{total} - Q_{block}}{Q_{total}} \right)$
n	Manning's coefficient
ν	Kinematic viscosity of water
θ	Attack angle or contraction transition angle in degree
p	Pressure (N/m^2)
q_1	Unit discharge at approach section
q_2	Unit discharge around abutment
Q_{block}	Discharge blocked by bridge embankment defined by approach average velocity on flood-plain times the area extending the bridge to approach section
Q_{total}	Total discharge
Q_{fp1}	Discharge on the floodplain in the approach section immediately upstream of the abutment
ρ	Unit mass of water
R_h	Hydraulic radius
Re	Reynolds number based on a or W_a
Re_{f2}	Reynolds number defined with local velocity V_{f2} and water depth in floodplain y_{f1}

S	Spacing of group piers or the energy slope
t	Elapsed time after start of scour (hour)
t_{equiv}	Equivalent time necessary for the highest velocity in the hydrograph to create the same scour depth as the entire hydrograph
t_{hydro}	Duration of the hydrograph
τ_c	Critical shear stress
$\tau_{max(Abut)}$	Maximum shear stress of around abutment
$\tau_{max(Cont)}$	Maximum shear stress of in the middle of channel
$\tau_{max(Pier)}$	Maximum shear stress of around pier
τ_s	Bed shear strength at depth z below initial bed-fluid interface
V_1	Approach average velocity
V_{f1}	Approach average velocity on the floodplain
V_{f2}	Velocity around the toe of the abutment
V_{fc0}	Critical velocity on the floodplain without back water effect
V_{fc}	Critical velocity on the floodplain
V_{max}	Maximum velocity in the hydrograph
V_{mc}	Critical velocity in the main channel
W	Water content (%)
W_a	Top width of the abutment or length of contraction channel
y_{Cont}	Total flow depth of scour in the contracted section (y_{m1}+$y_{s(Cont)}$)
y_{f0}	Water depth at the approach section on the floodplain without back water effect
y_{f1}	Water depth at the toe of the abutment estimated as the water depth immediately upstream of the toe of the abutment
y_{max}	Total flow depth of abutment scour depth (y_{f1}+$y_{s(Abut)}$)
y_{m1}	Water depth in the main channel at immediately upstream of bridge contraction
$y_{s(Abut)}$	Maximum abutment scour depth adjacent to the toe of the abutment
$y_{s(Cont)}$	Maximum contraction scour depth in the middle of channel
$y_{s(Pier)}$	Maximum pier scour depth
$y_s(t)$	Scour depth at time t
$\dot{z}_i$	Initial rate of scour
$\dot{z}_{i,mean}$	Mean initial rate of scour corresponding to the maximum velocity

REFERENCES

ABSCOUR. (Maryland SHA Bridge Scour Computer Program), Maryland State Highway Administration, Version 8, build 1.02, compiled August 14, 2006.

Benedict, S. T., and Caldwell, A. W. (2006). "Development and Evaluation of Clear-Water Pier and Contraction Scour Envelope Curves in the Coastal Plain and Piedmont Provinces of South Carolina." *U.S. Geological Survey Scientific Investigations Report 2005 - 5289*, U.S.G.S., Reston, VA, USA.

Briaud, J.-L. (2008). "Case Histories in Soil and Rock Erosion: Woodrow Wilson Bridge, Brazos River Meander, Normandy Cliffs, and New Orleans Levees." *J. Geotech. Geoinviron. Eng., ASCE*, 134(10), 1424 - 1447.

Briaud, J.-L., Brandimarte, L., Wang, J., and D'Odorico, P. (2007). "Probability of scour depth exceedance owing to hydrologic uncertainty." *Georisk*, 1(2), pp 77-88.

Briaud, J.-L., Chen, H.-C., Chang, K.-A., Oh, S. J., and Chen, X. (2009). "Abutment Scour in Cohesive Materials." *NCHRP Report 24-15(2)*, National Research Council: Transportation Research Board, Washington, DC, USA.

Briaud, J.-L., Chen, H. C., Li, Y., Nurtjahyo, P., and Wang, J. (2003). "Complex pier scour and contraction scour in cohesive soils." *NCHRP Rep. No. 24-15*, Transportation Research Board National Research Council.

Briaud, J.-L., Chen, H. C., Li, Y., Nurtjahyo, P., and Wang, J. (2004). "Pier and contaction scour in cohesive soil." Transportation reearch board, Washington, D.C.

Briaud, J.-L., and Oh, S. J. (2010). "Bridge Foundation Scour." *Geotechnical Engineering Joural of the SEAGS & AGSSEA*, 41 (2), 1 - 16.

Briaud, J.-L., Ting, F., Chen, H. C., Cao, Y., Han, S.-W., and Kwak, K. (2001). "Erosion function apparatus for scour rate predictions." *J. Geotech. Geoinviron. Eng., ASCE*, 127(2), 105-113.

Briaud, J.-L., Ting, F., Chen, H. C., Gudavalli, S. R., Perugu, S., and Wei, G. (1999). "SRICOS: Prediction of scour rate in cohesive soils at bridge piers." *J. Geotech. Eng. ,ASCE*, 125, 237-246.

Chen, X. (2008). "Numerical study of abutment scour in cohesive soils," Ph.D. Dissertation, Texas A&M University, College Station, TX.

Chow, V. T. (1959). *Open-Channel Hydraulics*, McGraw-Hill, New York, USA.

Chow, V. T., Maidment, D. R., and Mays, L. W. (1988). *Applied Hydrology*, McGraw-Hill.

Ettema, R., Nakato, T., and Muste, M. (2008). "Estimation of scour depth at bridge abutment." *NCHRP Rep. No. 24-20*, Transportation Research Board, Washington, D.C.

Froehlich, D. C. "Analysis of onsite measurement of scour at piers." *Proceedings of ASCE National Hydraulic Engineering Conference, 1988*, Colorado Springs, CO, USA.

Froehlich, D. C. "Local scour at bridge Abutment." *Proceedings of National Conference on Hydraulic Engineering, 1989*, New York, pp. 13-18.

Gill, M. A. (1981). "Bed erosion in rectangular long contraction." *J. Hydr. Div.*, 107(HY3), pp. 273 - 284.

Gudavalli, S. R. (1997). "Prediction model for scour rate around bridge piers in cohesive soils on the basis of flume tests," Ph.D. Dissertation, Texas A&M Uninversity, College Station, TX.

Komura, S. (1966). "Equilibrium depth of scour in long constrictions." *J. Hydr. Div.*, 92(HY5), pp. 17-38.

Kwak, K. (2000). "Prediction of scour depth versus time for bridge piers in cohesive soils in the case of multi-flood and layered soil systems," Ph.D. Dissertation, Texas A&M University, College Station.

Li, Y. (2002). "Bridge pier scour and contraction scour in cohesive soils on the basis of flume tests," Ph. D. Dissertation, Texas A&M University, College Station, TX.

Lim, S. Y. "Clear water scour in long contractions." *Prodeedings of the Institution of Civil Engineering - Water, Maritime & Energy*, London, UK, 101, No.9, June 1993, pp 93 - 98.

Moody, L. F. (1944). "Friction Factors for Pipe Flow." Transaction of the American Society of Civil Engineers, Vol. 66, Reston, Virginia, USA.

Muller, D. S., and Landers, M. (1996). "Channel scour at bridges in the United States." *FHWA-RD-95-184*, Federal Highway Administration, VA, USA.

Munson, B. R., Young, D. F., and Okiishi, T. H. (1990). *Fundamentals of fluid mechanics*, Wiley, New York.

Nurtjahyo. (2003). "Chimera RNAS simulations of pier scour and contraction scour in cohesive soils," Ph.D. Dissertation, Texas A&M University, College Station.

Oh, S. J. (2009). "Experimental Study of Bridge Scour in Cohesive Soil," Ph.D dissertation, Texas A&M University, College Station, TX.

Oh, S. J., Briaud, J.-L., Chang, K.-A., and Chen, H.-C. (2011). "Maximum Pier Scour Depth in Fine Grained Soil." *J. Geotech. Geoinviron. Eng., ASCE*.

Richardson, E. V., Simons, D. B., and Lagasse, P. F. (2001). "River engineering for highway encroachments - highways in the river environment." *FHWA NHI 01-004*, Federal Highway Administration, Hydraulic series No. 6, Washington, D.C.

Shields, A. (1936). "Application of similarity principles and turbulence research to bed-load movement." *Hydrodynamics Laboratory Publ. No. 167*, trans. by W. P. Ott J. C. van Uchelen, Laboratory of Hydraulic and Water Resources, Californial Institute of Technology.

Sturm, T. W. (2004). "Enhanced abutment scour studies for compound channels." *Rep. No. FHWA-RD-99-156*, Georgia Institute of Technology, School of Civil and Environmental Engineering, Atlanta, GA 30332.

Wang, J. (2004). "The SRICOS-EFA method for complex pier and contraction scour," PhD dissertation, Texas A&M University, College Station, TX, USA.

Webby, M. G. (1984). "General scour at a contraction." *RRU Bulletin 73*, Bridge Design and Research Seminar, New Zealand.

Wei, G., Chen, H. C., Ting, F., Briaud, J.-L., Gudavalli, S. R., and Perugu, S. (1997). "Numerical simulation to study scour rate in cohesive soils." *Reseach report to the Texas Department Transportation*, Department of Civil Engineering, Texas A&M University, College Station, TX.

WolframMathworld. (2007). "Erf function." available from http://mathworld.wolfram.com/Erf.html, (accessed 05January 2010).